A De-coupled Level Controller for Cascaded Flotation Processes

Jacobus P. van Heerden

Thesis presented in partial fulfillment
of the requirements for the degree of

Master of Science in Engineering
at the
University of Stellenbosch

Supervisor: Prof. J.J. du Plessis

Maart 2002

Declaration

I, the under-signed, hereby declare that the work contained in this thesis is my own original work and has not previously in its entirely or in part been submitted at any university for a degree.

Signature   :

Date   :   November 1, 2001

Abstract

Flotation was introduced early in the 20th century as a separation process for extracting valuable minerals from grinded ore. Today flotation is a dominant mineral concentration method and is used for almost all sulphide minerals and also for non-sulphide metallic minerals, industrial minerals, and coal.

Automation and control has become a basic requirement in flotation plants. Effective control of pulp levels plays a very important role in stabilising the flotation process and therefore requires careful attention.

This thesis presents a de-coupled level controller that has been developed for the control of levels in cascaded flow processes, including multi-tank cascaded flotation processes. The controller was developed on a two tank cascaded pilot plant using water as a flow medium. A simulation model was constructed for the cascaded flow process. The simulation model made it possible to develop and evaluate a de-coupled level controller in a simulation environment. Finally independent loop PID control and integrated PID control loops with feed-forward de-coupling were compared through simulation, as control strategies for the pilot plant.

Opsomming

Flotasie is vroeg in die 20ste eeu bekend gestel as 'n skeidingsproses om waardevolle minerale te onttrek uit fyngemaalde erts. Vandag is flotasie die dominante proses om minerale te konsentrasie en word gebruik vir byna alle sulfied minerale sowel as nie-sulfied metaal minerale, industriele minerale and steenkool.

Outomatisasie en beheer het 'n basiese vereiste geword in flotasie aanlegte. Die effektiewe beheer van pulpvlakke speel 'n baie belangrike rol in die stabilisering van die flotasie proses en verdien om hierdie rede deeglike aandag.

Hierdie tesis stel 'n ontkoppelde vlakbeheerstelsel voor wat ontwikkel is vir die beheer van vlakke in kaskade vloei prosesse byvoorbeeld multi-tenk flotasie prosesse. Die beheerstelsel is ontwikkel op 'n twee-tenk kaskade toetsaanleg met water as vloeimedium. 'n Volledige simulasiemodel is ontwikkel wat dit moontlik gemaak het om die vlakbeheerstelsel te ontwerp, toets en verfyn in 'n simulasie omgewing. Verder is die verskil tussen onafhanklike enkellus PID beheerders en ontkoppelde PID beheerlusse ondersoek en word in die tesis geillustreer.

Acknowledgements

Prof. Jan du Plessis, Dr. Herman Steyn and Dr. Derick Moolman for your mentorship and guidance.

All my colleagues at Crusader Systems who contributed to and supported my efforts in many ways.

Otto Strydom for your much-appreciated help with SIMuWIN.

My fellow students – I learnt a lot from you.

All my friends, family and loved ones who never ceased to support and encourage me.

Ties whom I love dearly – you believed in me and inspired me to push through.

My heavenly Father – You are the beginning of all knowledge and wisdom.

Contents

APPENDIX E SIMULATION MODEL EVALUATION 133

List of Figures

List of Tables

Keywords

flotation process

cascaded tanks

multi-tank system

pulp levels

level control

simulation model

non-linearities

hysteresis

Least Squares system identification

pole placement controller design

PID control

independent control loops

feed-forward de-coupling

Acronyms

PI	Proportional and Integral
PID	Proportional, Integral and Derivative
DCS	Distributed Control System
DC	Direct Current
LS	Least Squares
SISO	Single Input Single Output
PC	Personal Computer
MPC	Model Predictive Control
CL	Closed Loop
PLC	Programmable Logic Controller
A/D	Analogue to Digital
D/A	Digital to Analogue
PRBS	Pseudo Random Binary Sequence
ARX	Auto-Regressive with eXogenous input

Chapter 1

Introduction

1.1 Background

1.1.1 Flotation Process

Flotation was introduced early in the 20th century as a separation process for extracting valuable minerals from grinded ore. This separation is based on differences in the surface properties of the minerals. It's first commercial application was at Broken Hill in Australia where a great deal of early flotation research was done. Since then great advances have been made in both the chemical aspects of the process and the equipment used. Today flotation is the dominant mineral concentration method and is used for almost all sulphide minerals and also for non-sulphide metallic minerals, industrial minerals, and coal. Detail discussions on flotation as a process are given in [1], [2], [3], [4] and [5]. Information on flotation machines and equipment can be found in [6], [7], [8], [9], [10], [11] and [12].

The objectives of flotation are to maximise the recovery of valuables while maintaining a specific concentrate grade. The recovery in most flotation plants is at best 80 to 90% [13]. The reason for this is twofold: 1) Due to the limits of current grinding technology and available reagents, overlapping occurs between flotation properties of wanted and unwanted minerals, especially with composite particles of different compositions. This places a limit on maximum recovery and grade; 2) Flotation plants are not always operated optimally resulting in sub-optimal recoveries and grades.

The diminishing supply of raw materials and the increasing rate of consumption of metals and metal products together with the rising cost of energy, consumables and labour are demanding higher efficiency of metal extraction processes. Stricter pollution laws imposed by governmental regulations are placing additional economic

burden on the metal industry. Optimising process efficiency is therefore not a luxury any more, but a matter of survival in an increasingly competitive industry.

1.1.2 Automatic Control in Flotation

McKee [14] reports that during the early 1970's the first reliable on-stream analysis systems were developed, making assay information available, which is essential for on-line control. During more or less the same time mini-computers became available for process control and the first successful grinding control systems were reported. Thus all the important requirements for flotation control studies were met and by 1976 literature was reporting a number of initial control systems [15]. Today computer, measurement and instrumentation technology has developed to such an extent that control of flotation plants is largely automated using a PLC or a DCS.

Flotation plants are very susceptible to disturbances and therefore require careful control. Disturbances found in flotation plants mostly fall into one of three categories, namely 1) changes in throughput, 2) variations of ore types, metallurgical characteristics and flotation responses and 3) deliberate alteration of the metallurgical objectives of the circuit (grade and recovery) [14]. The main feed stream is normally a major source of disturbances to a flotation plant. Flow rates, densities, size distributions, shapes, surface properties and composites can all change, with significant impact on plant performance (grade and recovery) [13].

Effective optimisation and control of a flotation process can improve recovery by up to 5% [13]. Effective flotation control requires three different levels of control. 1) Stabilising process variables at set-points. This is a prerequisite to process optimisation. 2) The manipulation of process set-points to achieve specific grades and recoveries. 3) The manipulation of grade and recovery to optimise economic performance.

1.1.3 Stabilisation

Stabilising a process entails pinning process variables down to set-points despite of plant disturbances. For flotation processes these variables include reagent addition rates, pulp levels, froth height, wash water addition rates, aeration rates, impeller speeds and with the recent availability of visual froth characterisation sensors, visual froth parameters such as froth speed and bubble size.

This level of control relies directly on the controllability of the process determined by correct process configuration/topology, reliable high quality instrumentation and flotation equipment. In the early days of flotation control one of the main problems was the absence of reliable on-line measurements of process variables. Today reliable measurements of most of the important process variables can be obtained on-line. Combined with the availability of sophisticated modern control techniques, effective control is well within the reach of every flotation plant.

1.1.4 Pulp Levels

Pulp levels in flotation plants strongly contribute to the dynamic characteristics of the plant as a whole and must be controlled to ensure plant stability. It is closely related to grade and recovery and is therefore used as one of the cheapest and easiest ways to directly manipulate grade and recovery. For optimal grade and recovery, stable pulp levels at optimal set-points are necessary. Too low pulp levels result in losses in recovery whereas too high levels also negatively affect recovery and cause losses in grade.

Many techniques have been researched for measuring pulp levels of which several are in use today. These include bubble tubes, float sensors combined with ultrasonic or angle transmitters, conductivity probes [16], sonic devices [17], light attenuation sensors [18], capacitance probes and ultrasonic units. The float sensor ultrasonic combination seems to be one of the more accurate and robust methods and is popular today.

A single pulp-discharge valve is usually used to control the pulp level of each flotation unit.

1.2 Level Control

From the beginning of level control about 20 years ago, PI loops have been used for the control of each separate flotation unit.

Initially level controllers were retro-fitted to flotation units. Today in many cases the flotation cell and its level controller, consisting of the measuring device and control unit connected to the pulp discharge valve, is an integrated piece of equipment.

Connecting these units together in cascade results in a pulp flow system where each unit's level is controlled by a separate PI control loop.

It is however widely accepted, that separate controllers on each unit of cells is not the most suitable level control strategy, as each control valve is unaware of the actions of others, and propagates disturbances to downstream flotation units. The result is that disturbances are not damped, but propagated through the circuit.

An integrated control approach, where each control valve accounts for the actions of other control valves, has the potential to provide more effective neutralisation of level disturbances. [19]

A successful level control strategy should deal with the main difficulties in flotation level control namely pulp flow disturbances and interactions between tank units.

The best way to deal with pulp flow disturbances is to not burden the level controllers of the float section with the task, but to have a dedicated buffer mechanism for stabilising the feed before or right in the beginning of the flotation process.

Dealing with feed flow disturbances in the flotation process can be done in a feed-forward or feedback manner.

According to the feed-forward approach the pulp flow disturbance is measured directly and the measurement is fed forward to the control loops of the cascaded tank units to cancel the effect of the disturbance on the levels of the bank of flotation units. This approach is most viable if a reliable measurement of the pulp flow disturbance at, or very close to the inflow of the first tank can be obtained. If a measurement can be obtained, but not close to the inflow, a flow model of the pulp is needed from the point of measurement to the inflow to be able to cancel the effect of the disturbance on the first tank level control loop effectively. Such a flow model will change with the flow properties of the pulp. Obtaining a pulp flow measurement at the inflow to the first tank might be difficult in itself.

For the second approach no explicit measurement of the pulp flow is needed which makes it cheaper to implement. With feedback disturbance rejection, the disturbance is recognized as it results in measured level errors. The control system then compensates for it just as for any other error in pulp level.

Tank unit interactions are another major consideration in the level control of cascaded flotation units. The following ways exist of dealing with tank unit

Stellenbosch University http://scholar.sun.ac.za

Chapter 1. Introduction   1.3 Performance vs. Cost

interactions. Firstly a separate SISO control loop may be used for each individual unit. From the beginning level control was done in this way on cascaded flotation units. The approach does not address interactions however, but rather ignores it. Interactions are treated as pulp level disturbances and compensated for as level errors.

The other approach, which has proven superior and has become widely accepted recently, is an integrated control approach. In this case the interactions are modelled and de-coupling is accomplished actively by each pulp discharge valve considering the actions of the other and cancelling their affects on the level of its own unit in a feed-forward way. The result of this explicit de-coupling is that the level of each unit is only affected by the actions of the valve dedicated to controlling that specific level. This makes the units independently controllable. Level disturbances are therefore dealt with in the first unit of a cascaded bank of flotation units and have no affect on downstream levels.

1.3 Performance vs. Cost

The aim in developing any control system is to maximise the Performance/Cost-ratio, where Performance is the degree to which the control objectives are met, representing the requirements for maximum financial benefit, and Cost is the total cost of ownership including installation, operation, maintenance, lifetime and replacement costs.

1.4 Aim of this thesis

This thesis presents a de-coupled level controller that can be applied in cascaded flotation processes. It was developed using a cascaded two-tank pilot plant with water as a flow medium.

1.5 Overview of the chapters

Chapter 2 describes the pilot plant and experimental set-up. Chapter 3 focuses on the development of a comprehensive simulation model of the pilot plant. Chapter 4 considers suitable control technologies for the level control problem. Chapter 5 shows how linear models can be deduced for the purpose of controller design. In Chapter 6 and Chapter 7 two different control approaches are evaluated and

described. The last chapter, Chapter 8, is a summary of the findings of this study with some conclusions.

Chapter 2

Experimental Set-up

This chapter describes the equipment, instrumentation and software that were used for the level control research carried out for this thesis. It also defines the control objectives for the pilot plant experimental set-up.

2.1 Pilot Plant

A pilot plant was used for the level control research. Figure 1 is a schematic diagram of the pilot plant with the instrumentation interfaced to a PC, which is used for level control. The water level in each tank is controlled by a control valve on the outlet of the tank. A pressure sensor at the bottom of the tank measures the water level. The feed flow rate to each tank is not directly measured and is treated as a disturbance to the tank level.
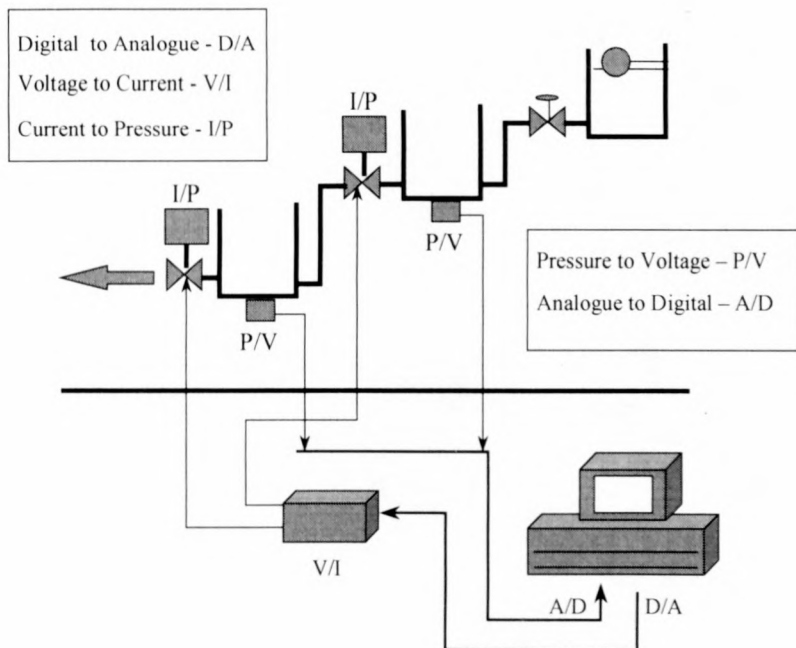
Figure 1: Schematic diagram of pilot plant

2.2 Level sensors

The two level sensors make use of LX06XXXD SenSym differential pressure transducer chips with one pressure inlet exposed to atmosphere and the other one to the pressure to be measured. The differential pressure signals from the transducer chips are then sent through amplifier circuitry with anti-aliasing filtering (Appendix A).

2.3 Control valves

An ADAS D/A (digital to analogue) converter gives a fixed voltage command signal from the PC at every sampling instant (0-10V), which is converted to current by a V/I (voltage to current) converter (4-20mA). The current command signal is applied to an I/P (current to pressure) transducer (Automax model 5100). The resulting pressure signal then serves as an input to a modular valve positioning system (Appex 5000) that positions a ¾ inch ball valve (VALPRESS PN40/DN20 AISI 316) by means of a pneumatic valve actuator (AUTOMAX MECAR Supernova Type SN050 DA).

2.4 ADAS

Analogue to digital (A/D) and digital to analogue (D/A) conversion is done with an ADAS card that slots into the PC. The ADAS card was designed by the Department Electrical and Electronic Engineering, University of Stellenbosch, South Africa.

2.5 SIMuWIN

SIMuWIN was software used for both the simulation and control of the process. SIMuWIN is a block diagram based environment for the simulation and control of dynamic systems. It was developed by the Department of Electrical and Electronic Engineering of the University of Stellenbosch, South Africa, and is commercially available from the department. SIMuWIN makes use of the ADAS card described above to output control signals to the plant and to sample the signals from the level sensors.

2.6 Control Objectives

The aim is to control each tank level at a fixed set-point despite changes in feed flow rate and to change each level from one level set-point to another in an acceptable way. In control terms this means guaranteed stability, good disturbance rejection and a well-damped transition from one level set-point to the next with acceptable rise time.

For the purpose of evaluating control system performance and comparing control strategies, the objectives for pilot plant level control are specified in Table 1.

Criteria	*Specification*	*Purpose*
Feed-flow Disturbance rejection	As good as possible	Stabilizing levels
Rise time	50 seconds for level change of 1 volt in pressure sensor reading (chosen to suit Pilot Plant flow capacity)	Controlling level transitions from one set-point to another.
Maximum Overshoot	5%	Preventing oscillations
Robustness	Performance specifications and Closed-loop Stability must be maintained in the presence of valve and hydrodynamic flow non-linearities and process disturbances.	Ensuring stability

Table 1: Control system specifications

2.7 Conclusions

In this chapter the pilot plant, instrumentation and software that were used for the research done for this thesis, have been described. Lastly, control objectives for the pilot plant were defined. In the next chapter a complete simulation model is developed for the pilot plant level control problem.

Chapter 3

Simulation Model

This chapter presents the development of a model that was used for the simulation of the pilot plant and the development of level control strategies in a simulation environment.

3.1 Variables & Dimensions

In modelling the pilot plant it was necessary to describe the dynamic relationships and interaction between the plant variables shown in Figure 2, over their respective operating ranges.
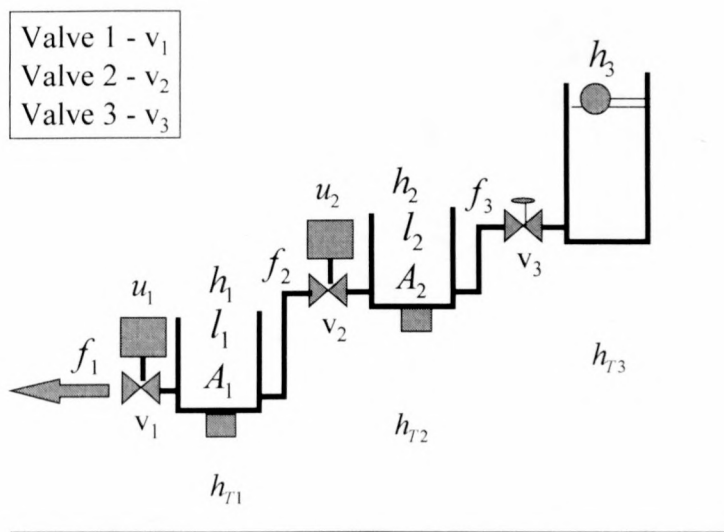
Figure 2: Valves, variables and dimensions

The system variables and dimensions are listed in Table 2.

Symbol	Variable/Dimension	Range/Value	Units
l_1	level sensor output	0 – 10	V
l_2	level sensor output	0 – 10	V
h_1	water level	0.030 - 0.311	m
h_2	water level	0.038 - 0.285	m
h_3	Reservoir water level	0.35	m
u_1	valve command input	3 – 10	V
u_2	valve command input	5 – 10	V
f_1	volumetric flow rate	0 – 4.3e-5	m^3/s
f_2	volumetric flow rate	0 – 4.3e-5	m^3/s
f_3	volumetric flow rate	0 – 2.8e-4	m^3/s
h_{T1}	tank elevation	0.57	m
h_{T2}	tank elevation	1.14	m
h_{T3}	reservoir elevation	1.71	m
A_1	tank cross sectional area	0.08	m^2
A_2	tank cross sectional area	0.08	m^2

Table 2: System variables and dimensions

3.2 Fundamentals

In developing a mathematical model of the flow system the first step was to look at the interdependencies of the system variables. In this system the independent variables are the valve command inputs u_1 and u_2 which are also used as model input variables. The flow f_3 in the pilot plant is dependent on levels h_2 and h_3 due to the effect of Toricelli's law[1]. For the purposes of the simulation model the latter dependencies are not taken into account, and f_3 is assumed to be an independent disturbance input variable to the model. The extend to which this assumption holds true and the full effect of Toricelli's law on flow f_3 were tested and are illustrated in Appendix B. The rest of the variables are all interrelated and dependent directly or indirectly on the three independent model input variables u_1, u_2 and f_3.

The relationships between the respective tank levels and water flow rates are derived from the mass flow equations for the two tanks.

---

[1] The speed of efflux of a liquid from a small hole at the bottom of an open tank is equal to that acquired by a body falling freely through a vertical distance equal to the height of the liquid level above the point of efflux. [20]

Flow rates are integrated to produce levels as shown in Equation 1 and Equation 2.

Equation 1

$$A_1 \frac{dl_1}{dt} = f_2 - f_1$$

Equation 2

$$A_2 \frac{dl_2}{dt} = f_3 - f_2$$

Toricelli's law that follows from energy considerations determines the steady state volumetric flow rates. It points out the quadratic relationship between the flow velocity of water from a small hole at the bottom of a tank and the tank level:

Equation 3

$$f_1 = K_1(u_1)\sqrt{h_1 + h_{T1}}$$

Equation 4

$$f_2 = K_2(u_2)\sqrt{(h_2 + h_{T2}) - (h_1 + h_{T1})}$$

K_1 and K_2 are valve gain constants that are unique for every valve position and are determined empirically from flow experiments for the full range of valve positions.

Equation 3 and Equation 4 are steady state equations and do not say anything about the dynamic characteristics of the valves and the resulting effects on flow response. The question here was: what are the transient effects of the flow rates in response to changes in valve commands (u) and/or levels (l) respectively.

3.2.1 Flow transients due to level changes:

The tank capacities (cross sectional area) are large compared to the cross sectional areas of the out flow pipes. This combined with the low density of water means low inertia of water in the out flow pipes. Therefore a change in level that translates to a change in pressure at the pipe outlet causes quick acceleration of water in the pipe and therefore a quick flow rate change compared to any other time constant in the

system. In this model flow rate changes due to level changes are therefore assumed to be immediate. For fixed valve commands it can be described by Equation 5 and Equation 6:

Equation 5

$$f_1(t) = K_1(u_1)\sqrt{h_1(t) + h_{T1}}$$

Equation 6

$$f_2(t) = K_2(u_2)\sqrt{(h_2(t) + h_{T2}) - (h_1(t) + h_{T1})}$$

3.2.2 Flow transients due to valve commands changes:

To investigate the flow response transients for the two respective valves, a step test was done for every valve. A square wave input of period 33.3s and amplitude 2 was first applied to valve v_2 and levels l_1 and l_2 were recorded while the contents of the upper tank emptied into the lower tank, with level l_2 dropping from full to empty. Secondly, a square wave of the same period and amplitude, but different offset, was applied to valve v_1 and level l_1 was recorded while l_1 dropped from full to empty. The respective flows were computed using Equation 1 and Equation 2 and plotted together with the valve command signal. The cut-off frequency of the anti-aliasing filters on the level sensors is 0.24Hz. The signals were sampled at a sample rate of 4Hz, about 20 times faster than the anti-aliasing filter cut-off frequency (Appendix A).
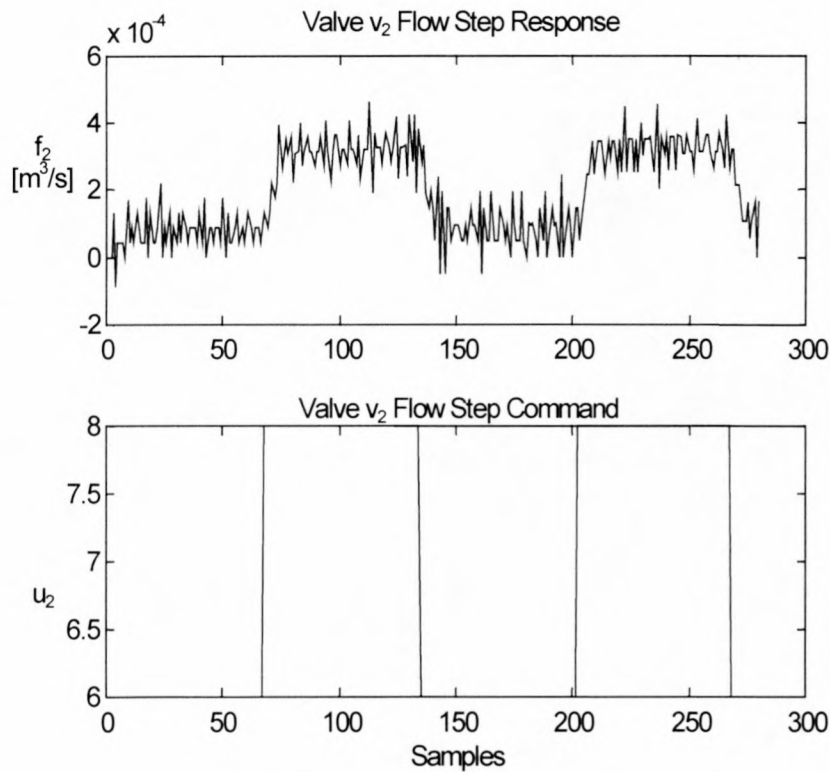
Figure 3: Flow rate step response of valve v_2
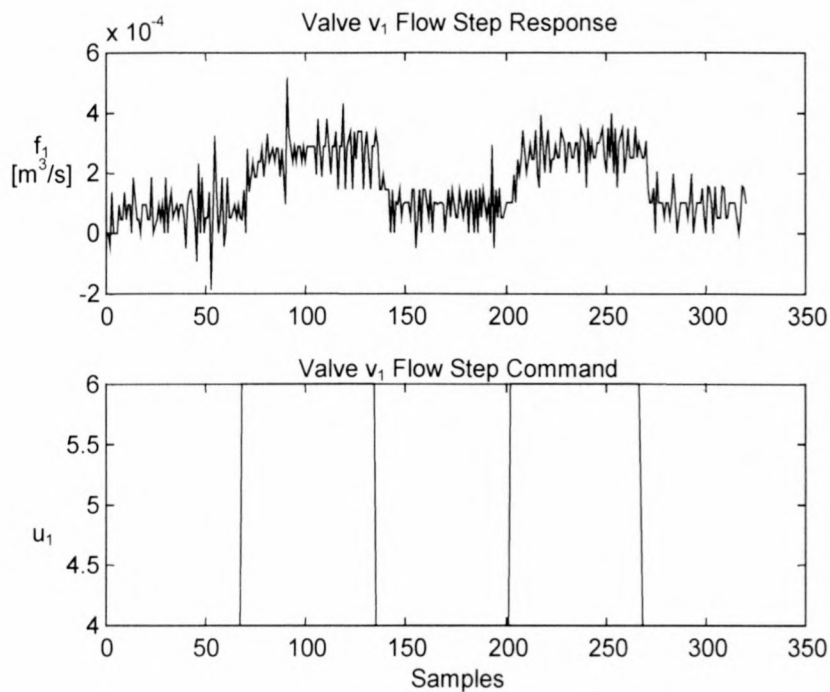
Figure 4: Flow rate step response of valve v_1

From the step responses in Figure 3 and Figure 4 the following conclusion can be made: The flow transients are of the first order. There are no significant delays between valve command signals and flow responses. The time constants are independent of the tank levels, because there is no notable difference between the

first and the second step responses. The settling times for both valves are in the order of 15 samples, implying time constants in the order of 0.75s.

The transient dynamics are included in the model in the following way. It is assumed to be of the first order and to include the effects from mechanical valve motion to level sensor time constants due to anti-aliasing filtering. It models the total transient response from valve command signal to measured flow rate response. The model makes provision for different flow rate step-up and step-down time constants. For fixed levels the flow transients can be written as shown in Equation 7 through to Equation 10:

Equation 7

$$f_1(t) = K_1(u_1(t))\left(1 - e^{-\frac{t}{\tau_{1o}}}\right)\sqrt{h_1 + h_{T1}} \quad \text{if} \left(\frac{du_1}{dt} > 0\right)$$

Equation 8

$$f_1(t) = K_1(u_1(t))\left(1 - e^{-\frac{t}{\tau_{1c}}}\right)\sqrt{h_1 + h_{T1}} \quad \text{if} \left(\frac{du_1}{dt} < 0\right)$$

Equation 9

$$f_2(t) = K_2(u_2)\left(1 - e^{-\frac{t}{\tau_{2o}}}\right)\sqrt{(h_2 + h_{T2}) - (h_1 + h_{T1})} \quad \text{if} \left(\frac{du_2}{dt} > 0\right)$$

Equation 10

$$f_2(t) = K_2(u_2)\left(1 - e^{-\frac{t}{\tau_{2c}}}\right)\sqrt{(h_2 + h_{T2}) - (h_1 + h_{T1})} \quad \text{if} \left(\frac{du_2}{dt} < 0\right)$$

3.2.3 Hysteresis

The model structure as described to this point proved successful in predicting flow response to square input signals, but showed significant errors in response to

triangular input signals. This initiated tests to identify and characterize possible hysteresis effects in the flow system.

Hysteresis is known to be a common non-linearity in control valve operation and can be graphically represented as shown in Figure 5 below.
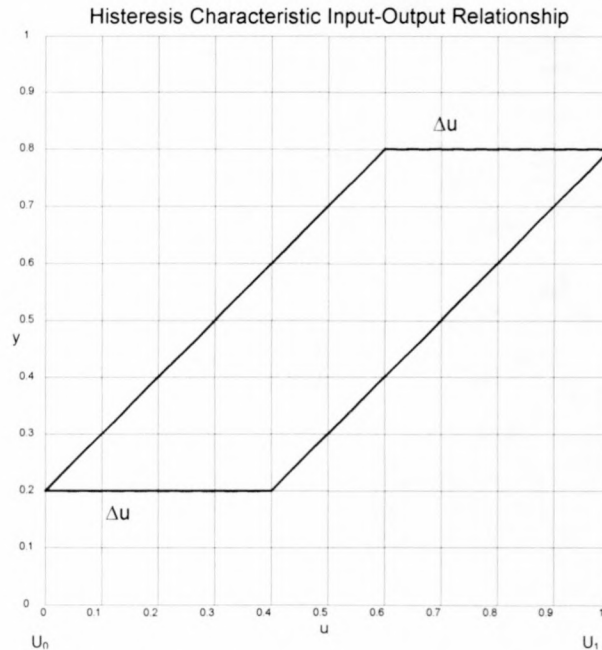
Figure 5: Hysteresis characteristic input-output relationship

It can be mathematically described in the following way with u being the input and y the output variable:

When the input u increases and u_0 is the value of u when it starts to increase, then the output y can be written as:

$$y = f(u_0) \text{ for } u_0 < u < u_0 + \Delta u,$$

$$y = f(u) \text{ for } u \geq u_0 + \Delta u,$$

When the input u decreases and u_1 is the value of u when it starts to decrease, then the output y can be written as:

$$y = f(u_1) \text{ for } u_1 - \Delta u < u < u_1,$$

$$y = f(u) \text{ for } u \leq u_1 - \Delta u,$$

with Δu describing the amount of hysteresis present in the system. A characteristic property of the Hysteresis non-linearity is that Δu is independent of the input signal frequency.

Appendix C more completely describes the Hysteresis non-linearity and shows how it can be identified and measured in dynamic systems.

With hysteresis defined, the structure and components of the dynamic simulation model of the pilot plant are completely specified. Unknowns in the model are the two gain functions $K_1(u_1)$ and $K_2(u_2)$, the time constants $\tau_{1_o}, \tau_{1_c}, \tau_{2_o}$ and τ_{2_c} and the amount of hysteresis Δu. h_1 and h_2 are related to level sensor outputs l_1 and l_2 as described in Appendix A.

The remainder of this Chapter describes how these unknowns were measured to complete the simulation model.

3.3 Gain functions

A set of experiments were performed on the pilot plant to determine the valve gain functions: With the tank water level at a maximum, the outlet valve was opened to a specific position and the tank allowed to run empty while level measurements were recorded at a fixed sample interval. From the recorded level data valve gain constants were computed at every valve position using Equation 5 and Equation 6. Once this was done for all valve positions in the range, a continuous function was fitted through the valve gain constants to obtain the valve gain function.

Important considerations were the following. Firstly levels were recorded over their full ranges dropping from full to empty to best capture the effect of Toricelli's law in the recorded data. Secondly, according to the Nyquist theorem, the sample frequency had to be at least 2 times higher than the -3dB cut-off frequency of the level sensors to prevent aliasing of possible high frequency signal content near the cut-off frequency of the anti-aliasing filter. In this case the sample frequency was chosen to be 4Hz, 20 times the level sensor cut-off frequency.

3.3.1 Computing $K_1(u_1)$:

Valve v_1 was opened to a specific position by applying a valve command signal u_1. The measured level l_1 was sampled with the lower tank running empty. This was done for each position of valve v_1 shown in Table 3 below.

Valve command (u_1) [Volt]
3
3.5
4
4.5
5
5.5
6
6.5
7
7.5
8
8.5
9
9.5
10

Table 3: Valve positions for valve gain experiments - valve v_1

The level signal samples were converted from volts (l_1) to meters (h_1) using the calibrated relationships from Appendix A and f_1 was computed using Equation 11.

Equation 11

$$f_1 = -\frac{dh_1}{dt} A_1 \quad [m^3/s]$$

This was done in a discrete way for every sample instance as shown by Equation 12

Equation 12

$$f_1(k) = -\frac{h_1(k+1) - h_1(k)}{T_s} A_1 \quad [m^3/s]$$

with T_s being the sample interval (0.25s) and k denoting the specific sample instance.

If f_1 is computed without pre-filtering the sampled level signals, measurement noise in the level signals results in extremely noisy computed values for f_1. This is due to the noise amplifying effect of taking the derivative of the noisy level signal. Before f_1 was computed the sampled level signals were filtered using a first order digital Butterworth filter. The filter cut-off frequency was chosen to be 0.24Hz, cutting out any noise energy above the anti-aliasing filter bandwidth.

$K_1(u_1(k))$ was then computed for every sample instance as indicated below, using Equation 13.

Equation 13

$$K_1(u_1(k)) = \frac{f_1(k)}{\sqrt{(h_1(k) + h_{T_1})}}$$

Figure 6 shows the computed $K_1(u_1(k))$ values for all of the different valve position experiments, for the complete duration of each experiment.
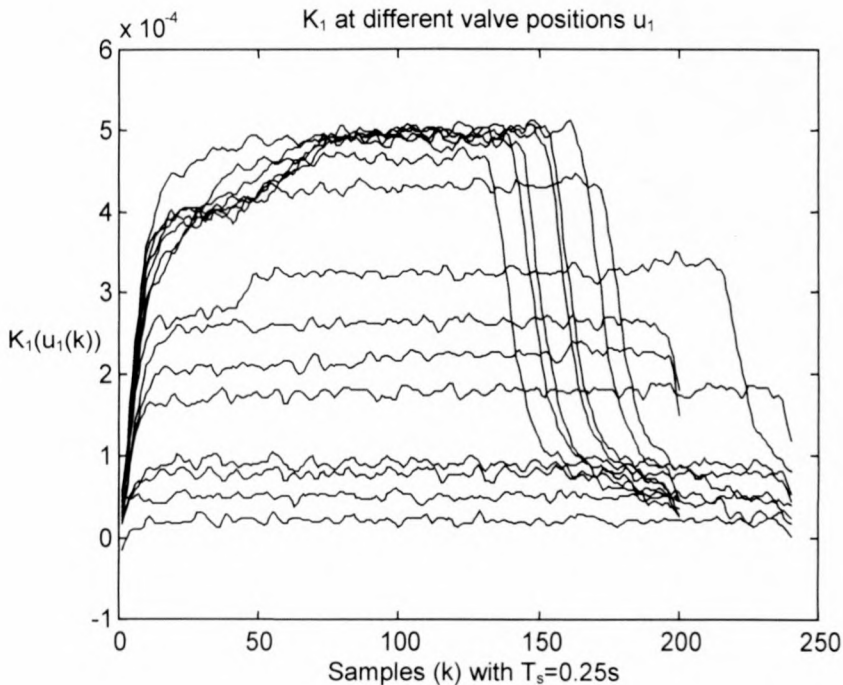
Figure 6: K_1 for different valve position experiments on valve v_1

The fact that $K_1(u_1(k))$ does reach a constant value during every experiment for every valve positions confirms the effect of Toricelli's law in the lower tank flow data

and therefore the validity of Equation 3 and Equation 4 describing the system. As illustrated in Figure 6, K_1 was obtained for every valve position by taking the mean of the values of $K_1(u_1(k))$ from samples 50 to 150 for the specific valve position experiment. Finally a continuous function $K_1(u_1)$ was obtained by fitting a seventh order polynomial trough the computed K_1 values as shown in Figure 7.
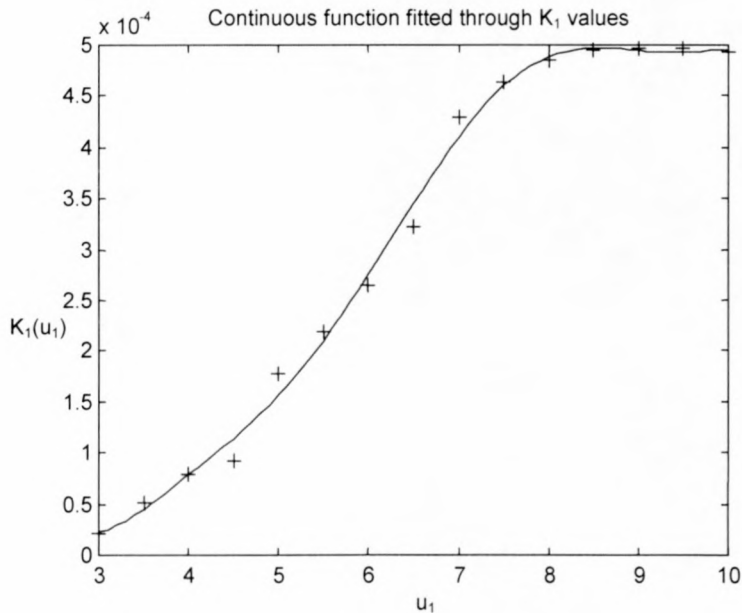
Figure 7: Continuous function $K_1(u_1)$

The coefficients of the resulting polynomial function are listed in Table 4.

Polynomial coefficient	Value
A7	-5.2168e-8
A6	2.3404e-6
A5	-4.3534e-5
A4	4.3418e-4
A3	-2.5061e-3
A2	8.3877e-3
A1	-1.5042e-2
A0	1.1139e-2

Table 4: $K_1(u_1)$ continuous function coefficients

The implementation of the polynomial function is presented in Appendix D in the model block *Kloflo*.

3.3.2 Computing K₂(u₂):

Valve v_2 was opened to a specific position by applying a valve command signal u_2. The measured levels l_1 and l_2 were sampled while the contents of the upper tank emptied into the lower tank. This was done for each position of valve v_2 shown in Table 5 below.

Valve position (u₂) [Volt]
5.3
5.6
6
6.5
7
7.5
8
8.5
9
9.5
10

Table 5: Valve positions for valve gain experiments - valve v₁

The level signal samples were converted from volts (l_1, l_2) to meters (h_1, h_2) using the calibrated relationships from Appendix A and f_2 was computed using Equation 14

Equation 14

$$f_2 = \frac{dh_1}{dt} A_1 \ \ [\text{m}^3/\text{s}]$$

This was done in a discrete way for every sample instance as shown by Equation 15

Equation 15

$$f_2(k) = \frac{h_1(k+1) - h_1(k)}{T_s} A_1 \ \ [\text{m3/s}]$$

with T_s being the sample interval (0.25s) and k denoting the specific sample instance.

Measurement noise in the level signals results in extremely noisy computed values for f_2 if f_2 is computed without pre-filtering the sampled level signals. This is due to the noise amplifying effect of taking the derivative of the noisy level signal. Before f_2 was computed the sampled level signals were therefore filtered using a first order digital Butterworth filter. The filter cut-off frequency was chosen to be 0.24Hz, cutting out any noise energy above the anti-aliasing filter bandwidth.

$K_2\big(u_2(k)\big)$ was then computed for every sample instance as indicated below, using Equation 16.

Equation 16

$$K_2\big(u_2(k)\big) = \frac{f_2(k)}{\sqrt{\big(h_2(k)+h_{T_2}\big)-\big(h_1(k)+h_{T_1}\big)}}$$

Figure 8 shows the computed $K_2\big(u_2(k)\big)$ values for all of the different valve position experiments, for the complete duration of each experiment
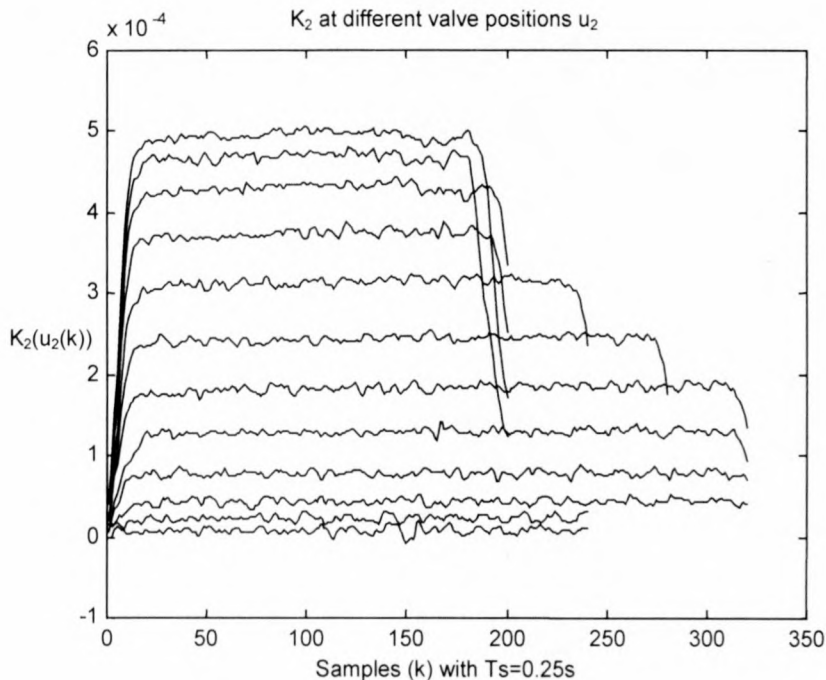
Figure 8: K_2 for different valve position experiments on valve v_2

The fact that $K_2\big(u_2(k)\big)$ reaches a constant value during every experiment for every valve position confirms the effect of Toricelli's law in the upper tank flow data and

therefore also confirms the validity of Equation 3 and Equation 4 to describe the system. From Figure 8, a value for $K_2(u_2)$ at every valve position was obtained by taking the mean of samples 50 to 150 of $K_2(u_2(k))$ for every valve position. Finally a continuous function was obtained by fitting a fourth order polynomial through the computed $K_2(u_2)$ values as shown in Figure 9.
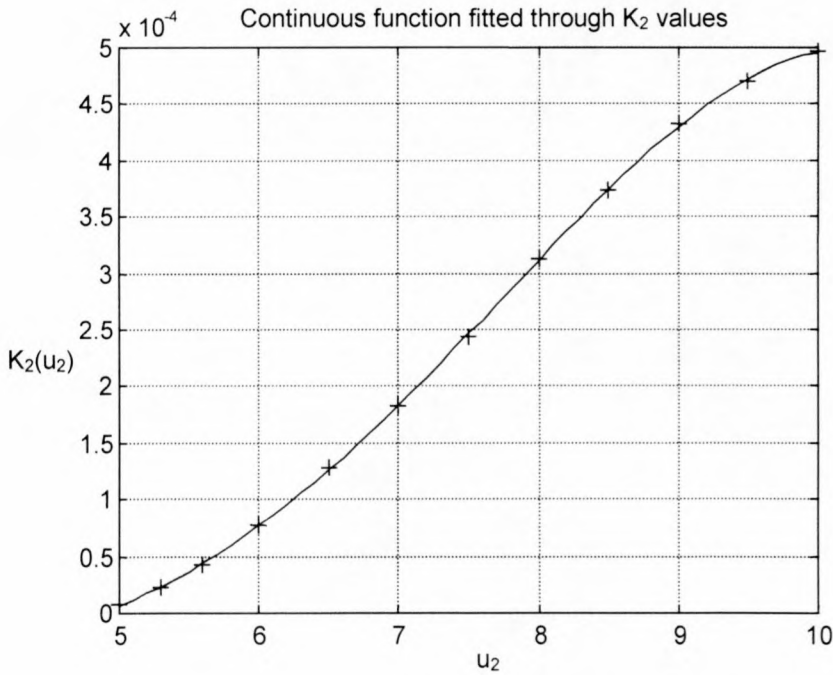
Figure 9: Continuous function $K_2(u_2)$

The coefficients of the resulting polynomial function are listed in Table 6 below.

Polynomial coefficient	Value
A4	-9.1209e-7
A3	2.2697e-5
A2	-1.9564e-4
A1	7.6884e-4
A0	-1.204e-3

Table 6: $K_2(u_2)$ continuous function coefficients

The implementation of the polynomial function is presented in Appendix D in the model block *KHHHFH*.

3.4 Time constants

To determine the time constants for the valves, experiments were performed, whereby a square wave was applied to the respective valves and the level responses recorded for a period of time equal to at least two cycles of the input signal. The frequency of the input square waves was chosen so that the period is at least twice the longest expected time constant. The different time constants of the model were then estimated using a Marquardt algorithm to minimize the sum square error between the model flow rate responses and the flow rates computed from the measured data. Figure 10 shows the model structure used to tune the time constants. It has the non-linear valve gain in series with one of the two time constants.
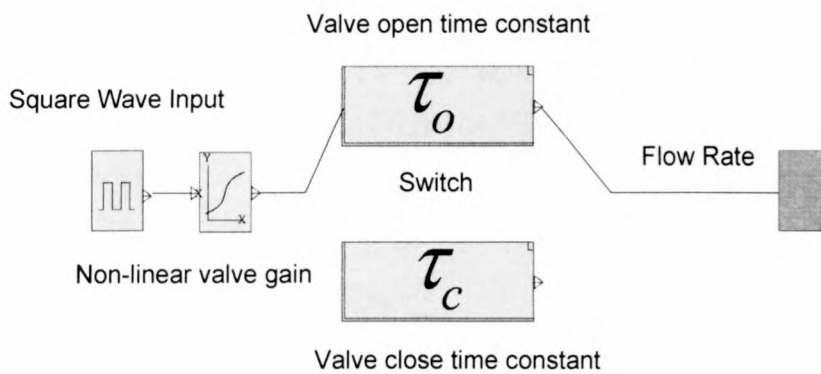
Figure 10: Valve time constants

3.4.1 Computing τ_{1_o}, τ_{1_c} :

The square wave input signal and the computed flow response of the valve is shown in Figure 4. The tuned values of the time constants is shown in Table 7 and the model response is compared to the measured response in Figure 11 below.

Time Constant	Value [s]
τ_{1_o}	1.53
τ_{1_c}	1.11

24

Table 7: Valve v_1 time constants

Valve v_1 Time Constant Tuning
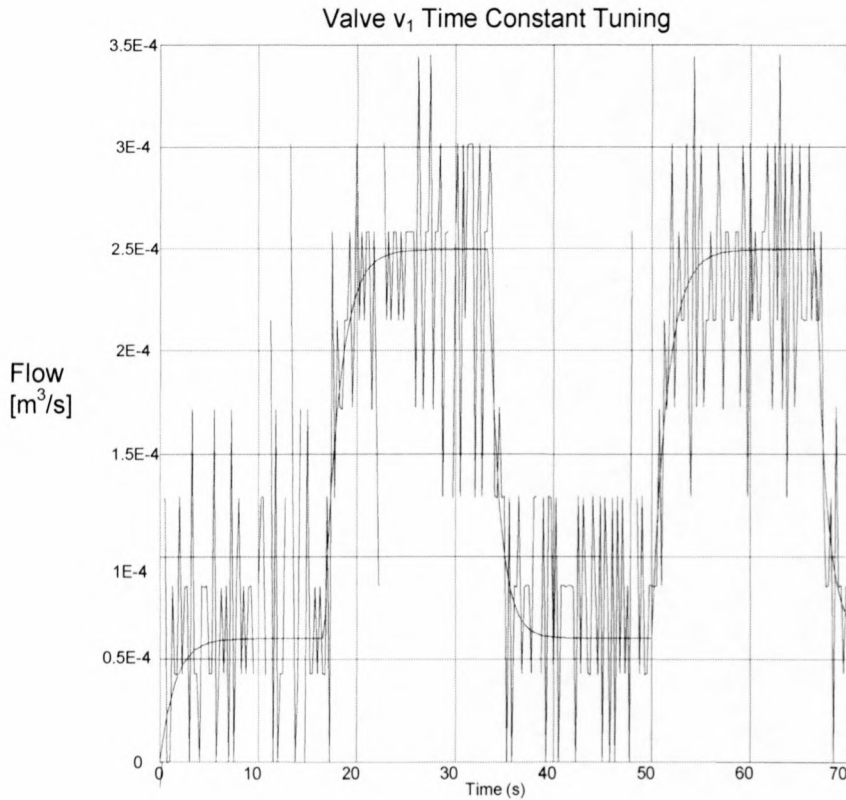
Figure 11: Valve v_1 time constant tuning

3.4.2 Computing τ_{2_o}, τ_{2_c} :

The square wave input signal and the computed flow response of the valve is shown in Figure 3. The tuned values of the time constants are shown in Table 8 and the model response is compared to the measured response in Figure 12 below.

Time Constant	*Value [s]*
τ_{2_o}	0.67
τ_{2_c}	1.25

Table 8: Valve v_2 time constants

25
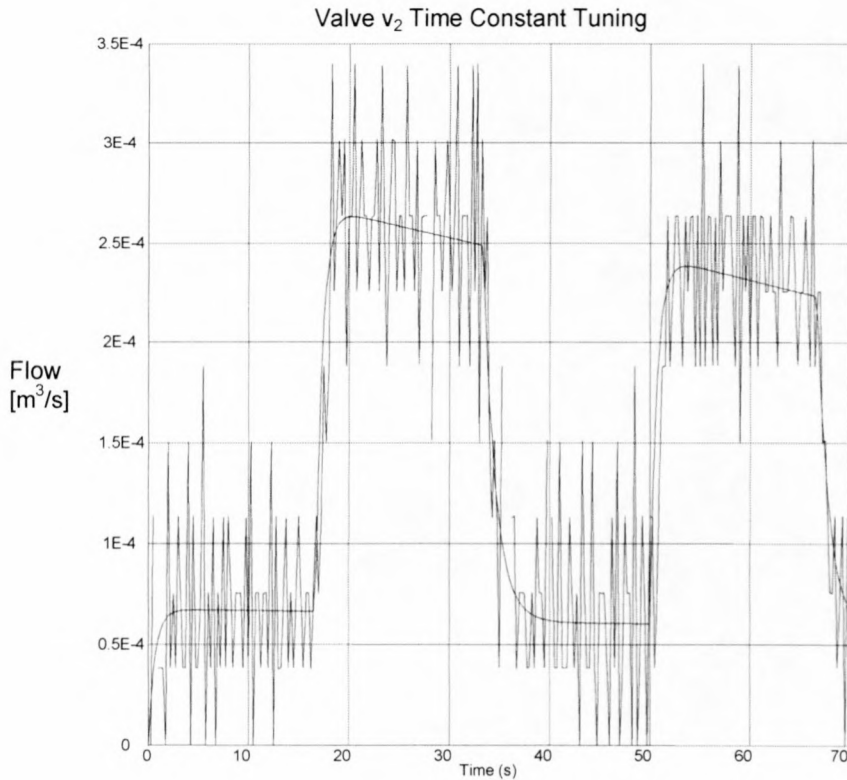
Figure 12: Valve v_2 time constant tuning

3.5 Valve hysteresis

Hysteresis was identified and a first estimate for each valve obtained using the methods described in Appendix C. The rough measurements were then optimised to a final hysteresis value for each valve.

3.5.1 Measuring hysteresis:

To get the first hysteresis estimates for the two valves the components of the flow system was assumed to be as shown in Figure 13.
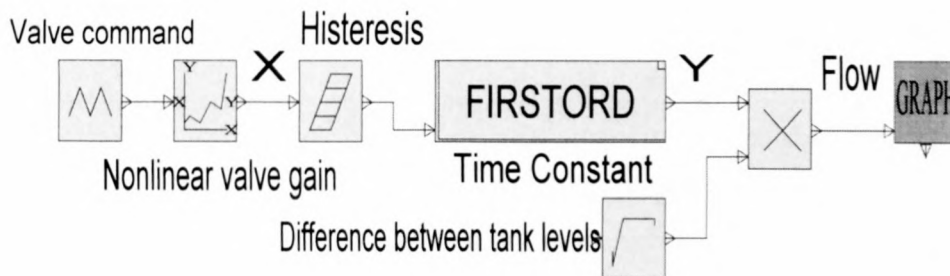
Figure 13: Flow rate model

A triangular signal of a low frequency (with a period much longer than the system time constant) was applied as a valve command input signal and the level response measured. The sampled level response was first order digitally filtered with a cut-off frequency equal to that of the anti-aliasing filter. This was done to eliminate any frequency components in the sampled signal above the anti-aliasing filter cut-off frequency. The flow rate and signals X and Y were computed from the filtered level response as indicated in Figure 13. Signals X and Y were plotted as a X-Y plot as shown in Figure 14. The same was done for a triangular input signal of a different frequency as shown in Figure 15. For each X-Y plot the resulting gap was measured in X-axis units and indicated on the plot. The amount of hysteresis was solved for from Equation 61 and Equation 62. The X-Y plots for the two valve experiments and the resulting hysteresis estimates are shown below.

3.5.1.1 Valve v_1:
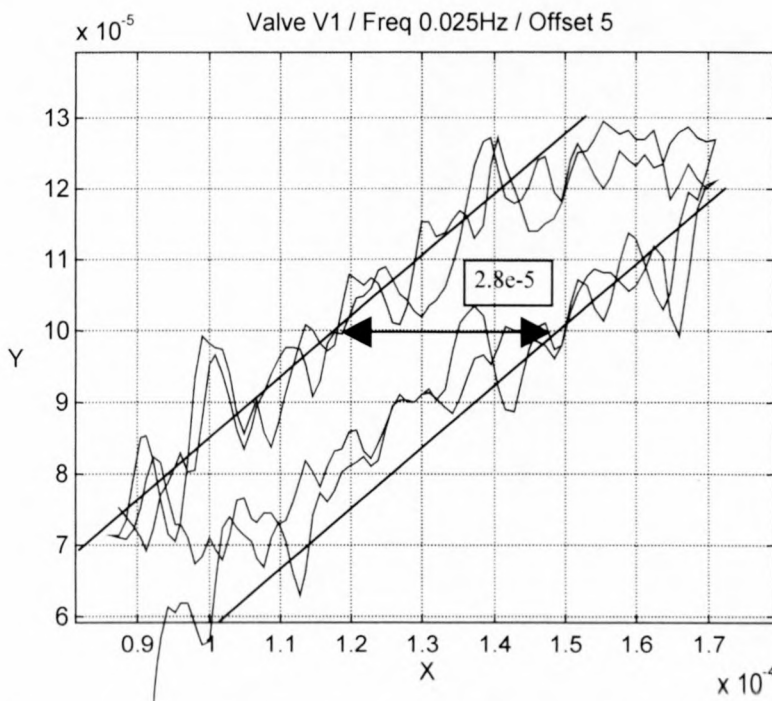
Figure 14: Valve v_1 hysteresis measurement – X-Y Plot – Frequency 1
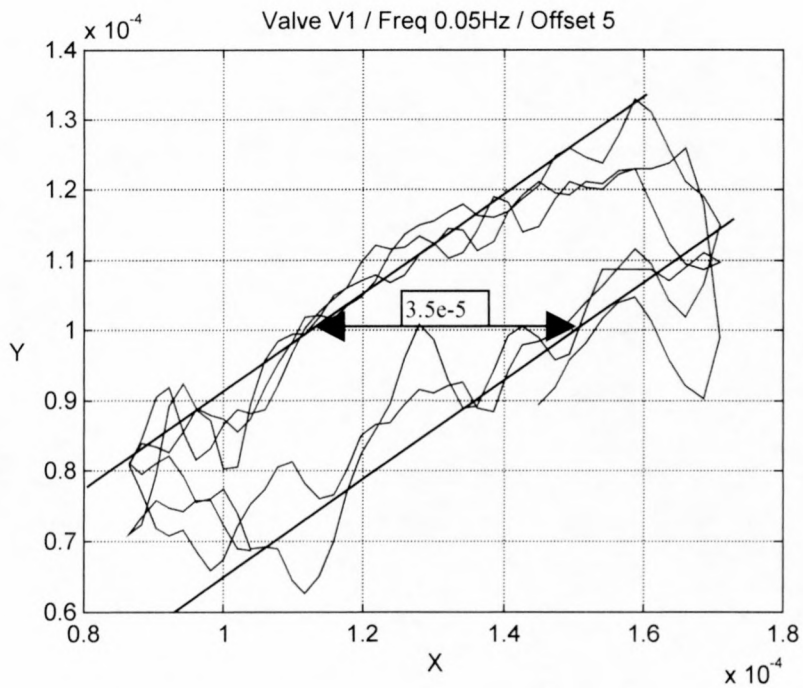
Figure 15: Valve v_1 hysteresis measurement – X-Y Plot – Frequency 2

Equations to solve from Figure 14 and Figure 15:

$$2.8e-5 = \Delta u + y$$
$$3.5e-5 = \Delta u + 2y$$

$$\Rightarrow \Delta u = 2.1e-5$$

where Δu is the portion of the gap due to hysteresis and y is the frequency dependant portion of the gap due to the time constant as manifested in Figure 14.

3.5.1.2 Valve v₂:
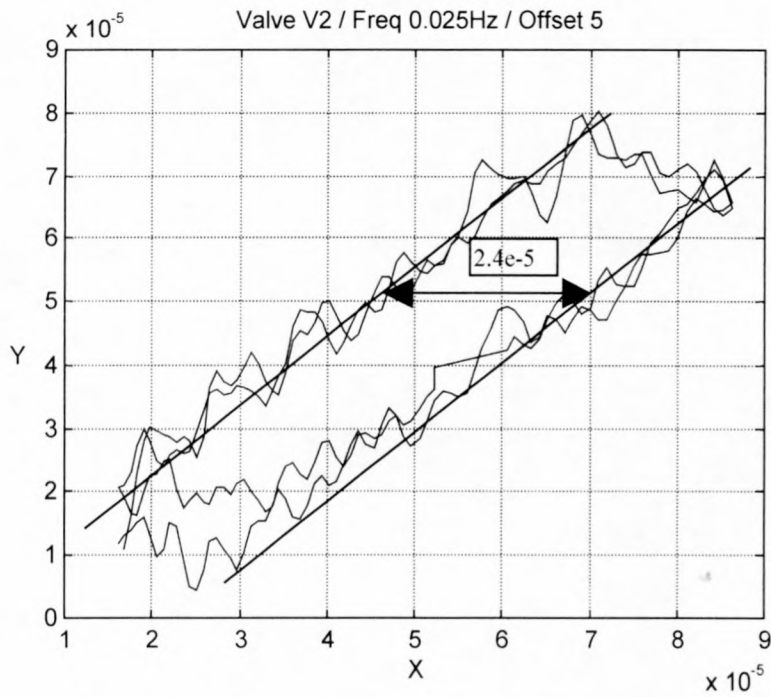
Figure 16: Valve v_2 hysteresis measurement – X-Y Plot – Frequency 1
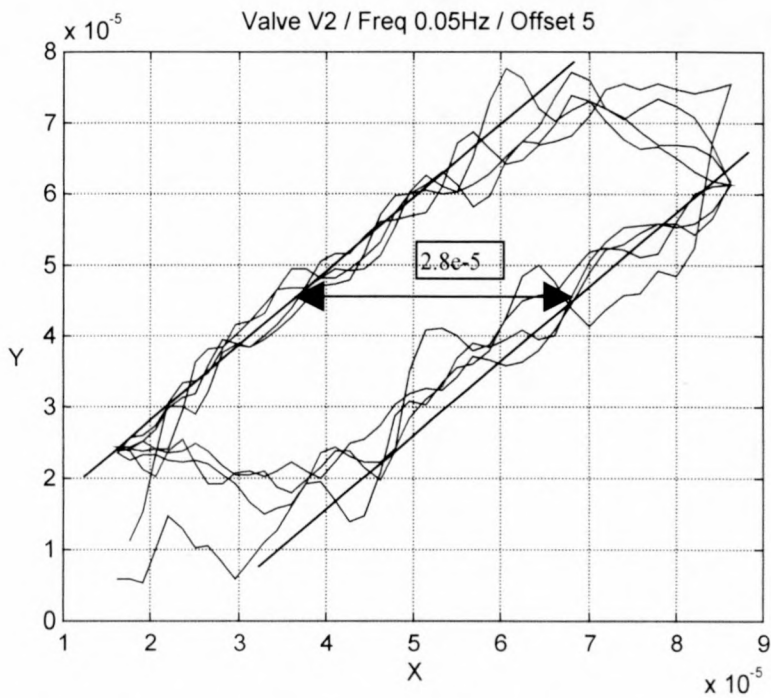
Figure 17: Valve v_2 hysteresis measurement – X-Y Plot – Frequency 2

Equations to solve from Figure 16 and Figure 17:

$$2.4e-5 = \Delta u + y$$
$$2.8e-5 = \Delta u + 2y$$

$$\Rightarrow \Delta u = 2e-5$$

where Δu is the portion of the gap due to hysteresis and y is the frequency dependant portion of the gap due to the time constant as manifested in Figure 16.

3.5.2 Optimising the measurements:

The hysteresis measurements shown above prove that the system contains a frequency independent non-linearity with a X-Y plot similar to the commonly known hysteresis. Due to the noise in the experimental data the exact form and value of the hysteresis present in the system is unknown. The simulation model proposed for the pilot plant assumes that the non-linearity present in the system is hysteresis. With this assumption and with all the other model parameters determined, the model was fit to a few experimental data sets to determine the amount of hysteresis per valve.

Four triangular valve command input signals with different offsets were applied to four instances of the model as shown in Figure 18, comparing the outputs with measured plant response data from files. The frequencies of the input signals were chosen to be low enough to allow for two cycles in the time the tank levels drop from full to empty. The squared errors of a selection of the four cases were added together and the sum minimized over the duration of the input signals by tuning the hysteresis parameter of the model instances. The model parameter was scanned through a range of values around the rough estimate obtained from the hysteresis measurements described above, to find the optimum value that minimizes the sum squared error. The results of this optimisation process for the two valves are described below.

3.5.2.1 Valve v_1:

From the data captured for valve v_1 only the data set with input signal offset 5 proved fit for use in the optimisation of the valve v_1 hysteresis parameter. The other three data sets, if taken into account during optimisation, would result in a hysteresis value that would compensate for errors not due to hysteresis. The simulation set-up that was used is shown in Figure 18.
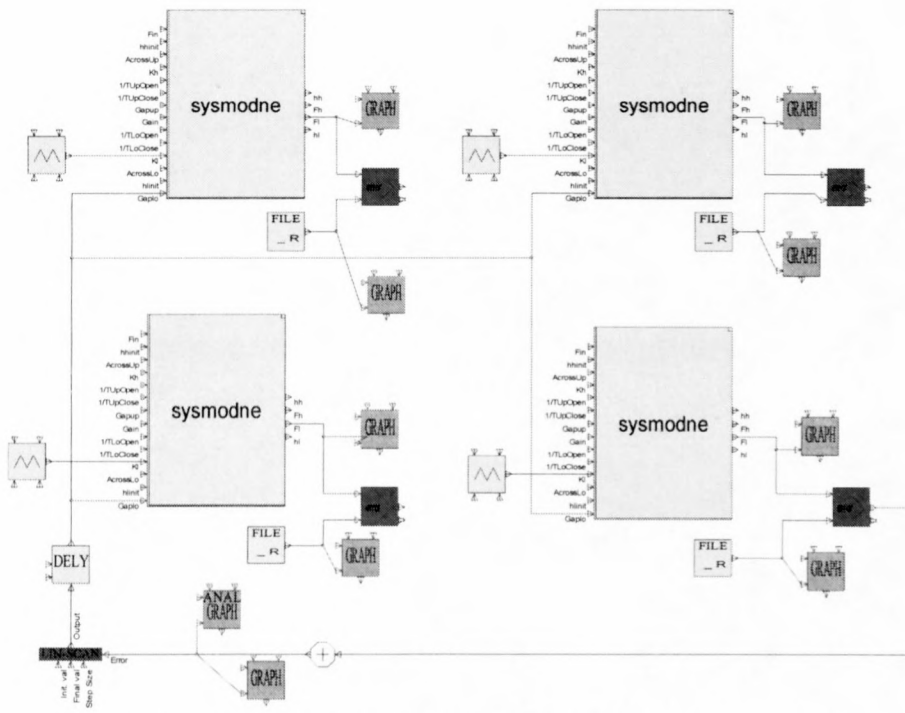
Figure 18: SIMuWIN diagram for valve v_1 hysteresis tuning

The hysteresis parameter, defined in SIMuWIN as $\frac{1}{2}\Delta u$, was scanned over the range 0.5e-5 to 1.5e-5 with steps of 0.1e-5. For every hysteresis value, the sum of the squared error over the duration of the input signal, is presented in Figure 19.
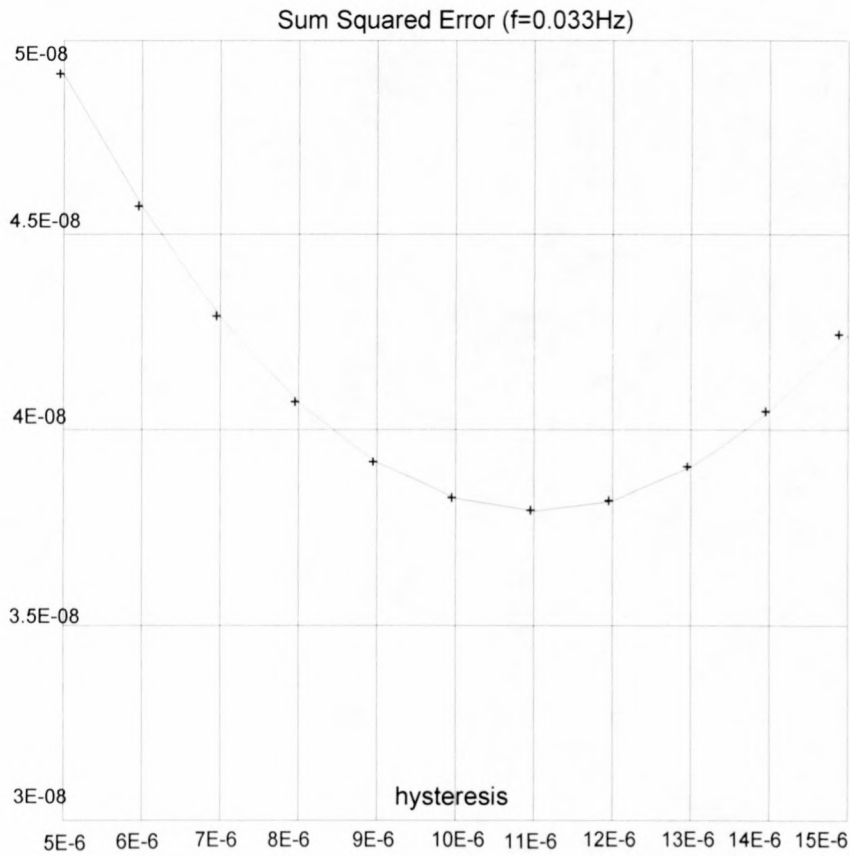
Figure 19: Valve v_1 error function vs. hysteresis values

The optimum hysteresis value that produced the best fit as seen from Figure 19 is

1.1e-5 according to the SIMuWIN definition ($\frac{1}{2}\Delta u$). The optimum amount of

hysteresis (Δu) is therefore 2.2e-5.

The resulting model fit to all four data sets using this optimum hysteresis value is shown in Figure 20 and in Figure 21. The following input signals were used in each of the two figures: amplitude 1; offsets 4,5,6,7; frequency 0.033Hz.
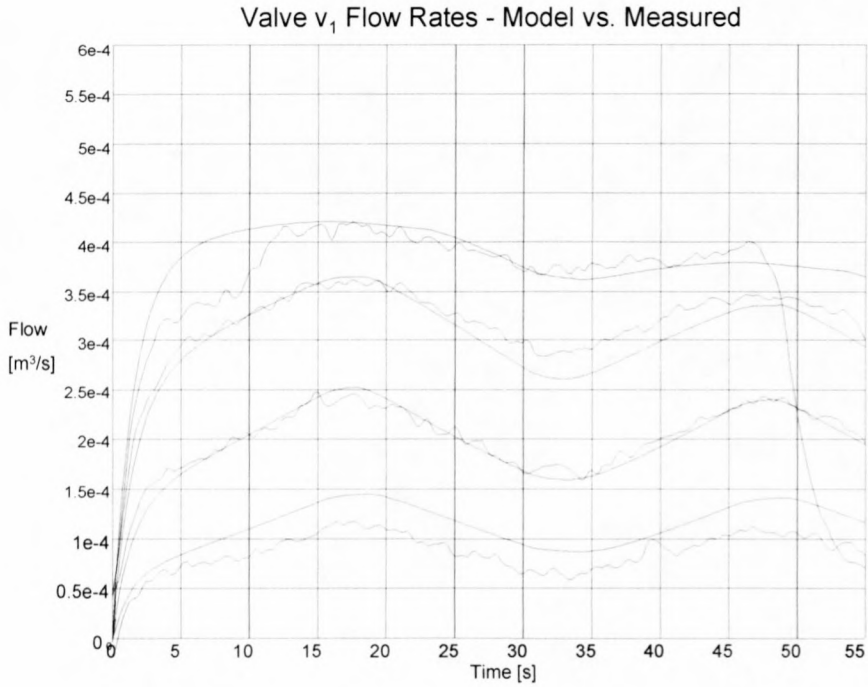
Figure 20: Valve v_1 flow rate – model vs. measured
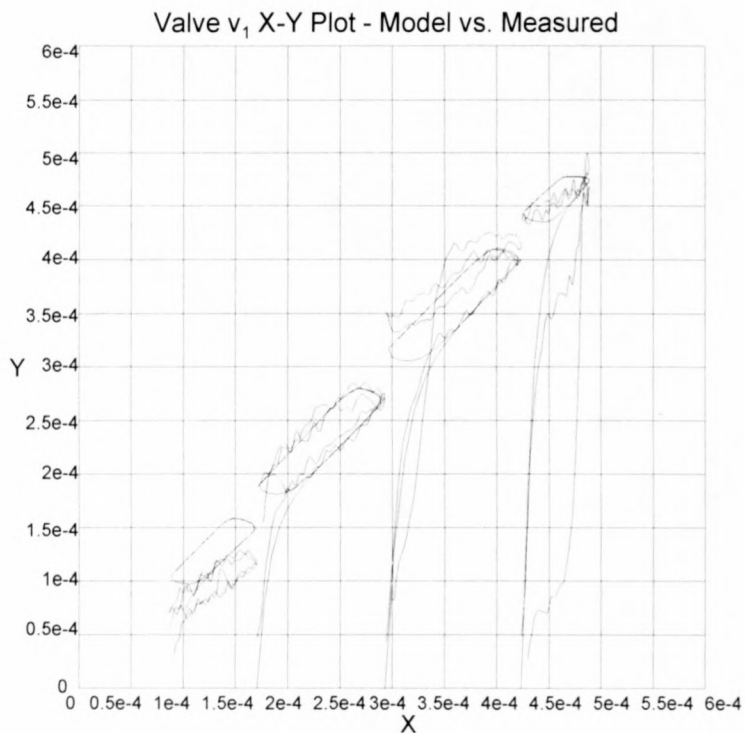
Figure 21: Valve v_1 X-Y plot – model vs. measured

3.5.2.2 Valve v_2:

In the hysteresis optimisation for valve v_2 the sum of the squared errors of all four data sets were minimised. This can be seen from the simulation set-up in Figure 22.
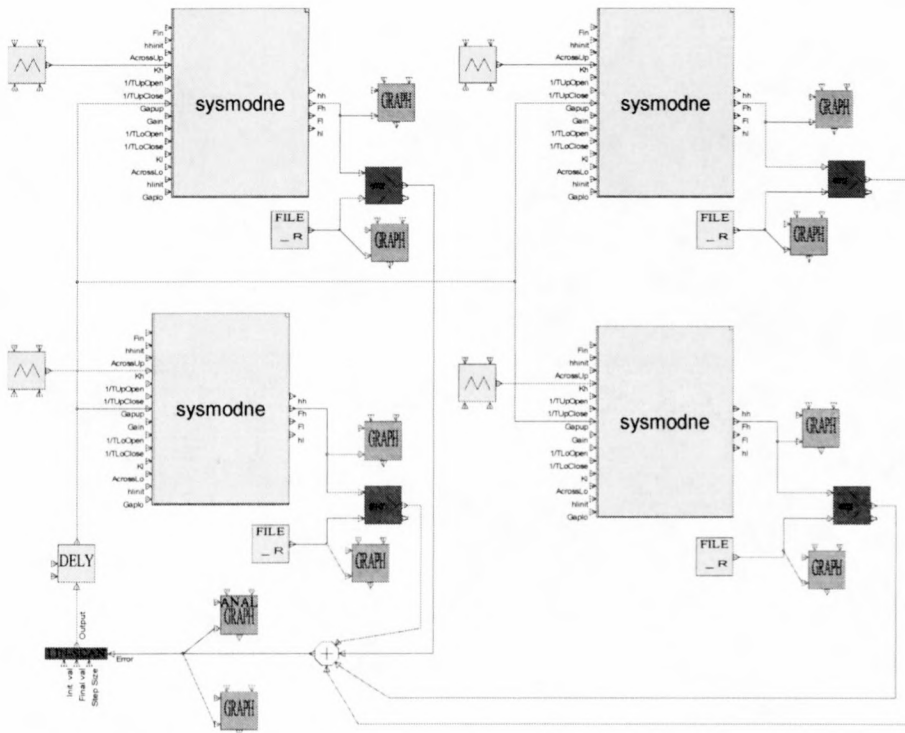
Figure 22: SIMuWIN diagram for valve v_2 hysteresis tuning

The hysteresis parameter was scanned over the range 0.5e-5 to 1.5e-5 with steps of 0.1e-5. The sum of the squared error for every value is presented in Figure 23.
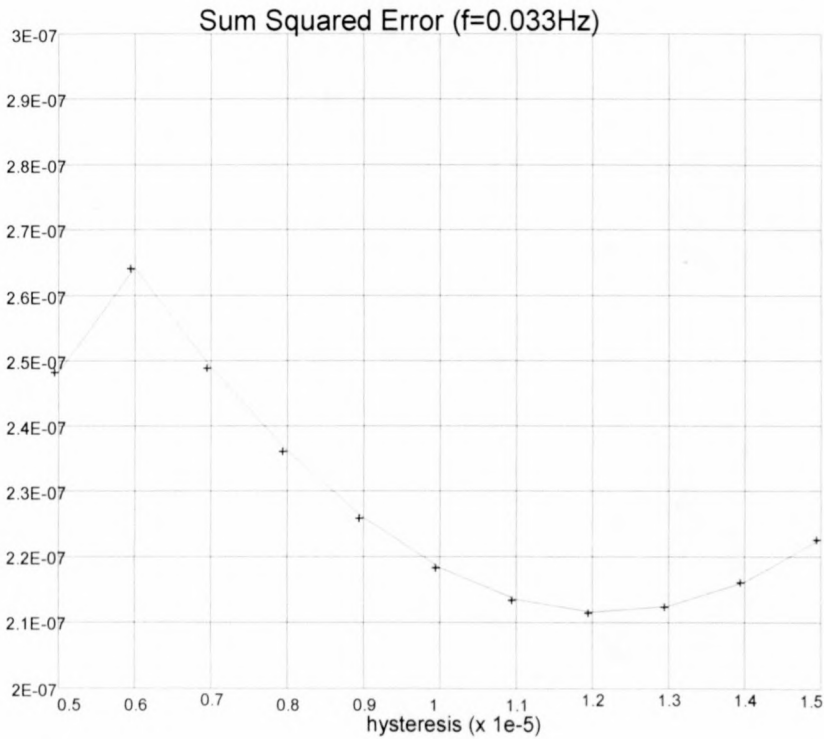
Figure 23: Valve v_2 error function vs. hysteresis

The optimum hysteresis value that produced the best fit as seen from Figure 23 is 1.2e-5 according to the SIMuWIN definition ($\frac{1}{2}\Delta u$). The optimum amount of hysteresis (Δu) is therefore 2.4e-5.

The resulting model fit to all four data sets is shown in Figure 24 and in Figure 25. The following input signals were used: amplitude 1; offsets 5,6,7,8; frequency 0.033Hz.
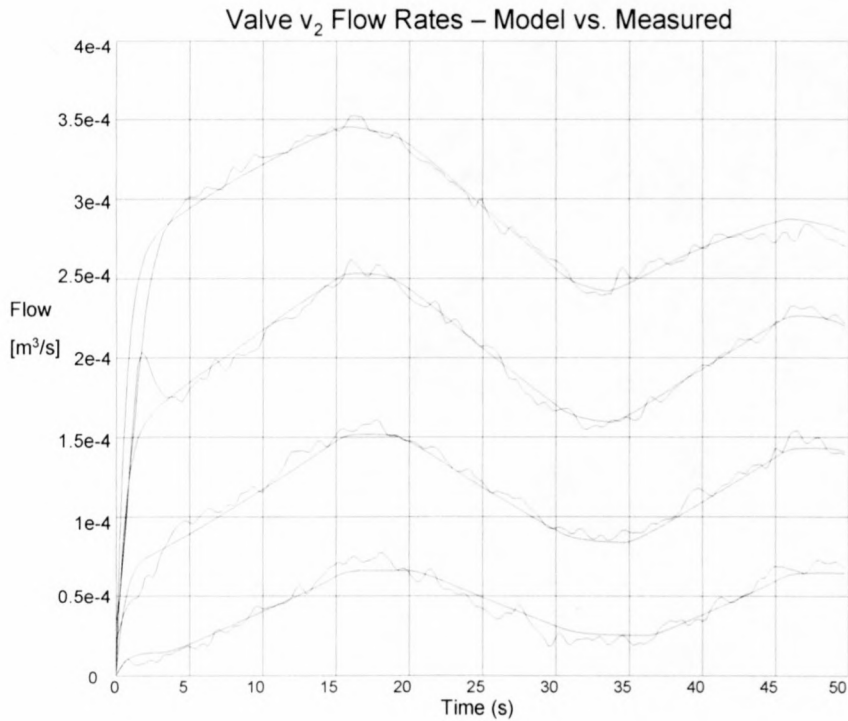
Figure 24: Valve v_2 flow rates – model vs. measured
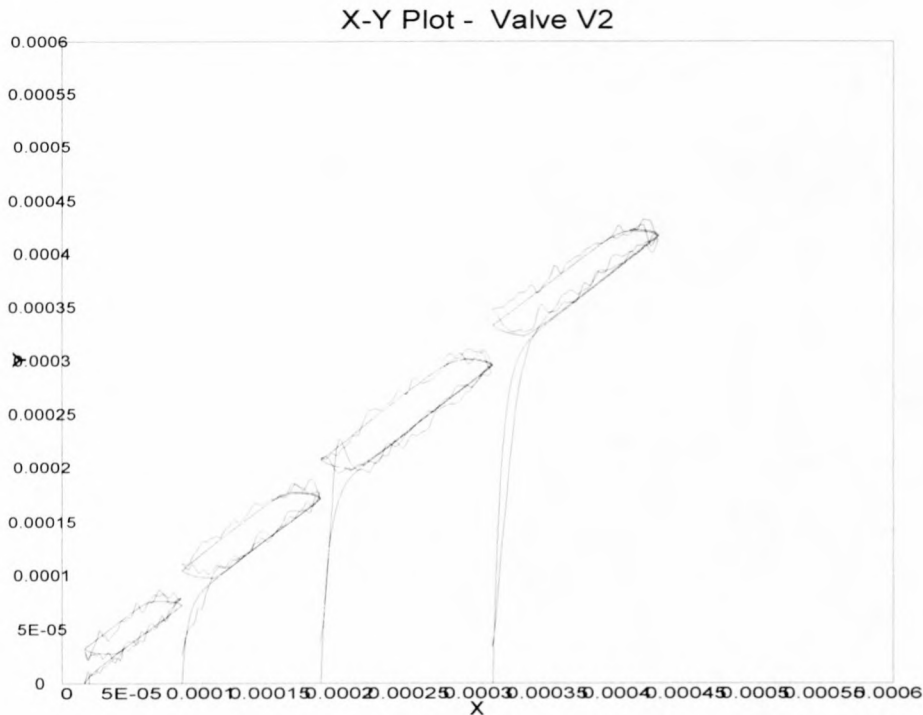
Figure 25: Valve v_2 X-Y plot – model vs. measured

This concluded the development of the simulation model with all model parameters determined.

3.6 SIMuWIN Implementation

The model described in this chapter was implemented in SIMuWIN as a simulation model of the cascaded flow process. SIMuWIN was then used as a simulation environment for the development and testing of a control strategy for the cascade flow system. The block diagrams and parameters of the SIMuWIN implementation of the simulation model are presented in Appendix D.

3.7 Model evaluation

This simulation model covers the full range of valve inputs and tank levels as presented in Table 2. The resulting model was evaluated using a few test signals. This evaluation is presented in Appendix E.

3.8 Conclusions

A simulation model of the pilot plant was developed in this chapter through a fundamental analysis of the process and the identification of gain functions, time

constants and valve hysteresis. Having obtained a complete simulation model of the pilot plant, the next step was to develop a suitable control strategy. Chapter 4 considers a range of possible control techniques.

Chapter 4

Control Technologies

A wealth of control theories and techniques are available today to address a wide range of control problems. Selecting the appropriate technique for a specific problem requires an understanding of the performance criteria to be achieved as well the spectrum of available techniques. This chapter briefly considers control criteria and a range of available control techniques.

4.1 Criteria for successful control

Performance	How accurately can the control objectives be met by the considered technology?
Cost	Initial costs; Controller lifetime; Maintenance costs; Repair and replacement costs; Total cost of ownership
Robustness	i.r.o operating point changes; i.r.o operating conditions such as plant environment and noise levels
Maintainability	Ease of maintenance; Frequency of maintenance
Transparency	Are the control actions and control performance transparent, easy to monitor, understand and evaluate?
Autonomy	How much interaction is needed by the operator/technician/engineer in order to consistently achieve the control objectives?
User friendliness	Are operator interactions with the controller easy, intuitive and a pleasant experience?

Table 9: Criteria for successful control

Table 9 presents some criteria for a successful control system that needs to be considered when an appropriate control technique is selected.

4.2 Range of available technologies

Before selecting an appropriate control technique it is necessary to qualitatively consider the range of available techniques.

4.2.1 Apparent Intelligent Techniques

In general, these techniques have a high total cost of ownership due to high complexity and specialised skills required for design and maintenance.

4.2.1.1 Expert systems/State Machines/ Sequence tables/Decision Trees

This group of techniques has the ability to switch to or select a controller state or output, or a sequence of controller states or outputs, based on a combination of the current and/or historical inputs, events, states and/or conditions. They are usually more suitable for supervisory control and control of discrete systems than for stabilisation control loops in continuous processes.

4.2.1.2 Neural Networks

The application of neural networks in closed loop control requires specialised skills and is more complex than most classical control techniques. It is also supported by complex theory to guarantee behaviour such as stability. A neural network needs to be trained on data, which makes it dependant on the availability and the integrity of the available data.

4.2.1.3 Fuzzy Logic

Fuzzy Logic is well suited for processes where controller design has to be based on expert knowledge and experience rather than on mathematical models. The technique has a strong non-linear ability, is very versatile and intuitive, and makes it easy to build in expert knowledge to the control strategy in the form of rules. There is however a lack of systematic methodologies for direct controller design and optimisation in cases where exact control performance specifications are required. It

might be necessary therefore to optimise initial rules and membership functions according to defined performance criteria, using formal optimisation techniques, to meet specific control objectives. The implementation of a fuzzy logic controller requires specialised computational functionality and will therefore be more complex to program than for instance a classical polynomial controller.

4.2.2 Switching and Sliding mode

Time optimal control is possible using Switching and Sliding mode control techniques. An exact mathematical model of the process is needed to compute the switching curve for time optimal behaviour. Non-linearities or model uncertainties will cause sub-optimal behaviour, which can be dealt with by over-switching to cross the optimal switching curve. Switching and Sliding mode techniques will usually lead to constant chattering or switching of control actuators like valves, which may shorten the lifespan of equipment.

4.2.3 Adaptive and Gain Scheduling

Adaptive and Gain Scheduling control techniques are useful to compensate for long-term performance changes in a control system. This can be due to effects like slow changes in dynamic characteristics of control valves over time and solids build-up in openings or valves connecting adjacent flotation units. It cannot however compensate for valve gain non-linearities or hydrodynamic non-linearities due to the high frequency or short-term nature of the effect thereof on controller performance. Furthermore these techniques are usually more complex to design, implement and guarantee stability for, than fixed controller techniques.

4.2.4 Model Based Linear Control

Model Based Linear Control techniques are the standard in many industry operations today. This group of control techniques requires a linear plant model for controller design. Many direct controller synthesis techniques exist for the control system design engineer to choose from, which are supported by well-established basis of theory. Direct design of time domain control system performance specifications is possible using these techniques which range from PID to MPC available to suit degree of complexity of control problem at hand in a specific operational environment. Deterministic approaches are available for directly manipulating signal

levels in low noise or deterministic processes and stochastic approaches for directly manipulating signal density distributions in high noise or stochastic processes. Model Based Linear Control techniques will usually be able to provide 90% of the benefits in 90% of the control problems.

4.3 Complexity of the problem

The in-depth analysis of the level control problem and the design of the simulation model have shown how the complexity and controllability of level control problems totally depend on the position, size and dynamic properties of the valves and the dimensions of the tanks or containers used. In most cases, like in the case of the pilot plant used for this study, all aspects of the problem are well defined and of relatively low order and complexity. There is therefore a strong case to use PID control wherever possible from a cost, performance and maintainability perspective.

PID control is nearly an industry standard in relatively low order Single Input Single Output (SISO) control problems due to its simplicity, low cost of ownership and versatility as a control technique.

4.4 PID level control

From the beginning of level control in flotation plants, the pulp level in each flotation unit was controlled separately by an independent control loop. A measurement of the pulp level was used by the control loop to adjust or actuate the pulp discharge valve of the unit to maintain the desired level. PI controllers were implemented as the standard technology for these single unit control loops of which PID is an extension. This is still the case in many flotation plants today.

The single unit level control problem, as defined above, is a low order control problem. The order of the system dynamics depends on the form of the flotation unit, the valve used and the flow characteristics of the pulp and will seldom have higher than second order dominant dynamics. The low order nature of this control problem usually renders the complexity of a PID controller sufficient for acceptable level control.

PID controllers are described by three gain parameters each having a strong intuitive meaning in the way the controller achieves its goals. Due to the unique structure of PID controllers, rules exist for tuning the three design parameters of the controller to

obtain acceptable closed loop performance [21]. Tuning of a PID controller is therefore possible without an explicit model of the system dynamics. The advantage is that stable control loops can be obtained without expert knowledge of control system theory or explicit models of the system dynamics.

The next few chapters will show how PID control technology was used to meet the closed loop level control objectives for the pilot plant in an effective way.

4.4.1 Adjusted PID control law

In standard PID control the controller output is calculated at every time step as the weighted sum of the tracking error, its integral and its derivative at the particular time step.

The PID control law can be expressed in the z-domain as shown in Equation 17

Equation 17

$$u(z) = K_p \left(1 + \frac{T_s z}{T_I(z-1)} + \frac{T_D(z-1)}{T_s z} \right) e(z)$$

$$e(z) = r(z) - y(z)$$

where K_p, T_D and T_I are the three design parameters, together with sample period T_s.

Consider a scenario where the plant model is as shown in Equation 18 and the control law as presented in Equation 19:

Equation 18

$$\frac{Y[z]}{U[z]} = \frac{b_0 z}{z + a_1}$$

Equation 19

$$\frac{U[z]}{E[z]} = \left(K_p + \frac{K_i z}{(z-1)} + \frac{K_d(z-1)}{z} \right)$$

$$= \frac{(K_p + K_i + K_d)z^2 + (-K_p - 2K_d)z + K_d}{z^2 - z}$$

The resulting closed loop (CL) transfer function is shown in Equation 20.

Equation 20

$$\frac{Y[z]}{R[z]} = \frac{b_0 z \left((K_p + K_i + K + _d)z^2 + (-K_p - 2K_d)z + K_d \right)}{(z^2 - z)(z + a_1) + b_0 z \left((K_p + K_i + K + _d)z^2 + (-K_p - 2K_d)z + K_d \right)}$$

From the CL transfer function the following can be concluded:

A desired first order CL response of the form $\frac{1+a}{z+a}$ can only be obtained by choosing $K_i, K_d = 0$ and K_p to place the pole at a, resulting in proportional control only which will not give good disturbance rejection and zero steady state error in the present of disturbances. It is not possible by any choice of K_i, K_d and K_P and for any chosen model order, to design for a specific first or second order CL response, apart for the proportional control only option mentioned above. Choosing the three design parameters to obtain the desired CL poles results in unwanted zeros that distort the desired CL response. This is a result of the structure of this particular PID control law. Directly designing for time domain specifications is therefore not possible and obtaining desired CL speed of response, reference tracking, disturbance rejection and steady state characteristics will have to be a case of approximation by tuning.

In this thesis a PID control of a slightly different form is proposed to enable the direct design of time domain specification using the pole assignment control design technique. This has the advantage of enabling the user to directly specify the controller in terms of specifications like rise time, settling and overshoot and have the controller redesigned instantly. This PID control law structure also lends itself to more advances strategies such as self-tuning.

The control strategy developed in this chapter must enable the control engineer to force specific time domain and other criteria by means of direct design and therefore PID control in its standard form is not an option. Changing the form of the PID control law slightly can however achieve this for a special plant model. The alternative PID control law below provides the designer with the necessary control over time domain response by filtering the reference and the feed back output signals with two different filters, placing the CL poles at the desired positions without resulting in unwanted CL zeros. This however requires a very specific plant model which proved to be applicable to the pilot plant level control problem and should be applicable in most flotation level control set-ups.

The plant model required for the alternative PID control law is shown in Equation 21

Equation 21

$$\frac{Y[z]}{U[z]} = \frac{b_1 z}{z^2 + a_1 z + a_2}$$

and the alternative PID control law in [22] in Equation 22.

Equation 22

$$U[z] = \frac{R[z](g_0 + g_1 + g_2)z^2 - (g_0 z^2 + g_1 z + g_2)Y[z]}{z^2 - z}$$

This alternative PID control law can be compared to the standard PID control law by the substitutions shown in Equation 23.

Equation 23

$$g_0 = \left(K_p + K_i + K_d\right)$$
$$g_1 = \left(-K_p - 2K_d\right)$$
$$g_2 = K_d$$

4.5 Pole assignment design

Pole assignment control design is a direct method of calculating controller parameters to achieve specified controller performance. It is presented in this thesis

because it is a standard way of designing PID and Polynomial control laws and is easily extended to more advanced strategies like self-tuning [22]. This design method assumes a linear plant model of the form shown in Equation 24.

Equation 24

$$y(z) = \frac{B}{A} u(z)$$
$$B = b_1 z^{n-1} + \ldots + b_n$$
$$A = z^n + a_1 z^{n-1} + \ldots + a_n$$

The control law parameters are then chosen to obtain desired CL polynomials A_{CL} and B_{CL} so the CL system can be written as shown in Equation 25.

Equation 25

$$y(z) = \frac{B_{CL}}{A_{CL}} u(z)$$

In standard PID control the B_{CL} polynomial cannot be specified and is automatically fixed by the choice of A_{CL}. This is an inherent property of the standard PID control law presented above and is because the control law does no independent filtering of the reference and feedback signals. In the case of general polynomial control B_{CL} can also be specified independently. This is a result of the structure of the control law, which makes it possible to filter the reference signal and the system output with different filters. This method can be easily automated and extended to adaptive strategies if necessary.

4.6 Conclusions

In this chapter a range of different control technologies were considered. A specific form of PID control was selected for the level control problem under discussion in this thesis and its advantages explained. Lastly the pole assignment design technique was introduced as a design technique suitable for the direct design of control laws to achieve specified CL performance criteria.

Chapter 5

Linear Models

This chapter considers the process of obtaining a linear discrete plant model, which can be used for linear controller design.

5.1 Model requirements

It is assumed that the controller must be implemented in discrete time using a digital computer, PLC or DCS; the model therefore must be a discrete time model suitable for digital controller design.

The order of the model must be as low as possible, capturing enough of the system dynamics to allow a complexity of control sufficient to achieve closed loop performance specifications.

The cost of obtaining the model must be weighed against the expected gains in controller performance.

5.2 Different approaches to linear modelling

5.2.1 Measuring the frequency response

This approach samples the frequency response of the system at a number of frequencies over the open loop system bandwidth of interest. At every frequency a sinusoid of suitable amplitude is injected at the input. The amplitude and phase of the output sinusoid is measured from which the gain and phase of the system frequency response at that particular frequency is computed. Having obtained the frequency response of the system a continuous time transfer function in the Laplace domain is fitted onto the frequency response using Bode plot rules. This continuous

time transfer function can then be discretized to obtain the discrete model. In a flotation plant it will be necessary to stop the normal operation of the plant because the frequency response needs to be measured in open loop conditions. Automation of the method will be difficult and manual application of the approach will be time consuming and costly.

5.2.2 Fundamental modelling

Here fundamental theory combined with the inherent physical and structural properties and specifications of the plant or process is used to deduce linear continuous time differential equations describing the open loop system dynamics. These can then be discretized to arrive at a suitable linear discrete time model. This is the method that was followed in Chapter 3 to derive an accurate simulation model of the pilot plant. The plant structure combined with fundamental theory will suggest the model structure and parameterisation. Model parameters will have to be measured and computed from open loop experiments. This approach therefore suffers from many of the same difficulties as the previous approach in terms of automation, plant operation shut-downs and time-consuming measurements.

5.2.3 Data driven system identification

These methods rely on input/output data to infer a model. In terms of model description the techniques can be classified as parametric or non-parametric. In terms of the process of arriving at the best model, the techniques can be divided into recursive and non-recursive (batch) techniques. The reliability of the models obtained from these methods is heavily dependent on the integrity of the data used. Reliable data will produce reliable models. In all of these methods the models obtained will capture the system dynamics in as much as the dynamics is represented in the data. For this reason, the choice of a suitable input signal or stimulus for generating the modelling data, is an important choice that will determine which dynamics of the system will be stimulated and will therefore be present in the data. Most of the non-parametric methods estimate the frequency response of the system by means of Fourier or Correlation techniques. Parametric methods estimate parameters for a suggested discrete model structure by minimising an error criterion. These methods are attractive in a flotation set-up because they directly provide linear model parameters, they can be applied during normal plant operation and can be automated easily. The important issue with parametric methods is choosing a

suitable model structure. If this is not done carefully the resulting model may be useless for the purposes of controller design. Recursive Parametric methods can be implemented on-line, which makes automatic controller tuning possible. Batch Parametric methods are very useful in selecting the best model structure for controller design. Once a reliable and representative input/output dataset has been collected the suitability of different model structures can be tested by means of Non-recursive (Batch) Parametric methods. A suitable model structure identified in this way should always be verified by a fundamental analysis of the system. A model structure obtained by Batch Parametric methods and validated by a fundamental analysis can then be safely used for controller design.

5.3 Fundamental considerations

In order to arrive at a suitable linear model for controller design, it is necessary to consider a few fundamental aspects of the cascaded flow process as shown again in Figure 26.
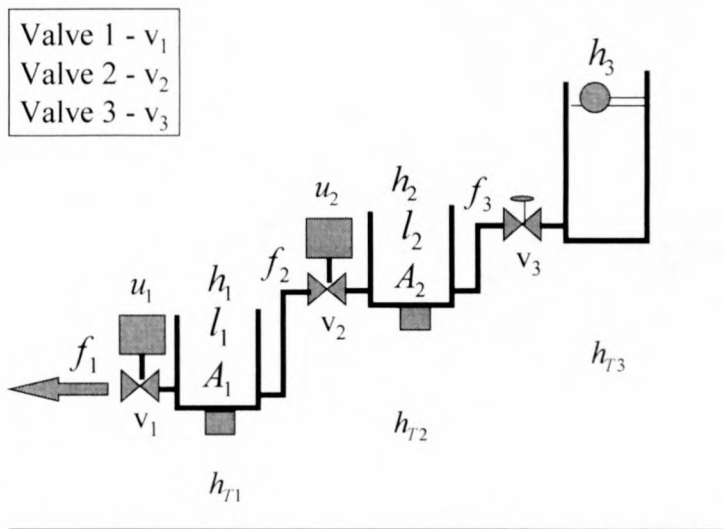
Figure 26: Cascaded flow process

5.3.1 Steady state scenario revisited

The flow system is said to be in a steady state when the volume flow rates into and out of each tank unit are equal resulting in no change in levels as shown in Equation 26.

Equation 26

$$f_1 = f_2 = f_3 = const$$
$$\frac{\partial h_1}{\partial t} = 0, \frac{\partial h_2}{\partial t} = 0$$

5.3.2 Dynamic scenario revisited

Level changes occur when volume flow rates deviate from the steady state scenario described in Equation 26. The situation can be described for the second tank unit by the following relationship:

Equation 27

$$A_2 \frac{\partial h_2}{\partial t} = \partial f_3 - \partial f_2$$

Equation 27 derives from the mass conservation principal. With the fluid or pulp density assumed to be constant it implies that the rate of increase of fluid volume inside a unit must equal the net volume flow rate of fluid into the unit. f_3, being the volume flow rate into the system, is assumed to be constant, equal to the steady state value and therefore $\partial f_3 = 0$. Any changes that occur in f_3 are ignored by the model and treated as disturbances to the system. Equation 27 can be rewritten in the Laplace domain as shown in Equation 28.

Equation 28

$$A_2 \partial h_2 [S] S = -\partial f_2 [S]$$

As seen in Chapter 3 Equation 4 and repeated here in Equation 29, a static relationship exists between the volume flow rate f_2, valve position u_2 and the fluid levels in the tanks on either side of the valve, h_1 and h_2.

Equation 29

$$f_2 = K_2(u_2)\sqrt{\left(h_2 + h_{T2}\right) - \left(h_1 + h_{T1}\right)}$$

A difference in the fluid levels causes a pressure differential to exist across the valve. The valve opening is related to the valve position. It provides a path between the absolute pressure on the one side of the valve and that on the other side. Given enough time, this will result in a steady volume flow f_2 through the valve, if u_2, h_1 and h_2 are to remain constant. The relationship is called static because it does not involve time as an independent variable and does not describe the transient behaviour of f_2 as a result of , for example, a step change in u_2.

Equation 29 is non-linear but can be linearized around set-point values of the three independent variables u_2, h_1 and h_2. This provides a linear equation, shown in Equation 30, that can predict small deviations in f_2 caused by small deviation in u_2, h_1 and h_2.

Equation 30

$$\partial f_2 = \partial f_{2_u} + \partial f_{2_H}$$
$$\partial f_{2_u} = k_1 \partial u_2 \qquad \text{where } H = (h_2 + h_{T2}) - (h_1 + h_{T1})$$
$$\partial f_{2_H} = k_2 \partial H$$

Equation 30 is a static relationship. The dynamic version can be written describing also the transient behaviour of f_2 for small step changes in u_2 as shown in Equation 31

Equation 31

$$\partial f_2[s] = \partial f_{2_u}[s] + \partial f_{2_H}[s]$$
$$\partial f_{2_u}[s] = k_1 \partial u_2[s] D_2[s]$$
$$\partial f_{2_H}[s] = k_2 \partial H[s]$$

where $D_2[s]$ is the unity DC gain Laplace transfer function from $\partial u_2[s]$ to $\partial f_{2_u}[s]$ representing the control valve dynamics. Combining Equation 28 and Equation 31 the dynamic scenario can be described by Equation 32.

Equation 32

$$A_2 \partial h_2[S]S = -k_1 \partial u_2[S]D_2[S] - k_2 \partial H[S]$$

5.3.3 Dynamic valve response

The ideal dynamic behaviour for a control valve would be rapid response with no oscillation, no overshoot, a linear valve gain and no other non-linear effects like hysteresis. Usually in level control loops, valve speed of response has little effect on the closed loop dynamics because it is usually quick compared to the overall closed loop time constants of the level control system. Referring to Equation 32, valve speed of response, $D[S]$, can usually be modelled as shown in Equation 33.

Equation 33

$$D[S] = \frac{1/T}{S + 1/T} e^{-STd}$$

In a system where the valve speed of response is of the same order of magnitude as the closed loop system time constants, the effect of the valve speed of response is to increase the model order by at least one, depending on the length of the valve delay. In a process in which the valve time constant is significant, it is important to check that the valve time constant is the same for both valve opening and valve closing actions. Especially under high load conditions the opening and closing time constants of the valve might differ, which adds to the dynamic non-linearity of the process. In such a case the maximum uncertainty must be determined and the average of the expected range of time constants taken. The maximum spread of opening and closing time constants would occur at maximum load and conversely, the minimum spread of opening and closing time constants would occur at minimum load.

5.3.4 Plant non-linearities

Non-linearities in the level response can be ascribed to a combination of valve non-linearities and the non-linear relationship between levels and flow rates. These non-linearities affect the flow rates as described by Equation 29 and the level response as described by Equation 27. Non-linearities present in the system will always be due to either non-linear component gains or due to structural imperfections inherent in the

system resulting in effects like hysteresis and dead band. It might be possible to compensate for mild gain non-linearities by using different controller setting for different gain regions. Pushing up loop gain, in other words, using stiff control loops, is the only way to compensate for structural non-linearities. This is not desirable in many applications, for example where instability or excessive noise is present. Structural non-linearities should be prevented as far as possible by ensuring the quality of the dynamic components in the control loops (like the control valves).

5.3.4.1 Effect of operating point changes

Levels

Level operating point changes have a direct effect on Equation 29 and affects the linearized Equation 30 by changing k_1 and k_2 as shown in Figure 27. Level set-point changes therefore have no effect on the order of the system model, but rather affect the system gains.

For a fixed value of u

Not on scale
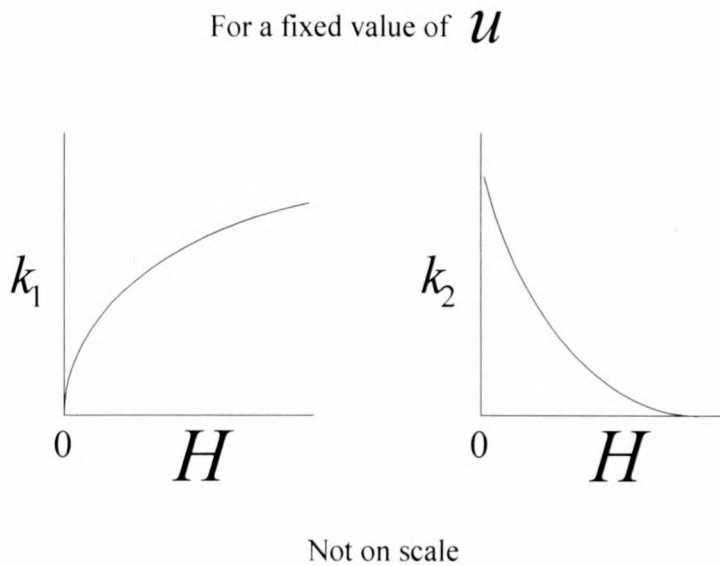
Figure 27: Effect of level operating point changes

Control valves

Valve operating point changes have a direct effect on Equation 29 due to the non-linear valve gain and affect the linearized Equation 30 by changing k_1 and k_2 as

shown in Figure 28. Valve set-point changes therefore have no effect on the order of the system model, but do affect the system gains.

For a fixed value of H

Not on scale
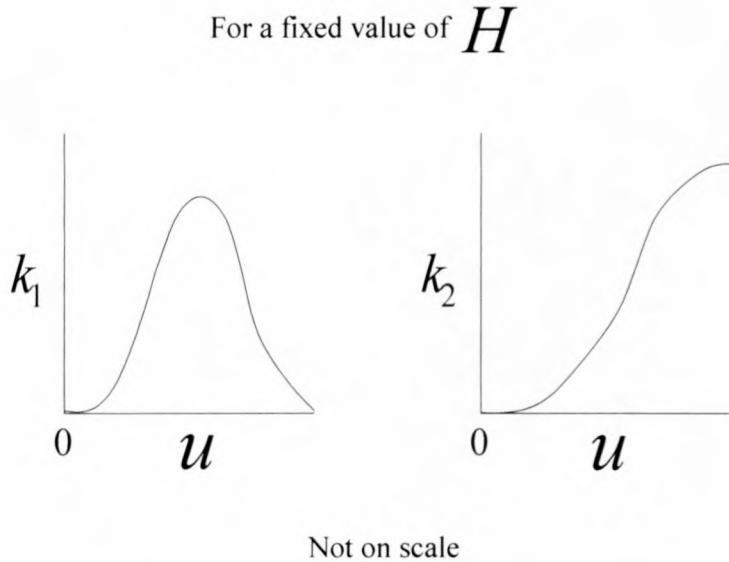
Figure 28: Effect of valve operating point changes

5.3.4.2 Unit cross-sectional area

Varying tank cross-sectional area will have a direct effect in Equation 27, resulting in changes to variables k_1 and k_2 in Equation 30 and Equation 31 as unit level operating points change. Varying unit cross-sectional area therefore affects the process gain and not the dynamic order of the system.

5.3.4.3 Pulp flow characteristics

Slurry, as opposed to water, is a Non-Newtonian fluid. Thus its viscosity is not constant, but changes with flow rate. Newtonian or Non-Newtonian, every fluid will have, at any point in time, a certain effective viscosity when flowing through a closed conduit. The fluid density, viscosity, flow rate and the conduit dimensions will result in a specific Reynolds number classifying the type of flow. A friction factor can then be computed for the specific flow situation, which is a direct function of the Reynolds number. $K_2(u_2)$ is then at any time equal to the friction factor times a constant relating the dimensions of the conduit. This implies that changes in the fluid properties like density, viscosity and operating conditions like temperature will have no effect on the order of the system model required. In other words, no dynamics are

added to the system. There is, however, an effect on the process gain and this results in changes in k_1 and k_2 shown in Equation 30 and Equation 31. The magnitude of the effect will have to be determined for a specific level control set-up.

5.3.4.4 Inlet and outlet positions

Inlet and outlet positions have no effect on model order, but determine the range over which the levels are controllable (limits of operation). If, for instance, h_2 drops below the unit outlet level, both levels h_1 and h_2 will become uncontrollable, thus destabilizing the level control system.

5.3.5 Number of units in cascade

Considering all the above-mentioned factors investigated, the number of units in cascade and the control valve dynamics are the only factors that introduce additional dynamics to the system and therefore add to the order of the open loops system model.

Consider a single unit flow system:

The cascaded two unit flow system shown in Figure 26, with the first (lower) unit detached or empty, is an example of such a flow system. Substituting $\partial H[S] = \partial h_2[S]$ in Equation 32 and assuming $D[S]$ to be negligible compared to the closed loop system time constant, Equation 32 can be rewritten to obtain the Laplace transfer function from $\partial u_2[S]$ to $\partial h_2[S]$ as shown in Equation 34.

Equation 34

$$\frac{\partial h_2[S]}{\partial u_2[S]} = \frac{-k_1}{A_2 S + k_2} = \frac{-\frac{k_1}{A_2}}{S + \frac{k_2}{A_2}}$$

Equation 34 shows that a single unit system model is of the first order. If the valve dynamics become significant it will be of the second order.

If the first (lower) tank unit is added in cascade, the two-unit system will be governed by two interdependent dynamic equations as shown in Equation 35, assuming the dynamics of valve v_1 also to be negligible.

Equation 35

$$A_2 \partial h_2[S]S = -k_1 \partial u_2[S] - k_2 \partial H_2[S]$$
$$A_1 \partial h_1[S]S = k_1 \partial u_2[S] + k_2 \partial H_2[S] - k_3 \partial u_1[S] - k_4 \partial H_1[S]$$

$$\partial H_2[S] = \partial h_2[S] - \partial h_1[S]; \quad \partial H_1[S] = \partial h_1[S]$$

From Equation 35 a transfer matrix $G[S]$ can be written for the interdependent two-unit system as shown in Equation 36 and Equation 37

Equation 36

$$\begin{bmatrix} \partial h_2[S] \\ \partial h_1[S] \end{bmatrix} = G[S] \begin{bmatrix} \partial u_2[S] \\ \partial u_1[S] \end{bmatrix}$$

$$G[S] = \begin{bmatrix} G_{22}[S] & G_{21}[S] \\ G_{12}[S] & G_{11}[S] \end{bmatrix}$$

where

Equation 37

$$G_{22}[S] = \frac{[k_1 k_2 - k_1(A_1 S + k_2 + k_4)]}{[(A_1 S + k_2 + k_4)(A_2 S + k_2) - k_2^2]}$$

$$G_{21}[S] = \frac{-k_2 k_3}{[(A_1 S + k_2 + k_4)(A_2 S + k_2) - k_2^2]}$$

$$G_{12}[S] = \frac{[k_1(A_2 S + k_2) - k_2 k_1]}{[(A_1 S + k_2 + k_4)(A_2 S + k_2) - k_2^2]}$$

$$G_{11}[S] = \frac{-k_3(A_2 S + k_2)}{[(A_1 S + k_2 + k_4)(A_2 S + k_2) - k_2^2]}$$

It can be seen from Equation 37 that the addition of another unit made the system second order. The terms $k_1 k_2, k_2 k_3$ and k_2^2 are negligible. Equation 37 can therefore be simplified without great loss of accuracy to Equation 38

Equation 38

$$G_{22}[S] = \frac{-k_1}{(A_2 S + k_2)}$$

$$G_{21}[S] = 0$$

$$G_{12}[S] = \frac{k_1}{(A_1 S + k_2 + k_4)}$$

$$G_{11}[S] = \frac{-k_3}{(A_1 S + k_2 + k_4)}$$

This simplification illustrates that the system retains a dominant first order dynamic response in the case where the valve dynamics are insignificant compared to the process time constant. It shows that the level of a tank unit is significantly affected by the control valves directly in front and after the tank unit. The effect of other control valves down stream and upstream in a multi-unit cascaded system is very small, decreasing the farther away a valve is from the level under investigation. This is important because it implies that first order linear discrete time models should be sufficient in many large-tank level control problems.

If the valve time constant becomes significant compared to the dominant time constant of the process, it will be important to include it in the model.

5.4 Data driven system identification

The Weighted Least Squares technique is a batch technique used to deduce a linear discrete time model directly from a representative dataset. Performing this technique entails obtaining data, selecting the best model structure and then applying the technique to obtain the estimated model parameters.

5.4.1 Getting reliable data

5.4.1.1 Choice of Sample Frequency

Reliable system identification requires a high sample frequency. The sample frequency should be at least four to ten times higher than the system open loop bandwidth. The upper limit for the sample frequency is determined by the availability of data storage space (for batch system identification) and the Analogue to Digital converter resolution. This is because a high sample frequency generates more data samples per time unit, which need to be stored. If the sample frequency is so high that consecutive samples do not differ by more than the A/D resolution, nothing can be gained by a faster sampling frequency.

If the only sample frequency possible is lower than the system open loop bandwidth, the system open loop bandwidth should be brought down by means of anti-aliasing filtering to prevent corruption of the sample signal due to the aliasing effect.

The following two techniques can assist in choosing an appropriate sample frequency for a specific application:

The Power Density Spectrum

Compute the power density spectrum of the sampled signal for a chosen sample frequency. If the signal power is squashed around 0 rad/sec sampling is unnecessarily fast. Signal power should fall off evenly across the frequency range 0 to π rad/sec, with negligible signal power (at least −40dB) at π rad/sec. If the power density spectrum is flat across the range without the signal power dropping to a negligible level before π rad/sec then sampling is too low, aliasing is occurring, or the output signal-to-noise ratio is unacceptable for good modelling and control.

Z-plane pole-zero plot

If estimated poles and zeros is squashed around zero in the Z-plane, sampling is too slowly. If estimated poles and zeros lie squashed against the unit circle then sampling is unnecessarily fast. Reasonable spread of poles and zeros in z-plane is an indication of correct sampling rate.

If it becomes evident that sampling was too fast then down sampling can easily be done. If on the other hand sampling was too slowly, the signal will have to be re-sampled at a fast enough rate.

5.4.1.2 Choice of input stimulus signal

The following signals are often used as input stimulus signals in system identification and have been widely documented: Square Wave, Pseudo-Random Binary Sequence (PRBS), Normally distributed noise and Gausian distributed noise [22].

A few important considerations in choosing an appropriate input stimulus signal follow below:

The signal used as stimulus for system identification should have a bandwidth greater or equal to the system open loop bandwidth, with sufficient power across the system open loop bandwidth to excite all relevant modes present in the system.

The following bandwidth check will give a good indication as to whether the bandwidth of the stimulus signal is correct:

Input signal of reasonable amplitude should result in a significant system output deviation. If significant output deviation cannot be achieved without input saturation the perturbation signal frequency is too high or an attempt is being made to control the system output with an inappropriate input.

The amplitude of the stimulus signal should be large enough to achieve an output deviation of at least 10% of the normal output range of the process. An advantage of choosing an input signal amplitude that achieves a significant output signal amplitude is that the A/D round-off errors in sampling the resulting output signal is minimized by utilizing the largest part of the full A/D scale. This will maximize the output signal-to-noise ratio.

The input signal should however, be small enough though not to saturate or drive the system into non-linear operation. If the aim is to obtain a small signal or locally linearized model around a particular set-point, then the input signal amplitude should be small enough only to effect small output deviations around the output set-point. Large sweeps across the linear input span will be necessary for a large signal model of the system.

Large input signal amplitude should excite reasonable output signal amplitude. If significant output deviation cannot be achieved without input signal saturation, the perturbation signal frequency is too high, or an attempt is being made to control the system output with an inappropriate input.

5.4.2 How much data is necessary?

Data should be collected for at least two times the period of the slowest significant or dominant mode or frequency of the system. A more optimal method would be to record data for four to ten times the duration of the slowest open loop system time constant.

5.4.3 Recording data for Pilot Plant model identification

Data for the pilot plant system identification was generated with the simulation model developed in Chapter 3.

The following data sets were recorded to data files:

- Level l_2 was recorded while perturbing valve v_2.

- Level l_1 was recorded while perturbing valve v_2.

- Level l_1 was recorded while perturbing valve v_1.

- Level l_2 was recorded while perturbing valve v_1.

Figure 29 shows the SIMuWIN diagram used to record level l_2 while perturbing valve v_2. All data sets were recorded in a similar way.
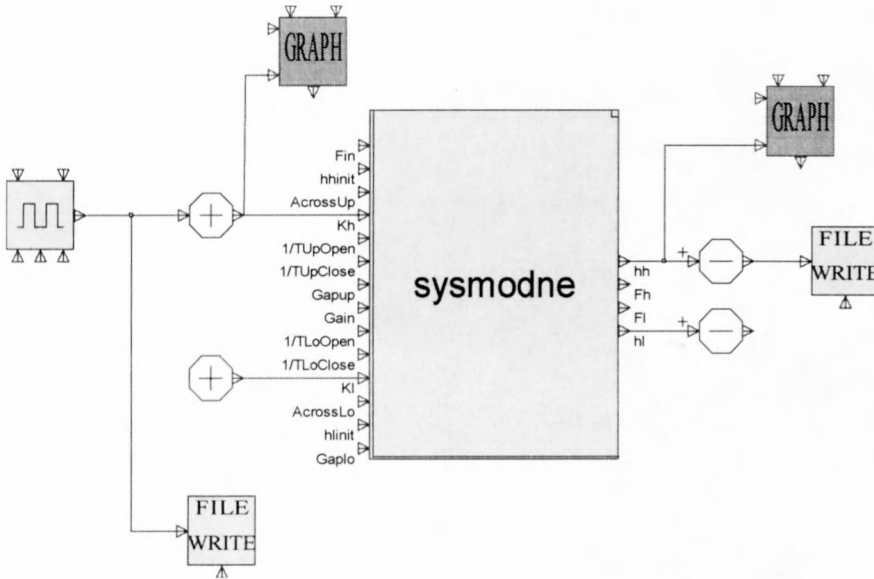
Figure 29: SIMuWIN – recording data for linear model identification

The recorded signals in the case of level l_2, valve v_2 is shown in Figure 30.
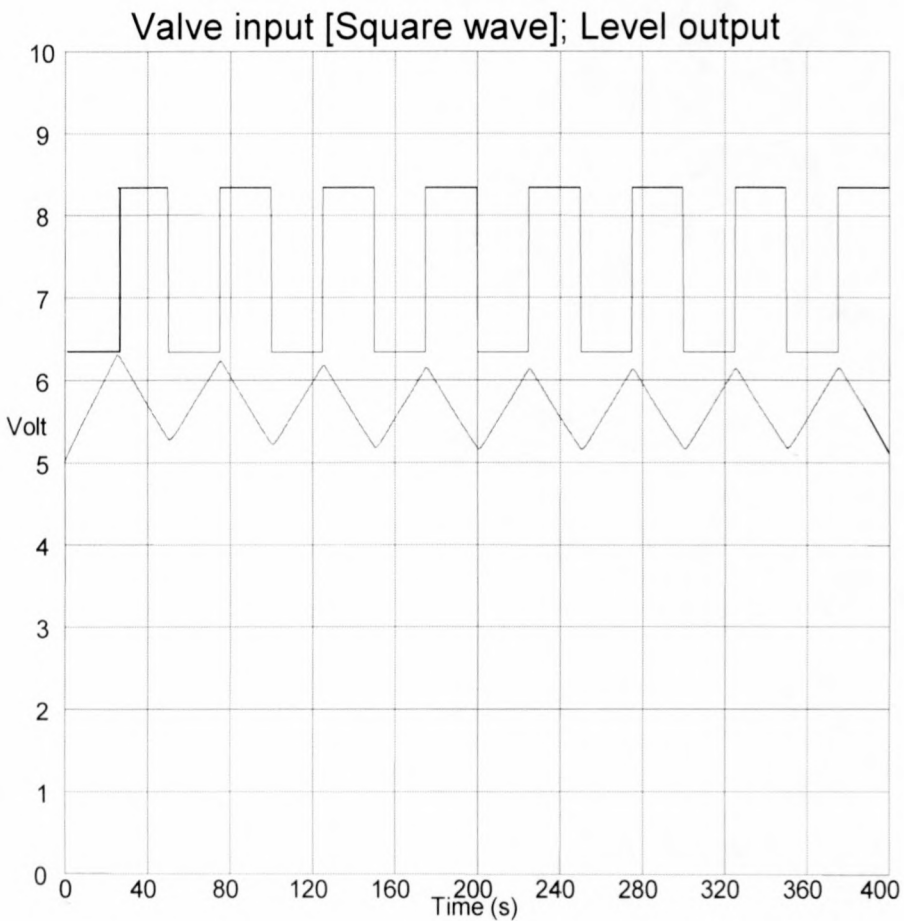
Figure 30: Valve input vs. Level

The perturbation valve input signal was a square wave with offset 7.4V, amplitude 1V, frequency 0.02 Hz. The resulting output level was recorded for a duration of 400

seconds (8 cycles) at a sample interval of 0.25 seconds, which is approximately four times faster than the valve dynamics.

5.4.4 Selecting the best model structure

5.4.4.1 Choosing the number of unit delays

System delay is defined as the number of samples when the output deflection is zero (or random and negligible), from the moment that a perturbation input signal is applied until it starts to deviate in a linear fashion. It can be read directly from the output data, where the output was initially at rest at a steady state before the input was applied to the system. A linear discrete model is taken to have at least one unit delay implying that when the output was sampled at the instant the input was applied, it was still zero. This indicates a finite propagation time through the system, which is a characteristic of any causal system.

If the number of unit delays is uncertain a safe alternative is to make the zero polynomial order greater than or equal to the maximum number of delays expected plus the order of the system dynamics. The pole polynomial order must then be at least the same, or of a larger order than the zero polynomial. When the model coefficients are estimated using Least Squares, the number of zero polynomial coefficients that turns out to be zero will indicate the number of system unit delays.

5.4.4.2 Evaluating different model orders using MATLAB

Once input/output data sets have been recorded different model structures can be evaluated as shown in the steps below using MATLAB's system identification toolbox.

Put the Input/Output data in one vector:

z = [y u];

Remove the straight-line trends from the data:

zd = detrend(z);

Break the data up in a Training and a Validation data set:

zdt = zd(1:800,:); zdv = zd(801:1601,:);

Specify the range of ARX model orders to be evaluated: ([an], [bn], [delays]):

NN = struc([1:3],[1:3],[0:3]);

with the ARX model structure being shown in Equation 39.

Equation 39

$$y(k) + a_1 y(k-1) + a_2 y(k-2) + \ldots + a_n y(k-n))$$
$$- b_1 u(k-1) - \ldots - b_n u(k-n)) = e(k; \theta)$$

Evaluate the different model structures plotting the Least Squares Criteria Loss Function (Summed Squared Estimate Error) for different numbers of parameters as shown in Figure 31:

VN = arxstruc(zdt,zdv,NN);
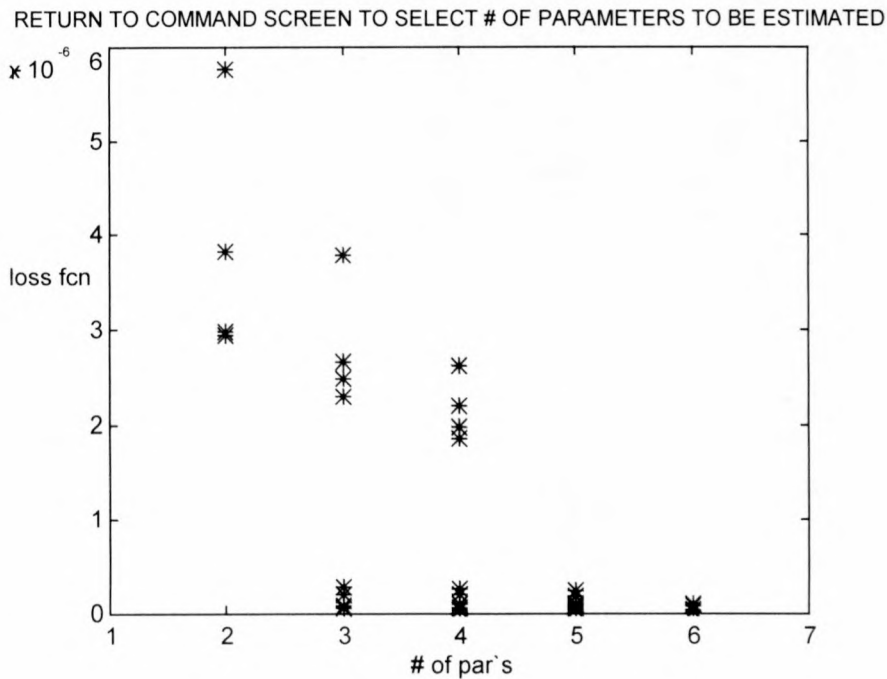
Figure 31: Comparing model orders

Table 10 shows the computed loss function for each model structure in the selected range of models structures as generated by the *arxstruc* command and found in the resulting VN vector (from top down: loss function, an, bn, delays).

1	2	3	4	5	6
5.7695e-006	3.8338e-006	2.9852e-006	2.9315e-006	3.7822e-006	2.6659e-006
1.0000e+000	1.0000e+000	1.0000e+000	1.0000e+000	1.0000e+000	1.0000e+000
1.0000e+000	1.0000e+000	1.0000e+000	1.0000e+000	2.0000e+000	2.0000e+000

0	1.0000e+000	2.0000e+000	3.0000e+000	0	1.0000e+000
7	**8**	**9**	**10**	**11**	**12**
2.2805e-006	2.4938e-006	2.6214e-006	1.9757e-006	1.8593e-006	2.1935e-006
1.0000e+000	1.0000e+000	1.0000e+000	1.0000e+000	1.0000e+000	1.0000e+000
2.0000e+000	2.0000e+000	3.0000e+000	3.0000e+000	3.0000e+000	3.0000e+000
2.0000e+000	3.0000e+000	0	1.0000e+000	2.0000e+000	3.0000e+000
13	**14**	**15**	**16**	**17**	**18**
7.4417e-008	6.5770e-008	1.9898e-007	2.7459e-007	4.7539e-008	6.1514e-008
2.0000e+000	2.0000e+000	2.0000e+000	2.0000e+000	2.0000e+000	2.0000e+000
1.0000e+000	1.0000e+000	1.0000e+000	1.0000e+000	2.0000e+000	2.0000e+000
0	1.0000e+000	2.0000e+000	3.0000e+000	0	1.0000e+000
19	**20**	**21**	**22**	**23**	**24**
1.9091e-007	2.5583e-007	4.3579e-008	5.6956e-008	1.8276e-007	2.3478e-007
2.0000e+000	2.0000e+000	2.0000e+000	2.0000e+000	2.0000e+000	2.0000e+000
2.0000e+000	2.0000e+000	3.0000e+000	3.0000e+000	3.0000e+000	3.0000e+000
2.0000e+000	3.0000e+000	0	1.0000e+000	2.0000e+000	3.0000e+000
25	**26**	**27**	**28**	**29**	**30**
4.1931e-008	5.8182e-008	8.9019e-008	9.6065e-008	3.9307e-008	3.4308e-008
3.0000e+000	3.0000e+000	3.0000e+000	3.0000e+000	3.0000e+000	3.0000e+000
1.0000e+000	1.0000e+000	1.0000e+000	1.0000e+000	2.0000e+000	2.0000e+000
0	1.0000e+000	2.0000e+000	3.0000e+000	0	1.0000e+000
31	**32**	**33**	**34**	**35**	**36**
8.8436e-008	9.6041e-008	1.5464e-008	3.4187e-008	8.7797e-008	9.6233e-008
3.0000e+000	3.0000e+000	3.0000e+000	3.0000e+000	3.0000e+000	3.0000e+000
2.0000e+000	2.0000e+000	3.0000e+000	3.0000e+000	3.0000e+000	3.0000e+000
2.0000e+000	3.0000e+000	0	1.0000e+000	2.0000e+000	3.0000e+000

Table 10: Model structure evaluation results by the *arxstruc* MATLAB command

Select a suitable model structure:

nn = selstruc(VN)

with nn containing the chosen model orders a_n, b_n and the chosen delay.

Model structure 14 as shown in Table 10 was used in this thesis to deduce linear models for the pilot plant in order to implement the alternative PID control law. A very low evaluated loss function value of 6.577e-8 shows how well this model structure suits the pilot plant level control problem.

The selected model structure has been shown in Equation 21 and is repeated here in Equation 40

Equation 40

$$\frac{Y[z]}{U[z]} = \frac{b_1 z}{z^2 + a_1 z + a_2}$$

5.4.5 Calculating model parameters using Least Squares

Once an appropriate model structure has been chosen the Weighted Least Squares Batch Technique, presented below, is used to obtain the optimum parameters for the chosen model structure.

Equation 41 presents the ARX model structure with equation error criterion.

Equation 41

$$y(k) + a_1 y(k-1) + a_2 y(k-2) + \ldots + a_n y(k-n))$$
$$- b_1 u(k-1) - \ldots - b_n u(k-n)) = e(k; \theta)$$

If the Parameter and State vectors are defined respectively in Equation 42 and Equation 43, N+1 instances of Equation 41 can be written in vector notation as shown in Equation 44.

Equation 42

$$\theta = \begin{bmatrix} a_1 \ldots a_n \ b_1 \ldots b_n \end{bmatrix}^T$$

Equation 43

$$\phi(k) = \begin{bmatrix} -y(k-1) \ldots -y(k-n) & u(k-1) \ldots u(k-n) \end{bmatrix}^T$$

$$Y(N) = \begin{bmatrix} y(n) \ldots y(N) \end{bmatrix}^T,$$
$$\Phi(N) = \begin{bmatrix} \phi(n) \ \phi(n+1) \ldots \phi(N) \end{bmatrix}^T,$$
$$\varepsilon[N; \theta] = \begin{bmatrix} e(n) \ldots e(N) \end{bmatrix}^T$$

Equation 44

$$Y = \Phi\theta + \varepsilon(N; \theta)$$

In Equation 43 n is the model order and $N+1$ is the number of consecutive input/output data samples used to compute the model parameters. The Parameter vector, θ, is then chosen to minimize the cost function shown in Equation 45.

Equation 45

$$J(\theta) = \sum_{k=n}^{N} w(k) e^2(k;\theta) = \varepsilon^T W \varepsilon$$

This can be achieved by selecting θ as shown in Equation 46.

Equation 46

$$\hat{\theta}_{WLS} = \left(\Phi^T W \Phi\right)^{-1} \Phi^T W Y$$

$$W(k,k) = w(k) I$$

$$w(k) = (1 - \gamma)\gamma^{N-k} \quad \text{with } \gamma \langle 1$$

The parameter γ is typically chosen between 0.95 and 0.99. When $W = I$ Weighted Least Squares becomes Normal Least Squares.

Using the model structure selected in section 5.4.4 and the data recorded from the pilot plant, as described in section 5.4.3, the Weighted Least Squares Technique was applied using MATLAB, to obtain the resulting process models presented in Equation 47.

Equation 47

$$\begin{bmatrix} \partial h_2[z] \\ \partial h_1[z] \end{bmatrix} = G[z] \begin{bmatrix} \partial u_2[z] \\ \partial u_1[z] \end{bmatrix}$$

$$G[z] = \begin{bmatrix} G_{22}[z] & 0 \\ G_{12}[z] & G_{11}[z] \end{bmatrix}$$

$$G_{22}[z] = \frac{-0.001337z}{z^2 - 1.862z + 0.862}$$

$$G_{12}[z] = \frac{0.001175z}{z^2 - 1.874z + 0.8749}$$

$$G_{11}[z] = \frac{-0.001615z}{z^2 - 1.848z + 0.849}$$

5.5 Conclusions

This chapter explained how linear models were obtained for controller design using both data driven and more fundamental approaches. It also considered concepts such as model order, model structure and possible causes of process non-linearities in the cascaded flow process. In the following chapters, the linear models are used to implement control strategies for the pilot plant.

Chapter 6

Independent Control Loops

This chapter presents a control approach where a separate independent control loop is used for the level control of each tank unit. This means that the control action of each outlet valve is only based on the level measurement of that particular tank unit fluid level. There is therefore no attempt to decouple adjacent tank units and interaction and level disturbances are dealt with using feedback control.

6.1 Operating conditions

To illustrate the strategy most effectively, a feed flow rate was selected for the Pilot Plant that placed the valves at steady state operating positions in the middle of their respective output ranges. This maximized system controllability and together with valve capacity, set an upper limit to closed loop speed of response. The rise time specification posed in Table 1 was chosen with this in mind. Table 11 shows the chosen operating regime.

Variable	Set-point
Feed flow rate f_3	1.8e-4 [m^3/s]
Resulting operating point of upper tank outlet valve v_2	75% of input span
Resulting operation point of lower tank outlet valve v_1	54% of input span
Level set-points chosen for both tanks	50% of full scale

Table 11: Operating conditions for control experiments

6.2 Model identification

A linear discrete time transfer function model was obtained for each tank unit from the control valve input to the level output by means of the data driven system identification explained in Section 5.4. The linear process models were assumed to be as shown in Equation 48.

Equation 48

$$\begin{bmatrix} \partial h_2[z] \\ \partial h_1[z] \end{bmatrix} = G[z] \begin{bmatrix} \partial u_2[z] \\ \partial u_1[z] \end{bmatrix}$$

$$G[z] = \begin{bmatrix} G_{22}[z] & 0 \\ 0 & G_{11}[z] \end{bmatrix}$$

$$G_{22}[z] = \frac{-0.001337z}{z^2 - 1.862z + 0.862}$$

$$G_{11}[z] = \frac{-0.001615z}{z^2 - 1.848z + 0.849}$$

6.3 Closed loop response specification

The desired closed loop response for the compensated pilot plant was a second order response with a maximum overshoot of approximately 5% and a rise time of 50 seconds, as specified in Table 1.

6.4 Pole placement design with Alternative PID control law

A discrete time model structure specified in the Z-domain with model parameters b_1, a_1 and a_2 was used, as shown in Equation 49.

Equation 49

$$\frac{Y[z]}{U[z]} = \frac{b_1 z}{z^2 + a_1 z + a_2}$$

It was combined with the Alternative PID control law in Equation 50.

Equation 50

$$U[z] = \frac{R[z](g_0 + g_1 + g_2)z^2 - (g_0 z^2 + g_1 z + g_2)Y[z]}{z^2 - z}$$

Equation 51 shows the desired second order CL response.

Equation 51

$$\frac{Y[z]}{R[z]} = \frac{(1 + t_1 + t_2)}{z^2 + t_1 z + t_2}$$

t_1 and t_2 are coefficients that achieve unit steady state gain as well as the CL specifications set out in Table 1. This was done by choosing the control law parameters as shown in Equation 52.

Equation 52

$$g_0 = \frac{t_1 + 1 - a_1}{b_1}$$

$$g_1 = \frac{t_2 + a_1 - a_2}{b_1}$$

$$g_2 = \frac{a_2}{b_1}$$

The desired CL specifications shown in Table 1 translate to the resulting CL response coefficients and control law parameters in Table 12.

| CL Response Parameter	Value
t_1	-1.9767
t_2	0.9769
Control Law Parameter	Value
g_{0_U}	-539.523

g_{1_U}	1065.050
g_{2_U}	-525.697
g_{0_L}	-662.177
g_{1_L}	1306.700
g_{2_L}	-644.727

**Table 12:** Closed Loop coefficients and Control Law parameters

6.5 Simulation of closed loop system

Two separate control loops were implemented for the cascaded two tank pilot plant to yield the desired CL response. These control loops utilized the alternative PID control law described above. The CL system was simulated for a few different scenarios and the results are presented below:
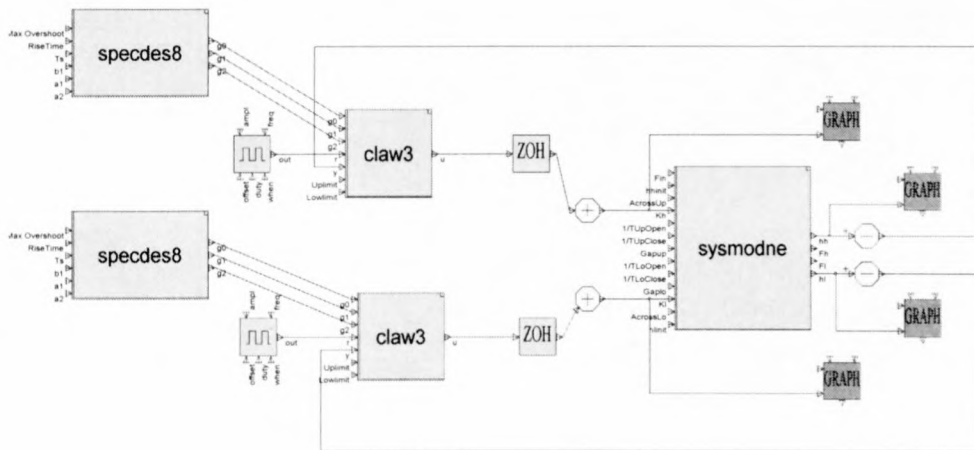
Figure 32: SIMuWIN – Independent controllers simulation

The simulation schematic (Figure 32) shows how two control laws were used to implement two separate discrete control loops. The sample rate was 0.25s. The simulation model (sysmodne) represents the cascaded two tank pilot plant. The upper control loop in Figure 32 controls the upper (second) tank unit level l_2 by adjusting valve v_2 as shown in Figure 2. The lower control loop in Figure 32 controls the lower (fist) tank unit level l_1 by adjusting valve v_1 as also shown in Figure 2. The valve command signals and level responses were plotted for each tank level. The simulation calculation time interval was 0.001s to simulate the continuous time response of the pilot plant to the implemented discrete control.
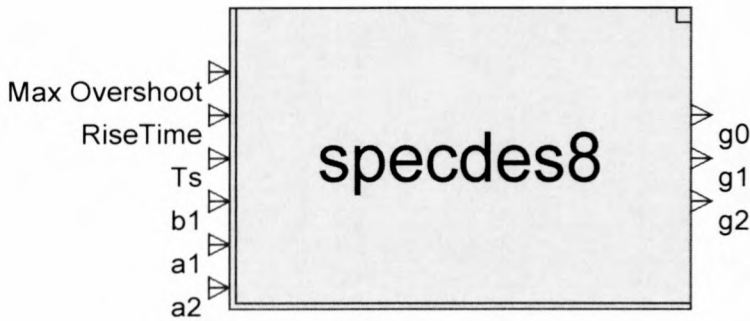
Figure 33: SIMuWIN – controller design block

The controller design block as shown in Figure 33 ("specdes8"), was used to compute the parameters of the proposed control law. This is based on the desired second order CL time domain specifications (max overshoot and rise-time) and the derived linear model of the plant. The ability of the resulting controller to produce the desired closed loop response depends directly on how well the linear model represents the true plant (the simulation model).
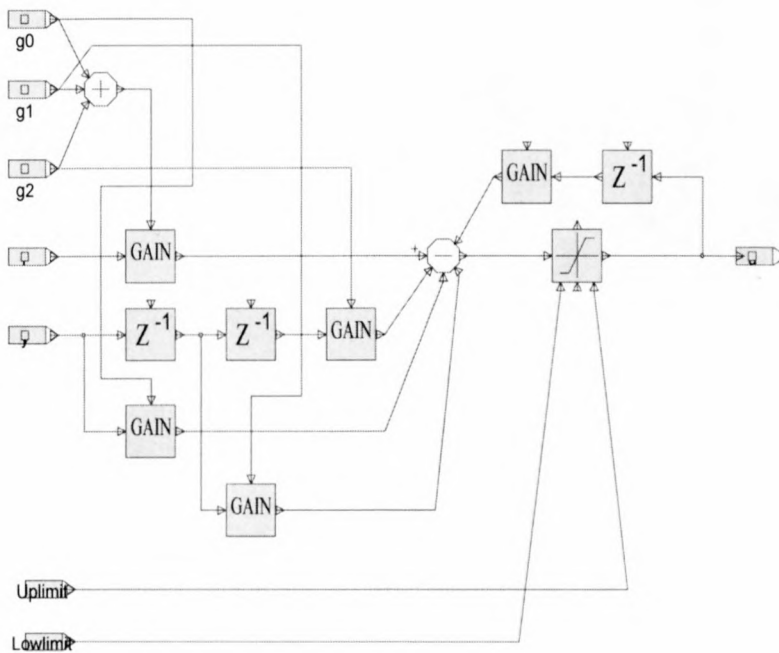

Figure 34: SIMuWIN – PID control law

The proposed control law (Figure 34) was implemented with gains and unit time delay blocks. The output of the control law was limited to take into account valve saturation. The limited output was fed back into the control law to prevent integrator wind-up.

Different scenarios were simulated to illustrate the performance of the two separate control loops on the pilot plant.
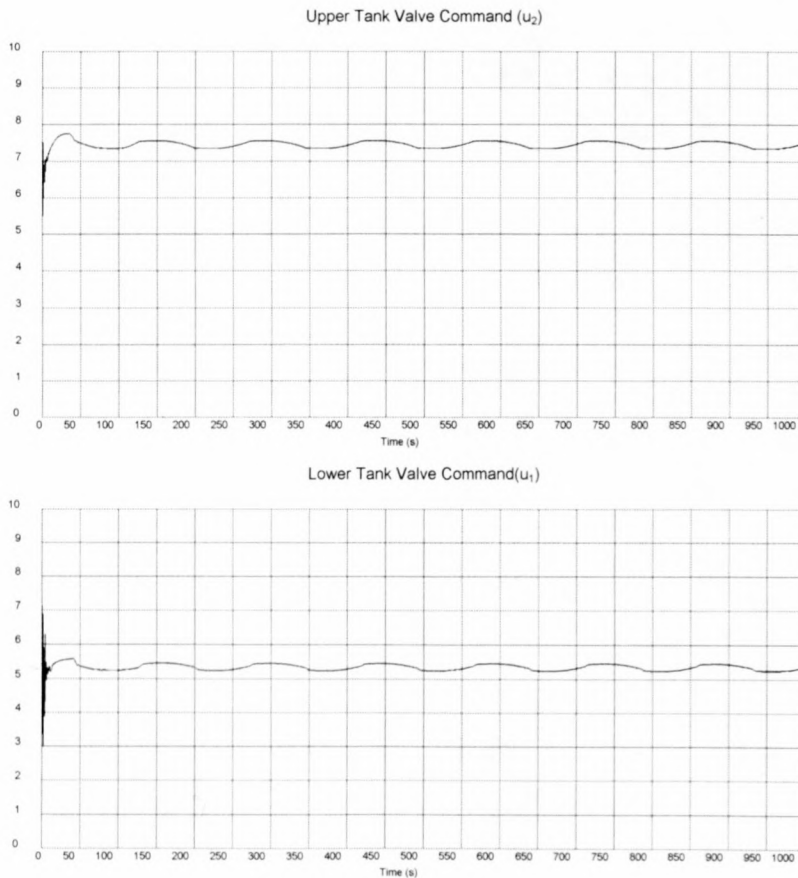
6.5.1 Scenario 1: Regulating levels at set-points

In this experiment both levels l_1 and l_2 were regulated to a set-point of 5V (50%). This was carried out using the SIMuWIN simulation schematic shown in Figure 32 . The square wave input block as reference input to the upper tank control loop was replaced with a constant block. This provided a constant reference input of 5V to the upper tank control loop. The square wave reference input to the lower tank unit control loop was also replaced with a constant block to provide the constant reference input of 5V to the lower tank unit control loop. The steady state feed flow rate to the upper tank unit, f_3, was as shown in Table 11. The full range of the level measurements was 0V to10V with 10V being full and 0V being empty. Full scale for the corresponding valve command signals was also 0V to 10V with 10V being open and 0V being closed. The level responses are shown in Figure 35 and the respective valve command signals in Figure 36. The level graphs are enlarged to give an idea of the variation of the levels around the set-points under conditions of steady state regulation with no feed flow rate disturbances (deviations in the feed flow rate to the upper tank unit from its steady state value). At time 0 the simulation started with a slight mismatch in flow rates of fluid entering and leaving each unit. This was due to the choice of initial valve positions and caused the level of each unit to deviate from its set-point. The respective controllers acted to bring the levels back to set-point and keep it there.

Upper Tank Level Response (l_2)

Lower Tank Level Response (l_1)
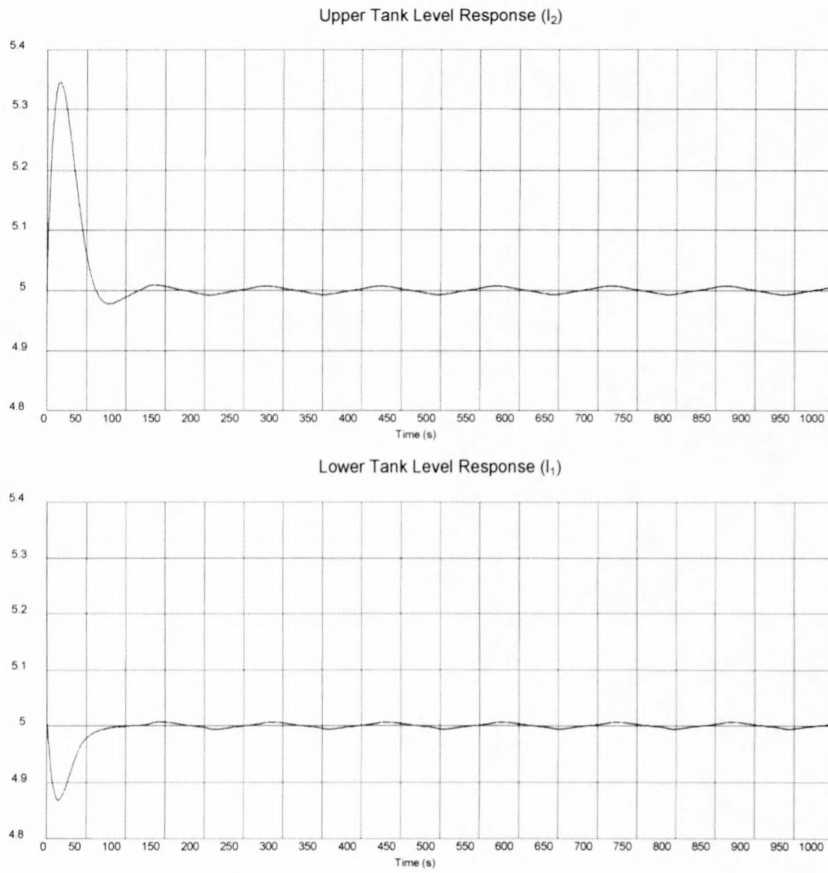
Figure 35: Scenario 1 – levels

Upper Tank Valve Command (u_2)


Lower Tank Valve Command(u_1)

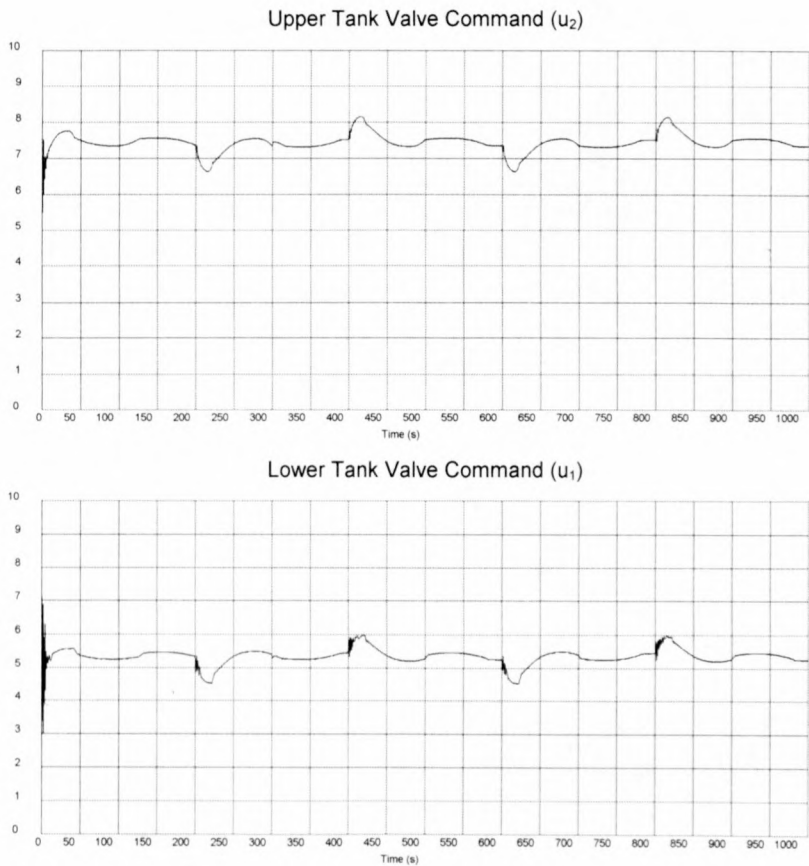**Figure 36:** Scenario 1 – valve command signals

73

A slight oscillation with damped natural frequency of 6.7mHz is visible. This is an indication of the degree of mismatch between the linear models used for controller design and the simulation model. If the linear models perfectly captured all the dynamic properties of the simulation model the controllers would have perfectly compensated for and cancelled the oscillation. The level regulation error was 0.1% of full scale (10V) for both the upper level, l_2, and the lower level, l_1.

6.5.2 Scenario 2: Regulating lower level while stepping upper level

In the second scenario the upper unit level, l_2, was stepped between level set-points 5V and 6V (which was a step size of 10% of level full scale) at a frequency of 2.5e-3Hz, while regulating the lower unit level, l_1, at a level set-point of 5V. This was done using the SIMuWIN simulation schematic shown in Figure 32 with the square wave input block as reference input to the upper tank unit control loop. The square wave reference input to the lower tank unit control loop was replaced with a constant block to provide the constant reference input of 5V to the lower tank unit control loop. The steady state feed flow rate to the upper tank unit, f_3, was as shown in Table 11. The full range of the level measurements was 0V to10V with 10V being full and 0V being empty. Full scale for the corresponding valve command signals was also 0V to 10V with 10V being open and 0V being closed. The level responses are shown in Figure 37 and the respective valve command signals in Figure 38.

Upper Tank Level Response (l$_2$)

Lower Tank Level Response (l$_1$)
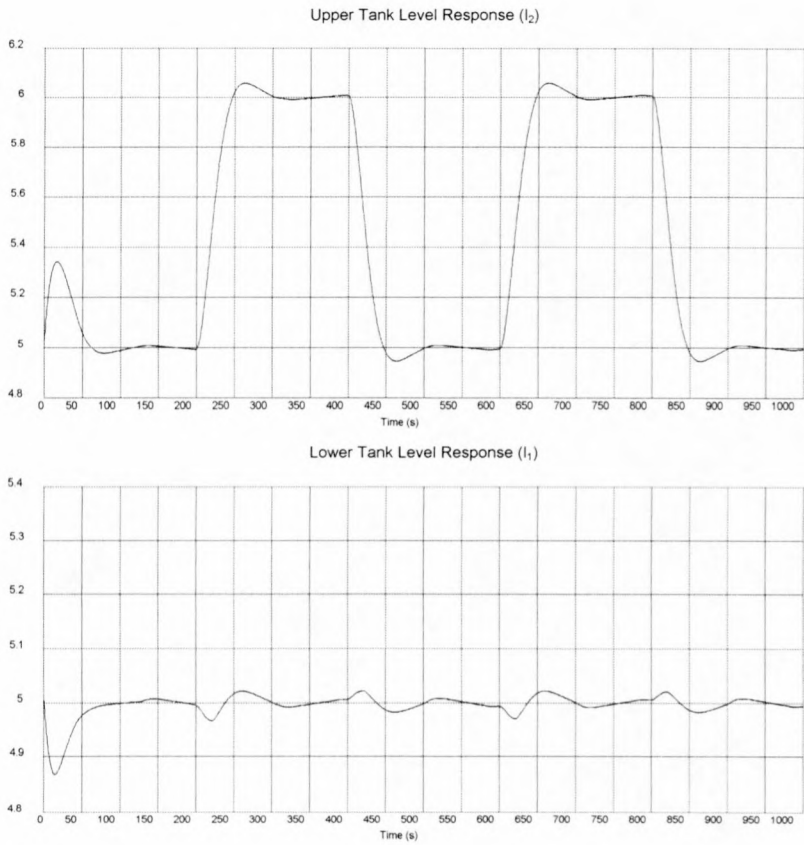
Figure 37: Scenario 2 – levels

Upper Tank Valve Command (u$_2$)
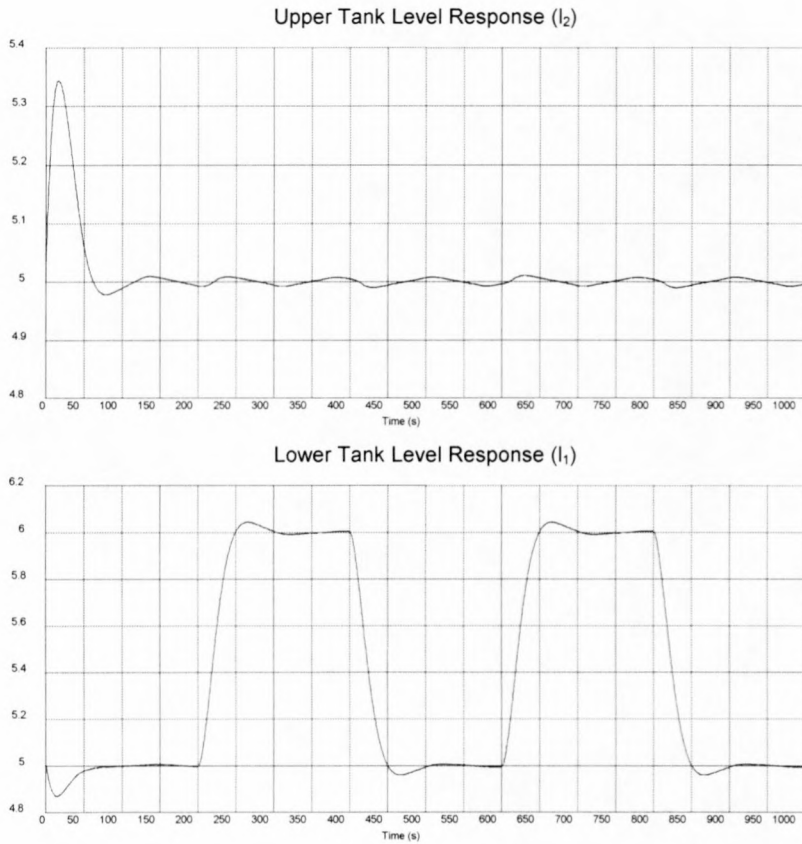
Lower Tank Valve Command (u$_1$)

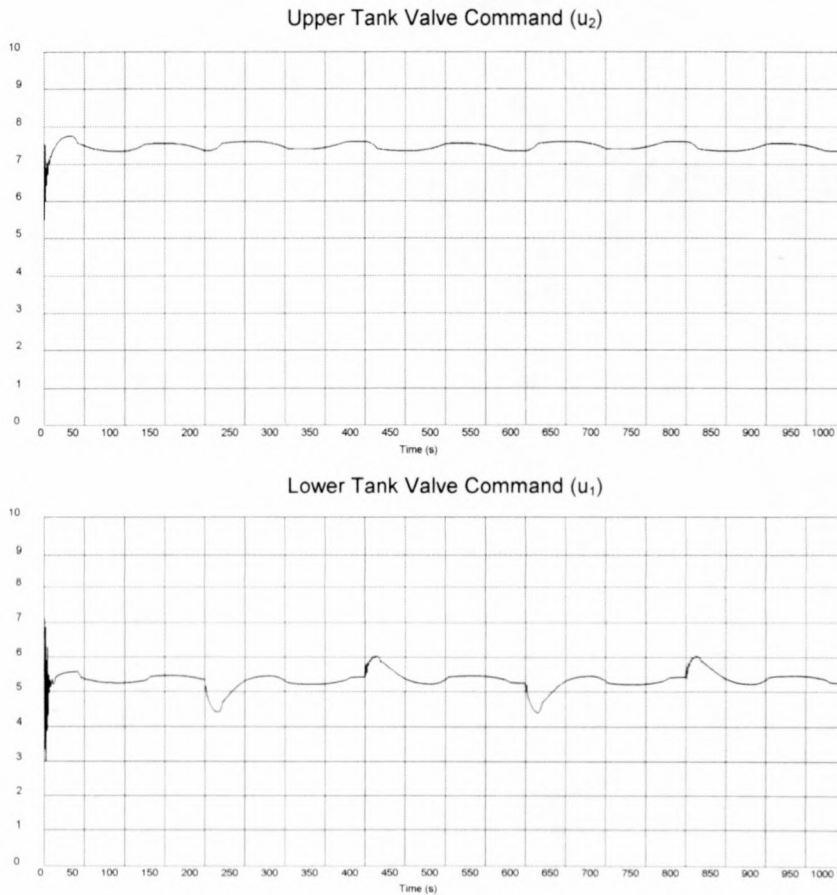**Figure 38:** Scenario 2 – valve command signals

The upper level control loop tracked the level set-point changes with a rise time of 47 seconds and was well damped with a maximum overshoot of 6% of step size (1V). Set-point changes of the upper level caused flow disturbances between the tank units that affected the lower level. The lower level control loop rejected the disturbances using the level error feedback and regulated the lower level at a set-point of 5V with a regulation error of 0.5% of level full scale (5% of step size). From this experiment it should be noted that the upstream control actions disturbed the down-stream control loop. This is evident in the large regulation error compared to the much smaller regulation error of scenario 1.

6.5.3 Scenario 3: Regulating upper level while stepping lower level

In this scenario level l_2 was alternated between level set-points of 5V and 6V at a frequency of 2.5e-3Hz, while level l_1 was regulated at a set-point of 5V. This was done using the SIMuWIN simulation schematic shown in Figure 32 with the square wave input block as reference input to the upper tank control loop replaced with a constant block to provide the constant reference input of 5V to the upper tank control loop. The square wave reference input to the lower tank unit control loop was used to step the lower tank level set-point between 5V and 6V. The steady state feed flow rate to the upper tank unit, f_3, was as shown in Table 11. The full range of the level measurements was 0V to10V with 10V being full and 0V being empty. Full scale for the corresponding valve command signals was also 0V to 10V with 10V being open and 0V being closed. The level responses are shown in Figure 39 and the respective valve command signals in Figure 40.

Upper Tank Level Response (l_2)

Lower Tank Level Response (l_1)

Figure 39: Scenario 2 – levels

Upper Tank Valve Command (u_2)
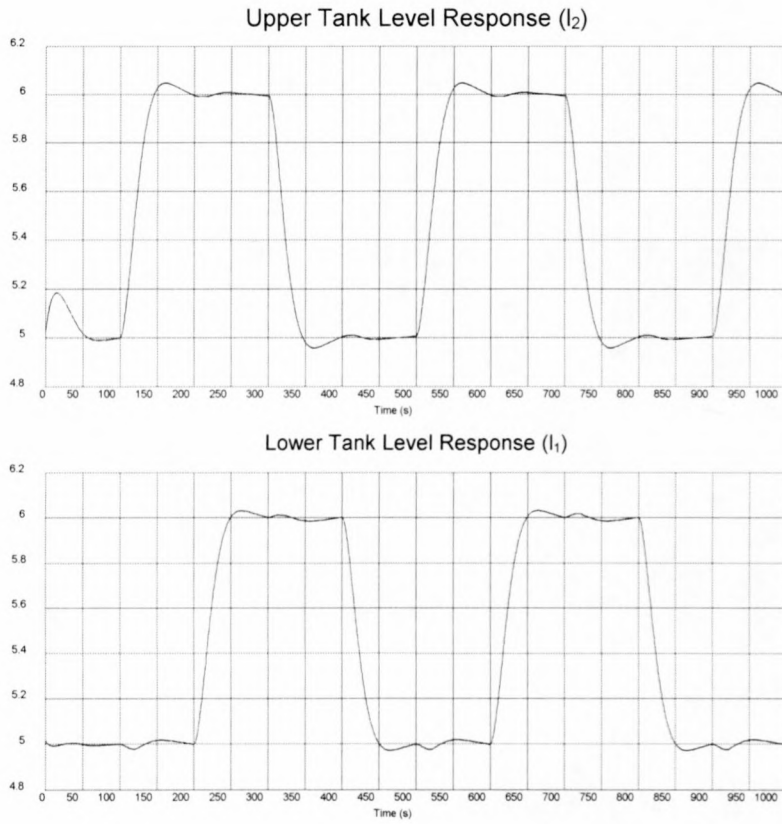
Lower Tank Valve Command (u_1)

Figure 40: Scenario 3 – valve command signals

The lower level control loop tracked the level set-point changes with a rise time of 50 seconds and was well damped with a maximum overshoot of 5%. Set-point changes of the lower level had little effect on the regulation of the upper level. The upper level control loop regulated the upper level at a set-point of 5V with a regulation error of 2% of step size (1V). It can be noted that downstream control actions have little effect on upstream control loops. This is evident in the 2% regulation error compared to the 5% regulation error in scenario 2.
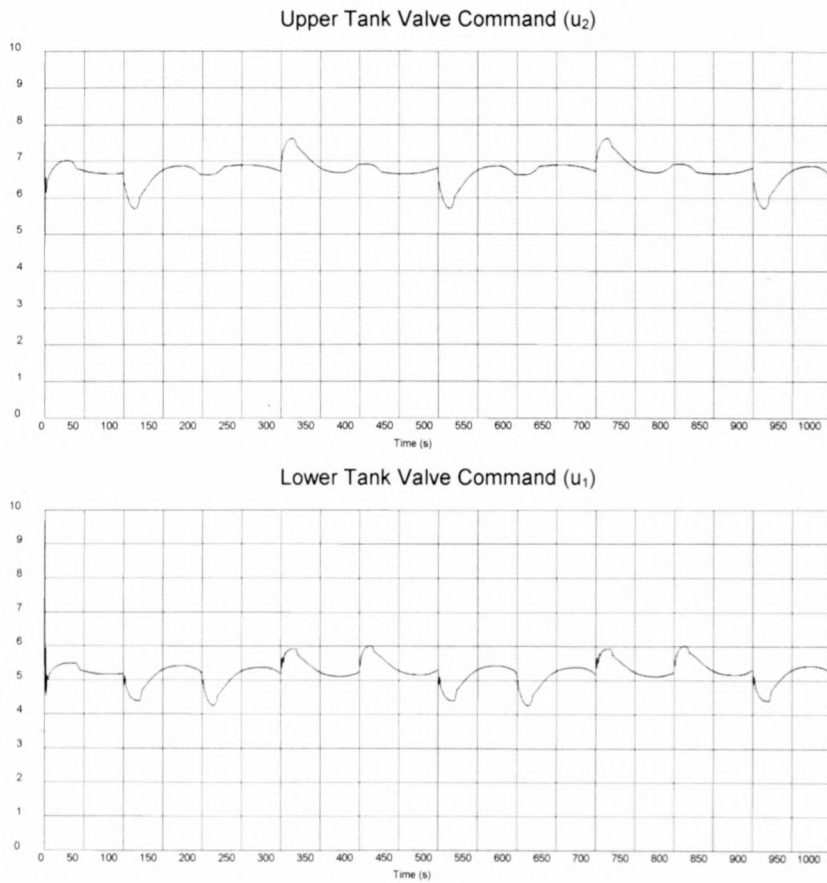
6.5.4 Scenario 4: Stepping both levels simultaneously

In scenario 4 levels l_2 and l_1 were stepped simultaneously between level set-points 5V and 6V at a frequency of 2.5e-3Hz. This was done using the SIMuWIN simulation schematic shown in Figure 32 with the square wave input block as reference input to the upper tank control loop. The square wave reference input to the lower tank control loop was used to step both the upper and lower level set-points between 5V and 6V. The steady state feed flow rate to the upper tank unit, f_3, was as shown in Table 11. The full range of the level measurements was 0V to 10V with 10V being full and 0V being empty. Full scale for the corresponding valve command signals was also 0V to 10V with 10V being open and 0V being closed. The level responses are shown in Figure 41 and the respective valve command signals in Figure 42.

Upper Tank Level Response (l_2)

Lower Tank Level Response (l_1)

Figure 41: Scenario 3 – levels

Upper Tank Valve Command (u_2)
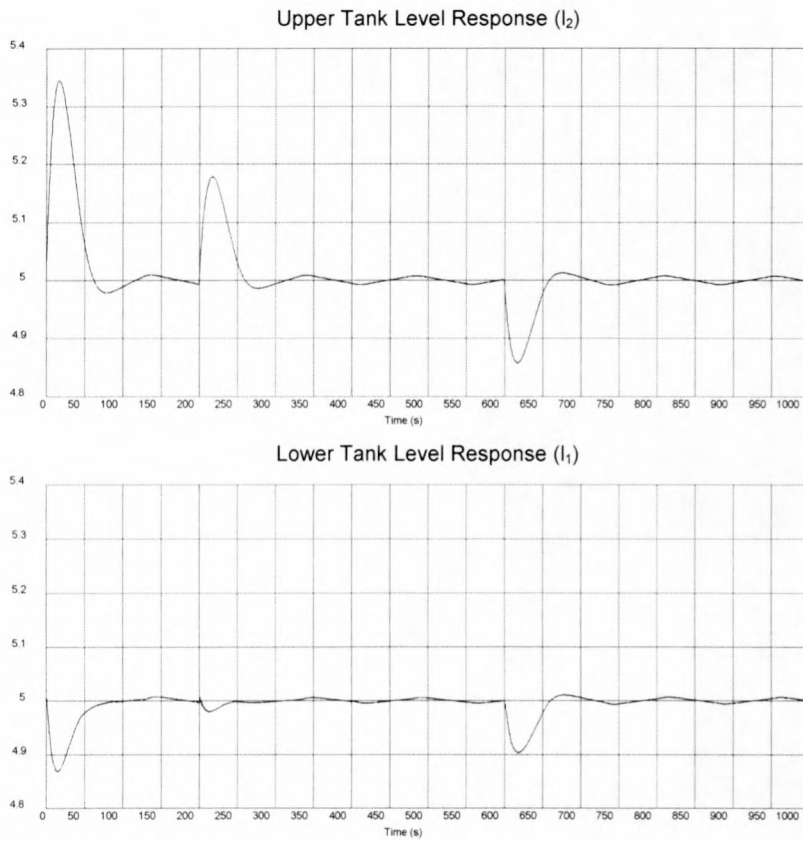
Lower Tank Valve Command (u_1)

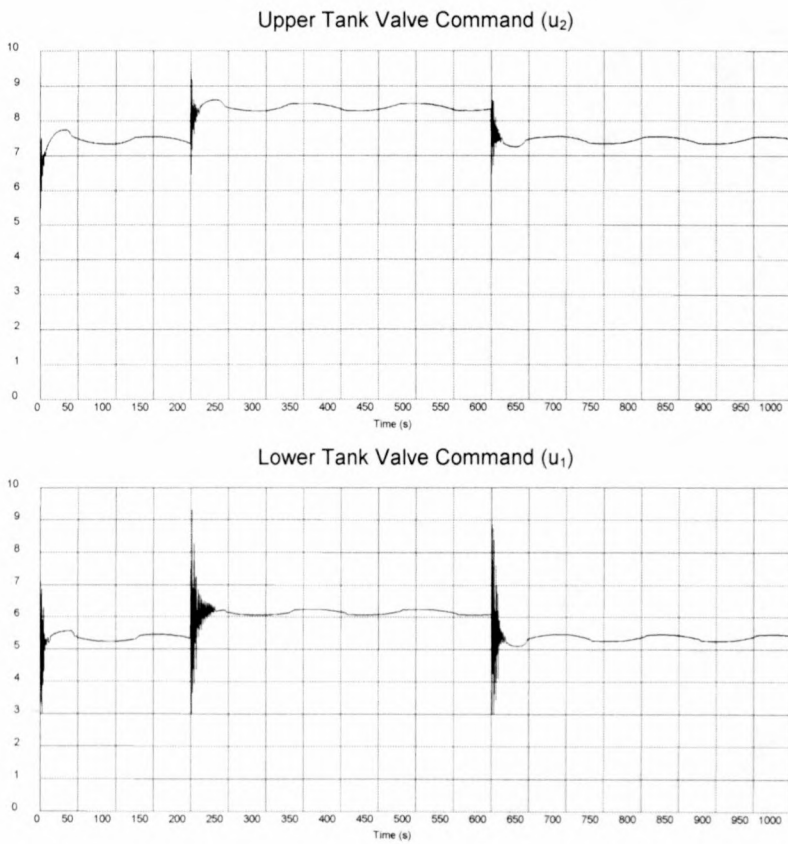**Figure 42:** Scenario 3 – valve command signals

The upper level tracked the set-point changes with a rise time of 45 seconds in a well damped fashion with a maximum overshoot of 5% and was disturbed by steps in the lower level set-point with a disturbance error of about 2% of step size. The lower level tracked the set-point changes with a rise time of 50 seconds in a well damped fashion with a maximum overshoot of about 4% and was disturbed by steps in the lower level set-point with a disturbance error of about 4% of step size. The disturbance effect of set-point changes in the upper level, l_2, on the lower level, l_1, response can be seen in Figure 41 and is clear from the difference in disturbance errors in the upper and lower levels as described above.

6.5.5 Scenario 5: Rejecting a Step disturbance in the feed flow rate

In scenario 5 levels l_2 and l_1 were regulated at level set-point 5V in the presence of a feed flow rate pulse disturbance (when 200 seconds, width 400 seconds, amplitude $0.9e-4$ m^3/s) at the inlet to the upper tank unit. This was done using the SIMuWIN simulation schematic shown in Figure 32 with the square wave input block as reference input to the upper tank control loop replaced with a constant block to provide a constant reference input of 5V to the upper tank control loop. The square wave reference input to the lower tank unit control loop was also replaced with a constant block to provide the constant reference input of 5V to the lower tank control loop. The steady state feed flow rate to the upper tank unit, f_3, as shown in Table 11, was disturbed using a pulse input block to provide a pulse in the feed flow rate to the upper tank unit as shown in Figure 45. The full range of the level measurements was 0V to10V with 10V being full and 0V being empty. Full scale for the corresponding valve command signals was also 0V to 10V with 10V being open and 0V being closed. The level responses are shown in Figure 43 and the respective valve command signals in Figure 44.
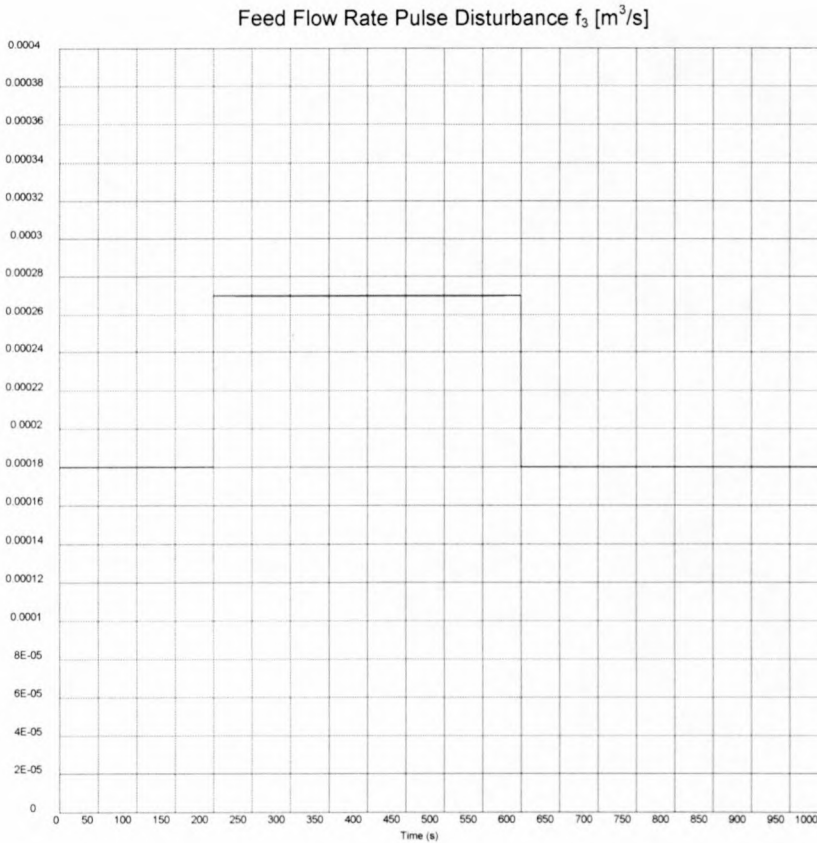
Figure 43: Scenario 5 – levels

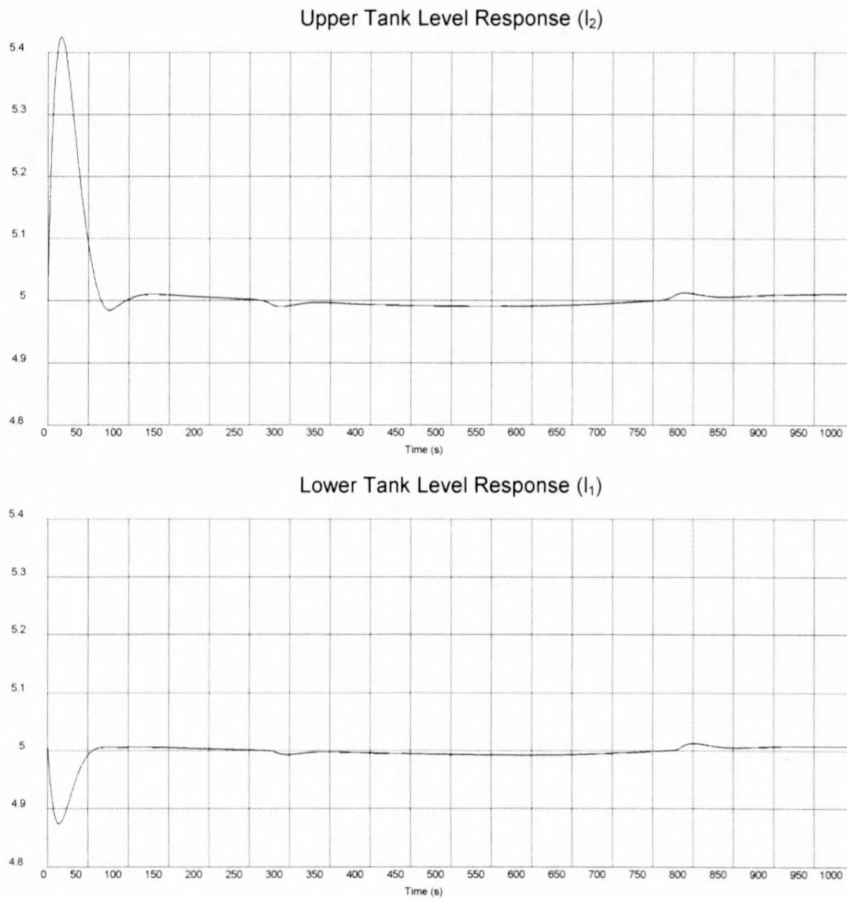**Figure 44:** Scenario 5 – valve command signals

Figure 45: Scenario 5 – disturbance signal

The step changes in the inlet flow rate of the upper tank disturbed both the upper and lower level control loops, which reflected in deviations in both levels. The upper level (l_2) was affected the most with a deviation of about 15% of step size from set-point. This was because the upper level was disturbed by a pulse disturbance, which had a higher bandwidth than the upper tank valve action, which consequently disturbed the lower level (l_1). The lower level was affected with a level deviation of about 10% of step size from the set-point. This experiment illustrates that disturbance dynamics faster than the closed loop response times of the control loops cannot be rejected perfectly by the controllers and will result in level deviations.

6.5.6 Scenario 6: Rejecting a sinusoidal disturbance in the feed flow rate

In this scenario levels l_2 and l_1 were regulated at level set-point 5V in the presence of a sinusoidal feed flow rate disturbance (Amplitude 1e-4 [m^3/s], Offset 2e-4 [m^3/s], Frequency 1e-3Hz) at the inlet to the upper tank unit. This was done using the SIMuWIN simulation schematic shown in Figure 32 with the square wave input block as reference input to the upper tank control loop replaced with a constant block to provide a constant reference input of 5V to the upper tank control loop. The square

wave reference input to the lower tank control loop was also replaced with a constant block to provide the constant reference input of 5V to the lower tank control loop. A sinusoidal signal input block was used to provide a sinusoidal feed flow rate, f_3, input to the upper tank unit as shown in Figure 48. The full range of the level measurements was 0V to 10V with 10V being full and 0V being empty. Full scale for the corresponding valve command signals was also 0V to 10V with 10V being open and 0V being closed. The level responses are shown in Figure 46 and the respective valve command signals in Figure 47.

Figure 46: Scenario 6 – levels

Upper Tank Valve Command (u₂)

Lower Tank Valve Command (u₁)
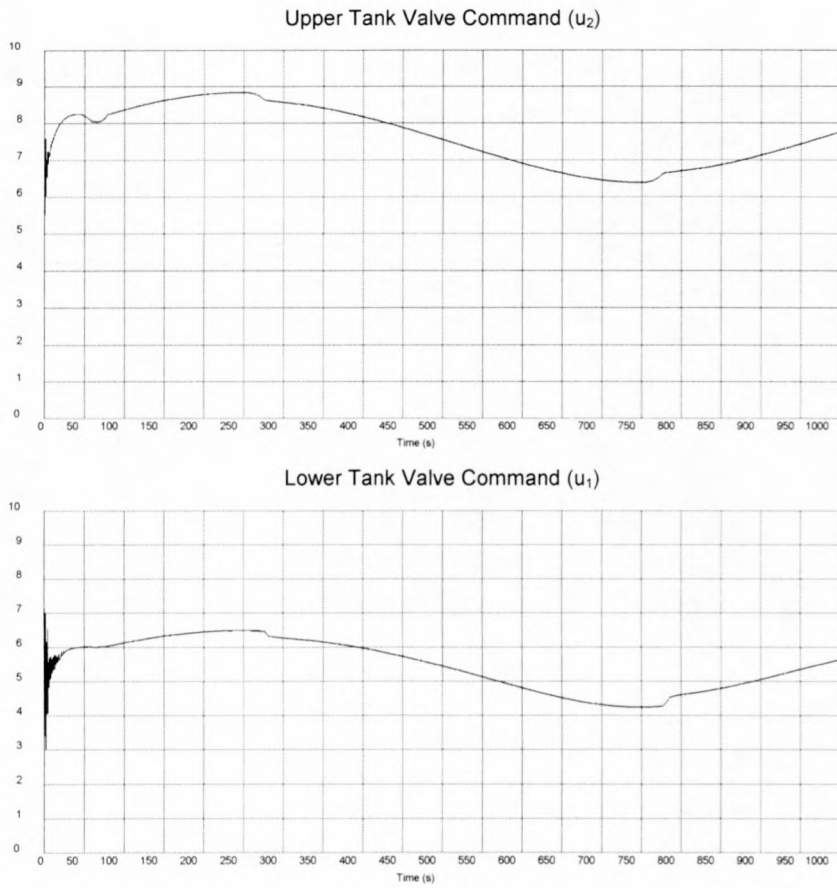
Figure 47: Scenario 6 – valve command signals

Feed Flow Rate Sinusoidal Disturbance f₃ [m³/s]
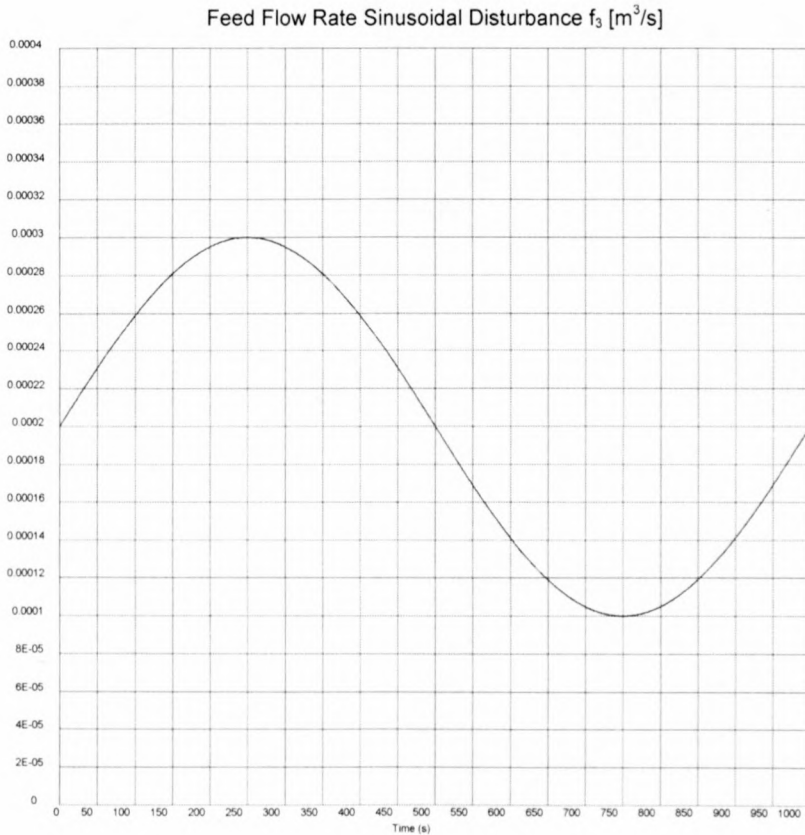
Figure 48: Scenario 6 – disturbance signal

This scenario showed that disturbance dynamics much slower than the closed loop response times of the control loops could be rejected by the controllers. Both controllers tracked the slow sinusoidal change in the inlet flow rate of the upper tank unit closely, resulting in little effect on the levels of both the upper and the lower tank units. The disturbance resulted in level deviations of about 2% of step size from the set-point in both upper and lower levels. Both levels were affected equally by the slow sinusoidal disturbance input flow rate (f_3). This was because both control loops tracked the disturbance closely resulting in the upper control valve (v_2) causing a sinusoidal flow rate (f_2) deviation of the same bandwidth than the feed flow rate disturbance input (f_3), which consequently had a equivalent disturbance effect on the lower level (l_1).

6.5.7 Scenario 7: Level responses to set-point changes at different steady state feed flow rates

In scenario 7 the results of two separate experiments were compared. In the first experiment levels l_2 and l_1 were alternated between level set-points 5V and 6V at a frequency of 2.5e-3Hz in the presence of a steady state feed flow rate (f_3) into the upper tank unit of 3e-4 m^3/s. In the second experiment levels l_2 and l_1 were again alternated between level set-points 5V and 6V at a frequency of 2.5e-3Hz, but this time in the presence of a different steady state feed flow rate (f_3) into the upper tank unit of 0.9e-4 m^3/s. Each of the experiments was done using the SIMuWIN simulation schematic shown in Figure 32 with the square wave input block as reference input to the upper tank control loop and the square wave reference input to the lower tank control loop used to step the upper and lower level set-points between 5V and 6V. The full range of the level measurements was 0V to10V with 10V being full and 0V being empty. Full scale for the corresponding valve command signals was also 0V to 10V with 10V being open and 0V being closed. The level responses are compared in Figure 49 and the valve command signals in Figure 50.
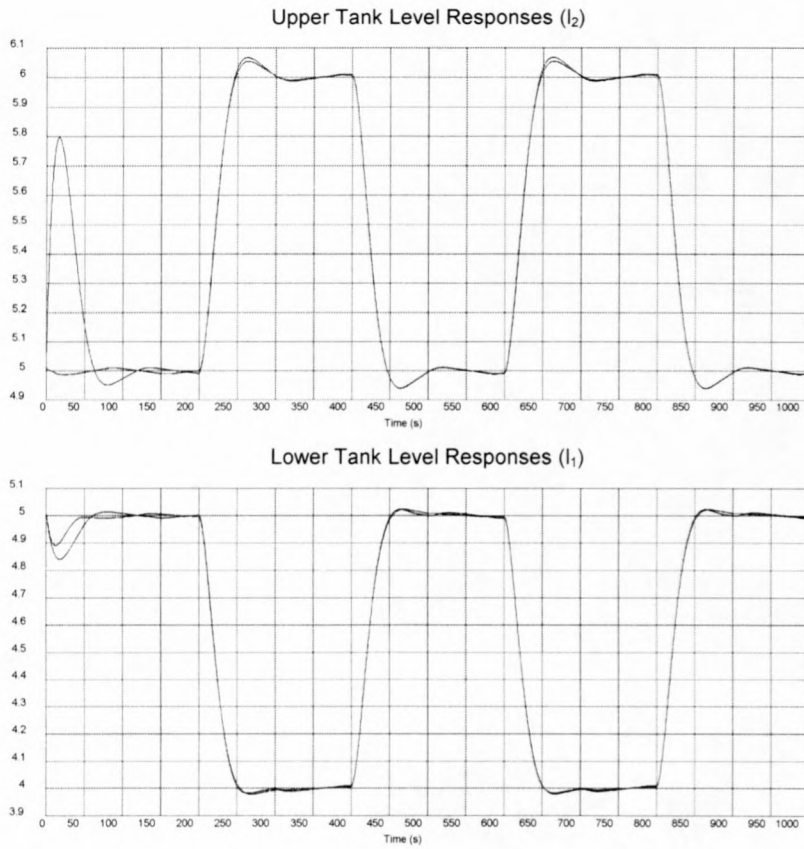
Upper Tank Level Responses (l₂)

Lower Tank Level Responses (l₁)

Figure 49: Scenario 7 – levels

Upper Tank Valve Commands (u₂)
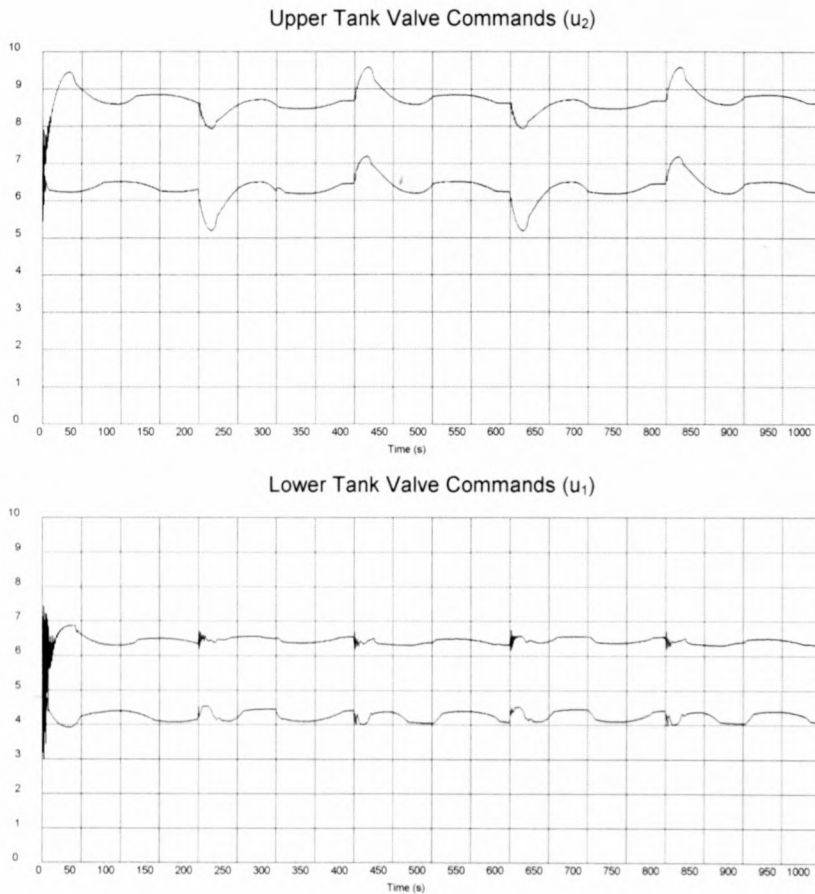
Lower Tank Valve Commands (u₁)

Figure 50: Scenario 7 – valve command signals

The upper tank valve command signal was centred around 8.75V and the lower tank valve command signal around 6.5V during the first experiment due to the higher steady state feed flow rate. In the same way the upper tank valve command signal was centred around 6.5V and the lower tank valve command signal around 4.25V during the second experiment due to the lower steady state feed flow rate.

Non-linearities in the valves gains resulted in different effective valve gains at different valve operating points. This caused a slight difference in closed loop responses of about 1% of step size in both upper and lower control loops. In this case the effect was small due to only a slight non-linearity in the valve gains. Non-linearity of valves is difficult to compensate for in control because movement through the valve operating range is usually too fast for adapting the controller settings. Correct sizing and choice of valves should rather ensure a linear operating range.

6.6 Summary of independent control loop simulation results

The different scenarios investigated in this chapter provided the following results:

The upper tank closed loop level response specifications were met with 90% accuracy and that of the lower tank unit with more than 99% accuracy. This implies that the upper tank linear control model was less accurate than the lower tank linear control model. The accuracy of the closed loop responses depends directly on the accuracy of the available linear models around the operating points.

Disturbances to upstream control loops were also passed on as disturbances to downstream control loops because the control loops acted independently. Because of the independence of the control loops, the lower level was disturbed by upper loop control actions with response times faster or in the same order than lower level closed loop response times. Flow disturbances of a low frequency nature however were tracked by the control loops and could therefore be rejected to a large extent.

Non-linearities in the control valve gains resulted in different closed loop level responses at different valve operating regions. This can not be compensated for by adapting controller settings because the valves move too quickly through their respective ranges during normal valve operation, which cause linear models to change much quicker than controllers can adapt to.

In the next chapter it will be shown how the two control loops were de-coupled in control so that feed rate disturbances only affected the upper level (l_2) and did not have an effect on the down-stream tank level (l_1).

Chapter 7

De-coupled Control Loops

This chapter presents a control approach, which recognises that each control loop is predominantly affected by the control loop upstream from it, and seeks to cancel this effect by means of feed-forward de-coupling. The result is control loops with no disturbance effects on downstream neighbours. The effects of feed flow rate disturbances on tanks levels of the cascaded tank system are therefore cancelled in the first tank and have no downstream effects on tank levels.

7.1 Operating conditions

Operating conditions were the same as described in section 6.1.

7.2 Model identification

A linear discrete time transfer function model was obtained for each tank unit from the control valve input to the level output by means of data driven system identification explained in Section 5.4. The linear process models were assumed to be as shown in Equation 47 and repeated here in Equation 53.

Equation 53

$$\begin{bmatrix} \partial h_2[z] \\ \partial h_1[z] \end{bmatrix} = G[z] \begin{bmatrix} \partial u_2[z] \\ \partial u_1[z] \end{bmatrix}$$

$$G[z] = \begin{bmatrix} G_{22}[z] & 0 \\ G_{12}[z] & G_{11}[z] \end{bmatrix}$$

$$G_{22}[z] = \frac{-0.001337z}{z^2 - 1.862z + 0.862}$$

$$G_{12}[z] = \frac{0.001175z}{z^2 - 1.874z + 0.8749}$$

$$G_{11}[z] = \frac{-0.001615z}{z^2 - 1.848z + 0.849}$$

7.3 Closed loop response specifications

The desired closed loop response for the compensated pilot plant was a second order response with a maximum overshoot of about 5% and a rise time of 50 seconds, as specified in Table 1.

7.4 Feed-forward de-coupling

In section 5.3.5 it was shown that each control valve has a primary effect on the tank levels directly upstream and downstream from it. It also has a secondary effect on levels further up and down stream that is usually negligible.

The effect of $\partial u_2[z]$ on $\partial h_1[z]$ can be cancelled through Equation 54 and Equation 55

Equation 54

$$\partial u_1[z] = \partial u_C[z] + \partial u_D[z]$$

where $\partial u_C[z]$ is the control signal from the second tank level controller

Equation 55

$$\partial u_D[z] = -\frac{G_{12}[z]}{G_{11}[z]} \partial u_2[z]$$

and where $\partial u_D[z]$ is the upper tank level control signal $\partial u_2[z]$ filtered with a feed-forward de-coupling filter.

Importance to note is that the approach of feed-forward de-coupling is not valid if the transfer function $G_{11}[z]$ has non-minimum phase zeros. This will cause the de-coupling filter to be unstable, destabilising the whole system.

Level control problems often contains delays that, if modelled with a linear transfer function model, result in non-minimum phase zeros. A way to overcome this is to look for a model structure with all minimum-phase zeros, or no zeros, or all zeros at $z = 0$, providing a reasonable approximation to the system that can be used for feed-forward de-coupling. If such a model structure cannot be found, feed-forward de-coupling is not possible. Furthermore, if it is the aim of the designer to combine feed-forward de-coupling with recursive LS estimation in an adaptive strategy, it is essential to use a model structure without zeros, or with all zeros at $z = 0$. This is to ensure that at no instant during estimator convergence or parameter tracking the model estimate contains a non-minimum phase zero that can destabilise the system.

In the case of the pilot plant, the model structure used in the alternative PID control design proved to be a good approximation to the system with resulting control loops achieving acceptable CL responses in Chapter 6. This second order model contains one zero at $z = 0$ and is perfectly suited for feed-forward de-coupling. If feed-forward de-coupling is added to the PID control design of section 6.4, the result is an integrated control strategy, which achieves the desired CL transient responses and in addition has the property that adjacent control loops have no disturbance effect on each other.

For this pilot plant the tank sizes and valves were identical and therefore the poles of $G_{12}[z]$ and $G_{11}[z]$ were more or less the same. The result was that de-coupling was possible by subtracting a scaled version of the upper valve command (u_2) from the lower valve command input (u_1). If this was not the case due to different valve types or sizing or differences in pressure potentials across the valves, the de-coupling

signal had to be a filtered version of the upper valve command signal as shown in Equation 55.

De-coupling was therefore achieved for this cascaded two tank system by subtracting a constant, $\dfrac{G_{12}}{G_{11}}$ = 0.001175/(-0.001337) = -0.88, from the lower valve command input (u_1), as shown in Figure 51.

7.5 Simulation of closed loop system

Simulations of the integrated PID design with feed-forward de-coupling were compared to the independent control loop PID design simulations of section 6.5 and the results are presented in the rest of this chapter. The simulations were done using the exact same SIMuWIN schematic as shown in Figure 32 and described in Chapter 6 except for a de-coupling gain block that was added to the schematic as shown in Figure 51.
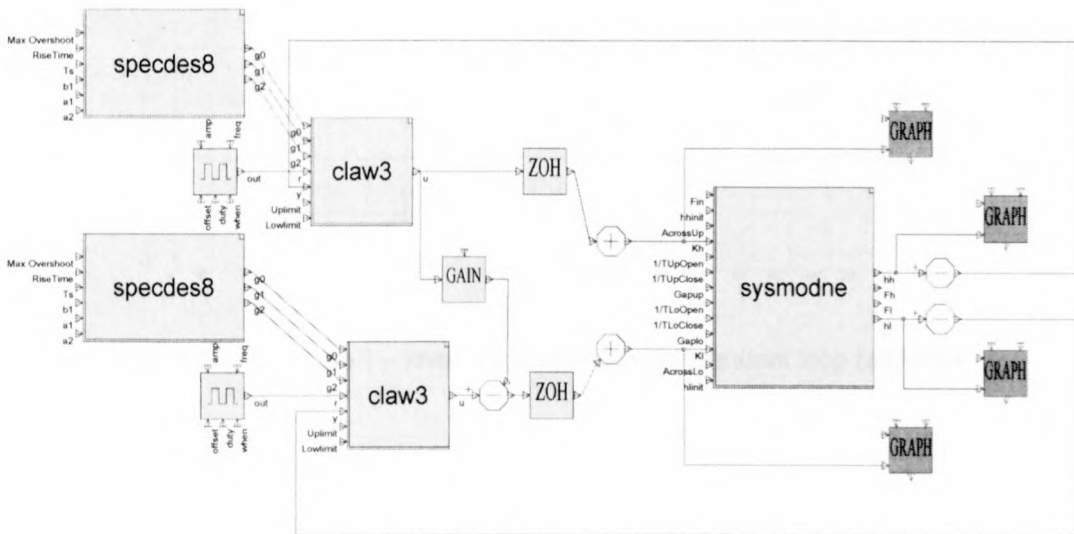

Figure 51: SIMuWIN – De-coupled controllers simulation

Different scenarios were simulated to illustrate the performance of the two separate control loops with feed-forward de-coupling on the pilot plant. In each figure the simulation results of the de-coupled control loops are compared with the results of the same scenario outlined in Chapter 6.
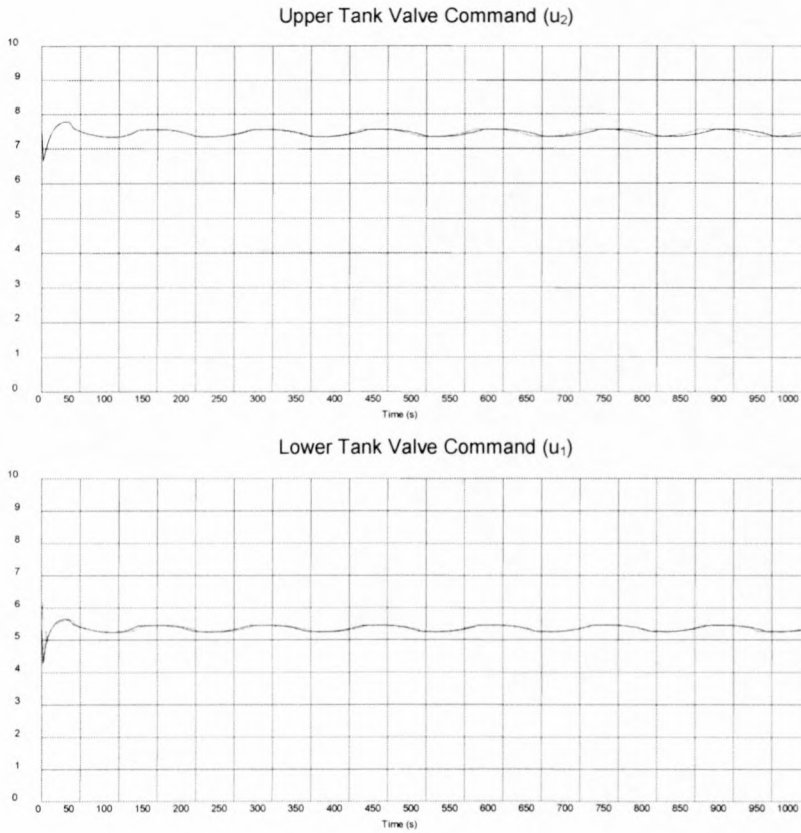
7.5.1 Scenario 1: Regulating levels at set-points.

Scenario 1 as described in section 6.5.1 was repeated here for the SIMuWIN schematic shown in Figure 51. The results are discussed below and shown in Figure 52 and Figure 53. The dotted lines in the figures are the compared responses of the equivalent scenario in Chapter 6.
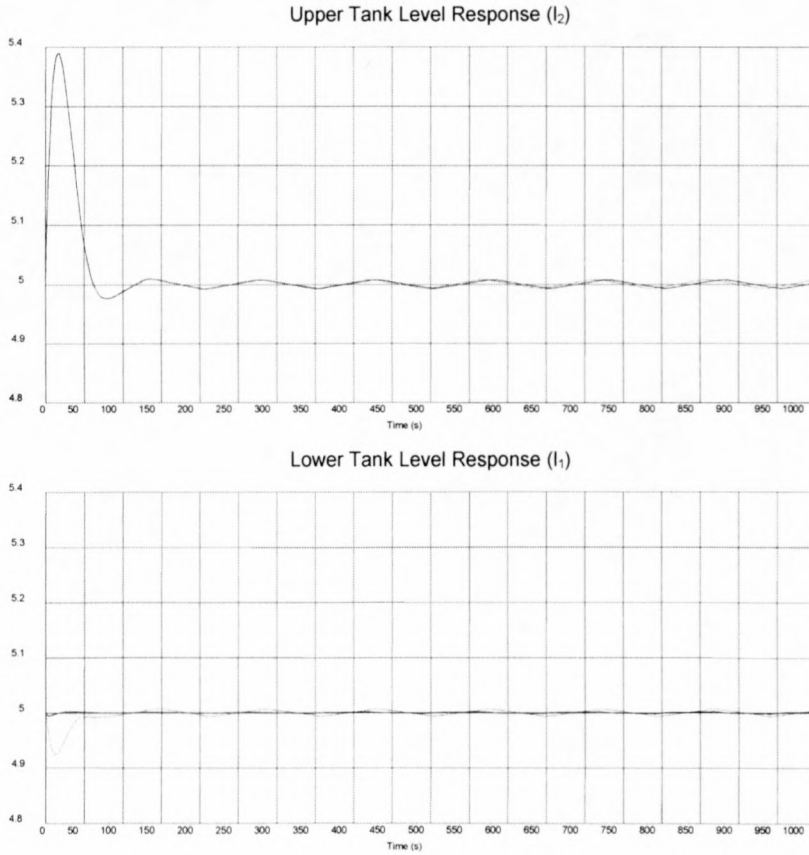
Figure 52: Scenario 1 – levels (dotted line is independent loop response)

Upper Tank Valve Command (u_2)
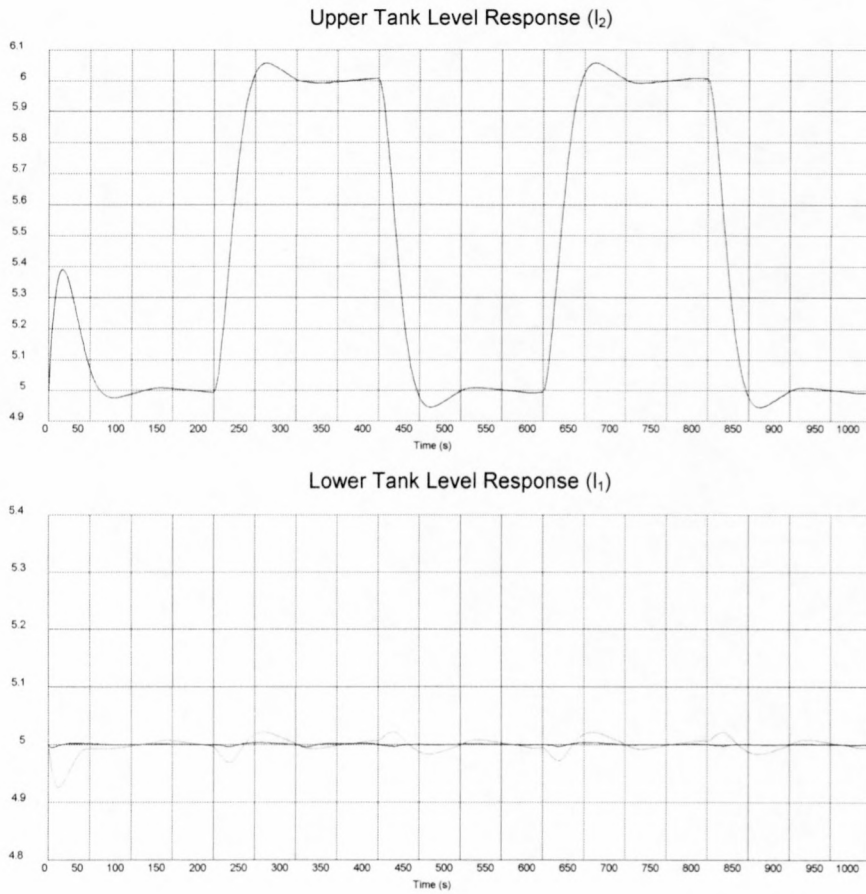
Lower Tank Valve Command (u_1)

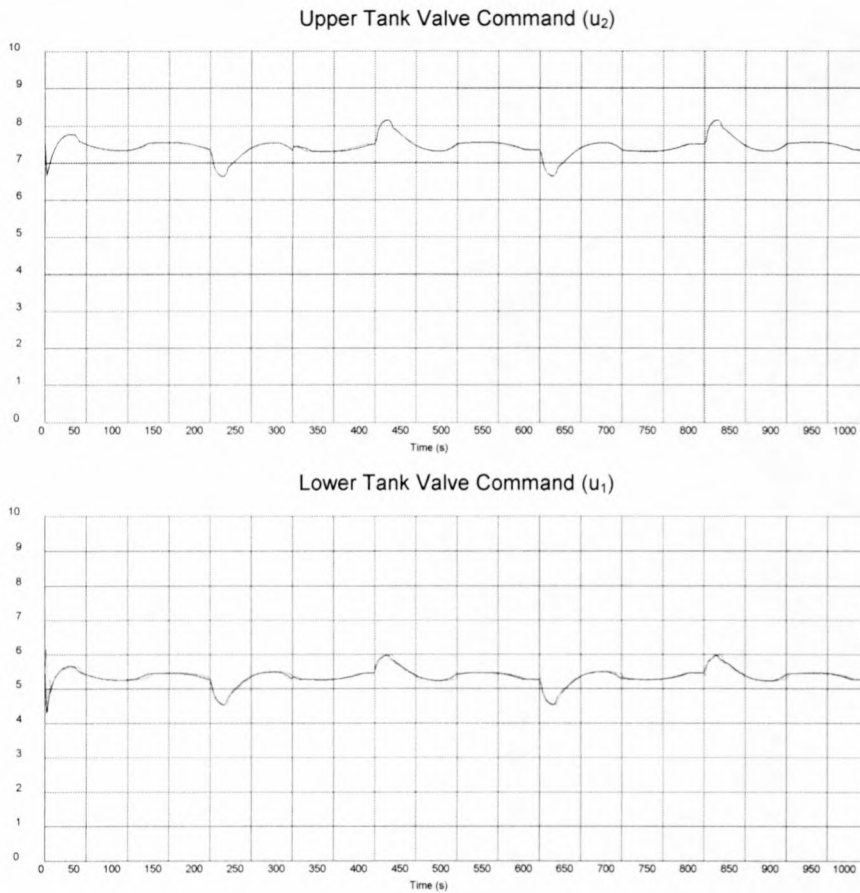**Figure 53:** Scenario 1 – valve command signals (dotted line is independent loop response)

Feed-forward de-coupling only affects the lower level response. The de-coupling signal cancels any disturbance effects that the upper tank control valve (v_2) may have on the lower tank level (l_1). This resulted in a negligible lower level regulation error compared to the lower level regulation error of 1% of step size (1V) without feed-forward de-coupling as shown in section 6.5.1.

7.5.2 Scenario 2: Regulating lower level while stepping upper level.

Scenario 2 as described in section 6.5.2 was repeated here for the SIMuWIN schematic shown in Figure 51. The results are discussed below and shown in Figure 54 and Figure 55. The dotted lines in the figures are the compared responses of the equivalent scenario in Chapter 6.

Upper Tank Level Response (l_2)

Lower Tank Level Response (l_1)

Figure 54: Scenario 2 – levels (dotted line is independent loop response)
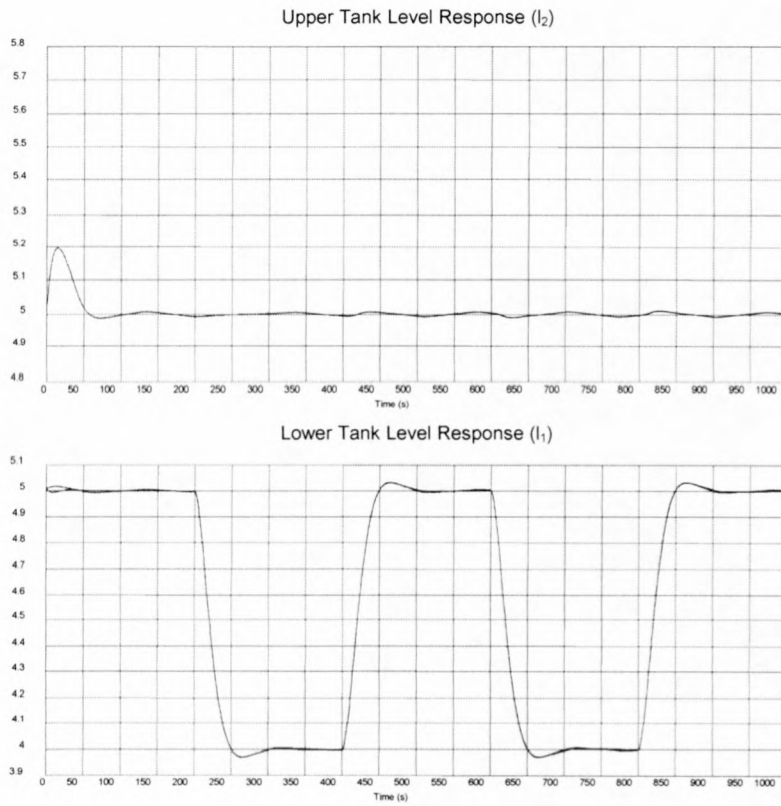
Figure 55: Scenario 2 – valve command signals (dotted line is independent loop response)

Without de-coupling the upper tank control valve actions disturb the lower tank level. The de-coupling signal cancels any disturbance effects that the upper tank control valve (v_2) may have on the lower tank level (l_1). This resulted in a negligible lower level regulation error of less than 1% of step size (1V) compared to the lower level regulation error of 5% of step size without feed-forward de-coupling, as shown in section 6.5.2.

7.5.3 Scenario 3: Regulating upper level while stepping lower level.

Scenario 3 as described in section 6.5.3 was repeated here for the SIMuWIN schematic shown in Figure 51. The results are discussed below and shown in Figure 56 and Figure 57. The compared responses were almost identical in this case.

Figure 56: Scenario 3 – levels (de-coupled response compared with independent loop response – almost identical)
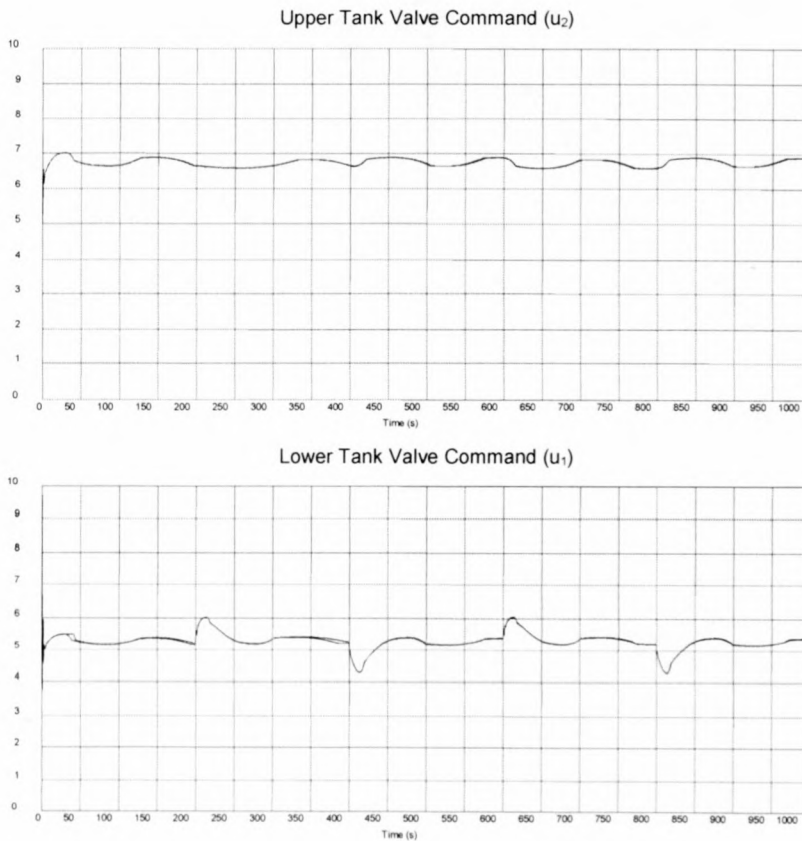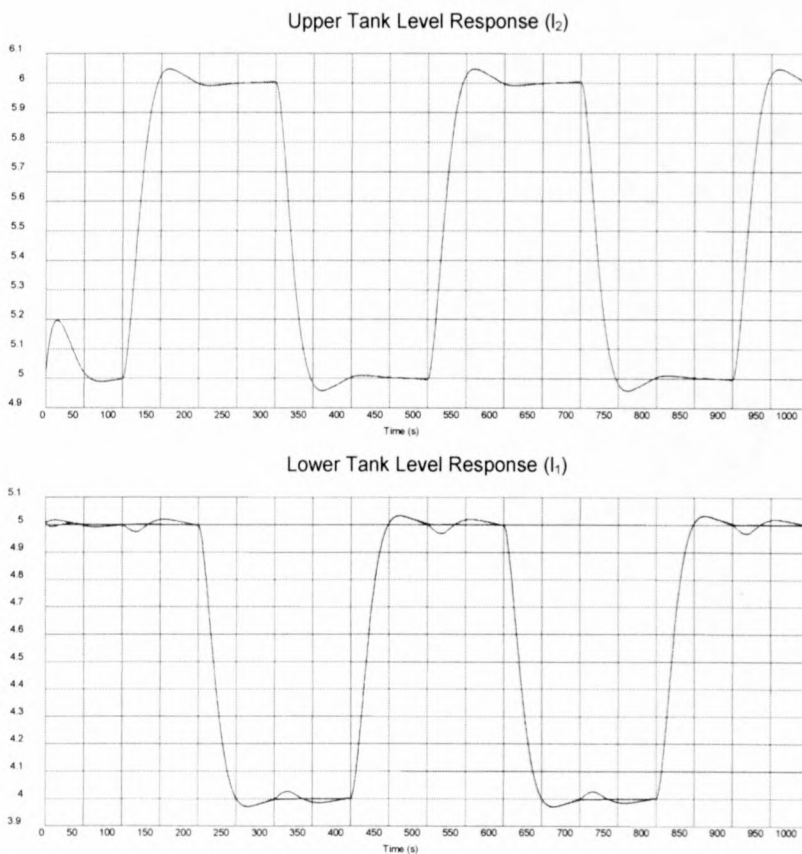

Figure 57: Scenario 3 – valve command signals (de-coupled response compared with independent loop response – almost identical)

In this scenario the level responses with and without feed-forward de-coupling were almost identical. This was because changes in the lower tank control valve (v_1) do not have any disturbing effect on the upper tank level (l_2). Furthermore the feed-forward de-coupling only cancels upper tank control valve (v_2) effects on the lower level (l_1). In this case there were no changes in the upper tank control valve that could disturb the lower tank level and would have needed to be cancelled.

7.5.4 Scenario 4: Stepping both levels simultaneously.

Scenario 4 as described in section 6.5.4 was repeated here for the SIMuWIN schematic shown in Figure 51. The results are discussed below and shown in Figure 58 and Figure 59.

Figure 58: Scenario 4 – levels (de-coupled response compared with independent loop response – de-coupled is the less disturbed response of the lower tank level)
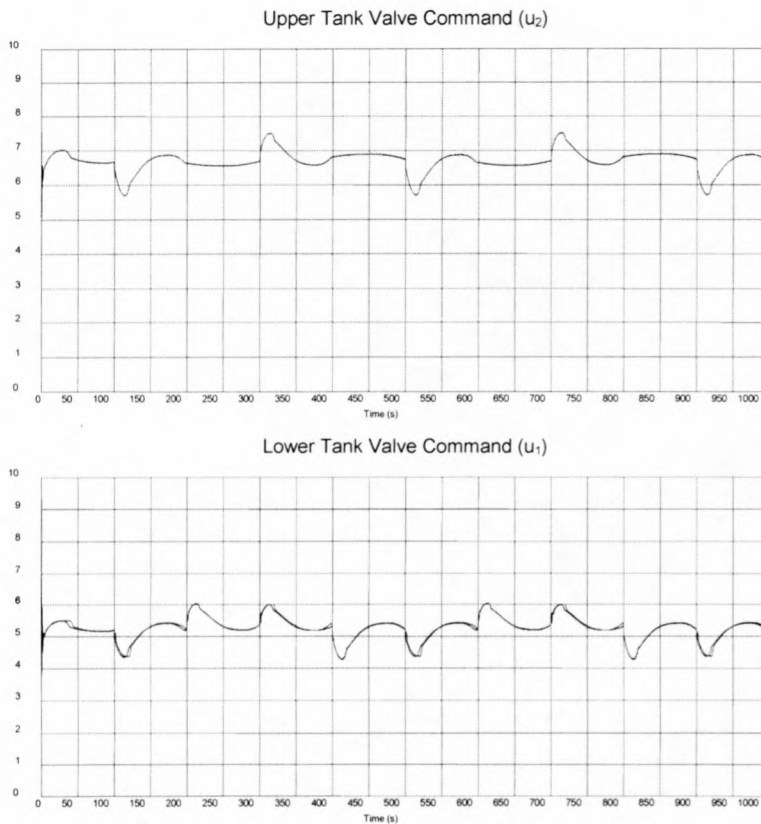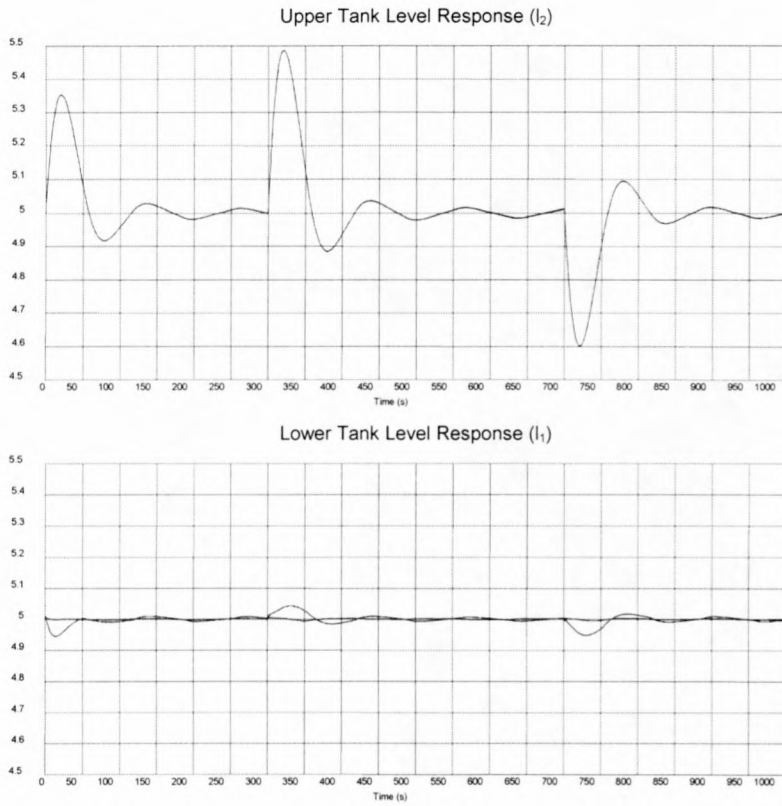
Figure 59: Scenario 4 – valve command signals (de-coupled response compared with independent loop response)

Step changes in the upper tank level set-point disturbed the closed loop set-point tracking performance of the lower tank level in the absence of feed-forward de-coupling as shown in section 6.5.4. With feed-forward de-coupling these disturbance effects are cancelled resulting in upper level set-point changes having no effect on the set-point tracking performance of the lower tank level as specified in section 7.3.

7.5.5 Scenario 5: Rejecting a Step disturbance in the feed flow rate.
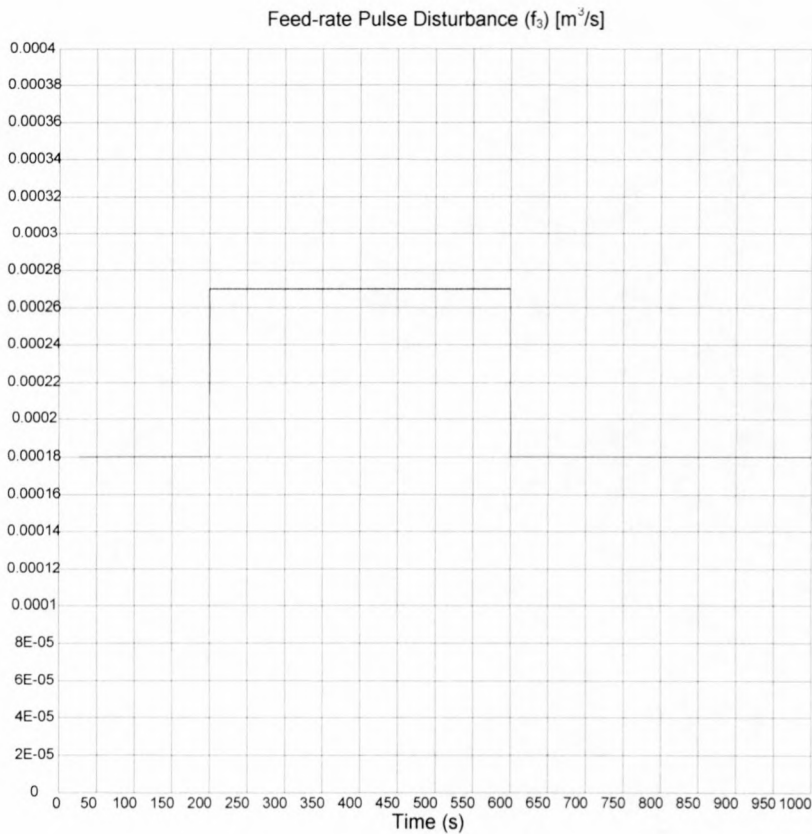
Scenario 5 as described in section 6.5.5 was repeated here for the SIMuWIN schematic shown in Figure 51. The results are discussed below and shown in Figure 60, Figure 61 and Figure 62.

Figure 60: Scenario 5 – levels (de-coupled response compared with independent loop response – de-coupled is the less disturbed response of the lower tank level)
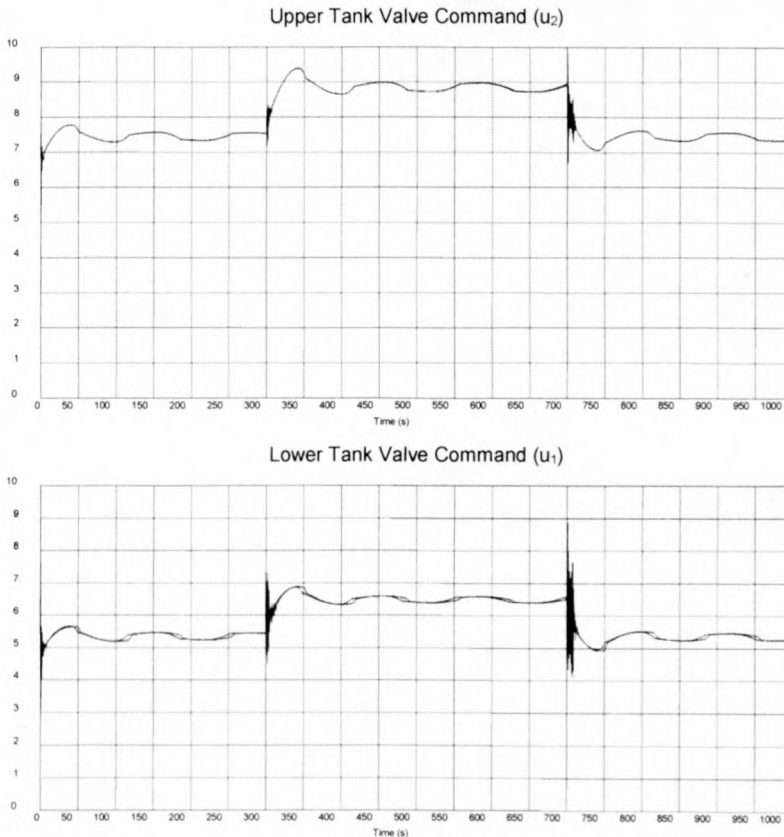
Figure 61: Scenario 5 – valve command signals (de-coupled response compared with independent loop response)

Figure 62: Scenario 5 – Feed-rate flow disturbance

Any high bandwidth feed flow rate (f_3) disturbance disturbs the upper tank level and without feed-forward de-coupling also the lower tank level as seen in section 6.5.5. Feed-forward de-coupling cancels the effect that this flow disturbance might have on the lower level, resulting in the lower level not being affected by the flow disturbance as shown in Figure 60.

7.5.6 Scenario 6: Rejecting a Sinusoidal disturbance in the feed flow rate.

Scenario 6 as described in section 6.5.6 was repeated here for the SIMuWIN schematic shown in Figure 51. The results are discussed below and shown in Figure 63, Figure 64 and Figure 65. The dotted lines in the figures are the compared responses of the equivalent scenario in Chapter 6.
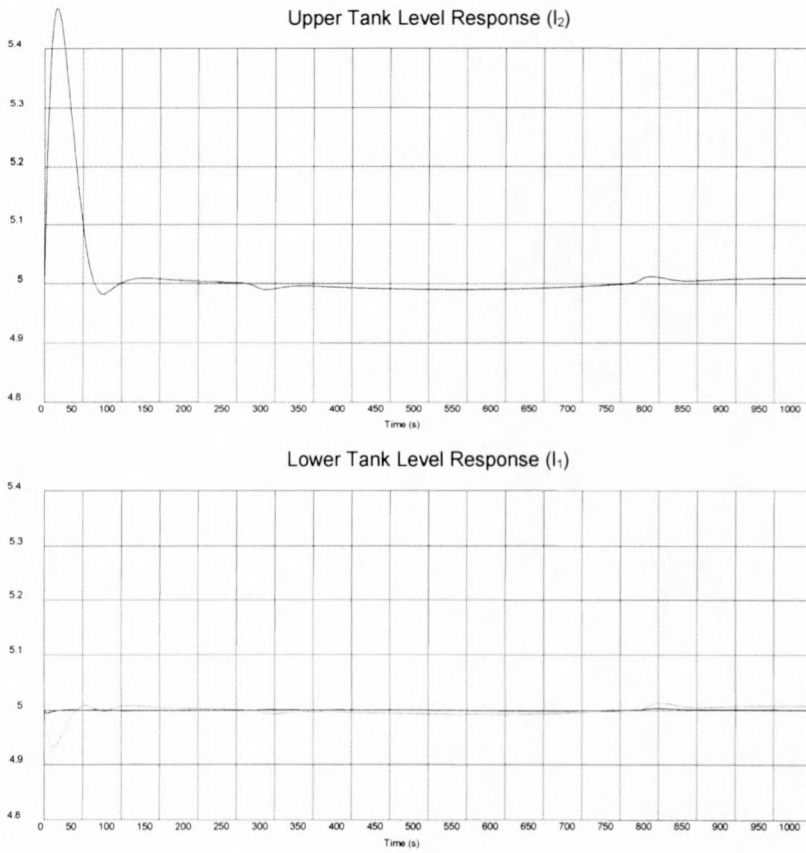
Figure 63: Scenario 6 – levels (dotted line is independent loop response)
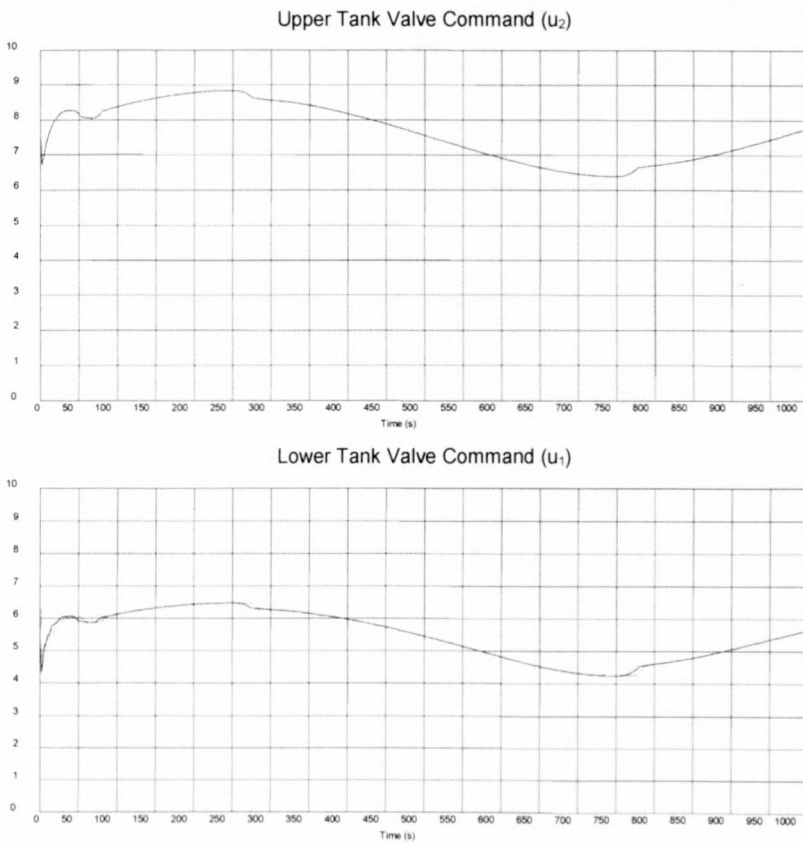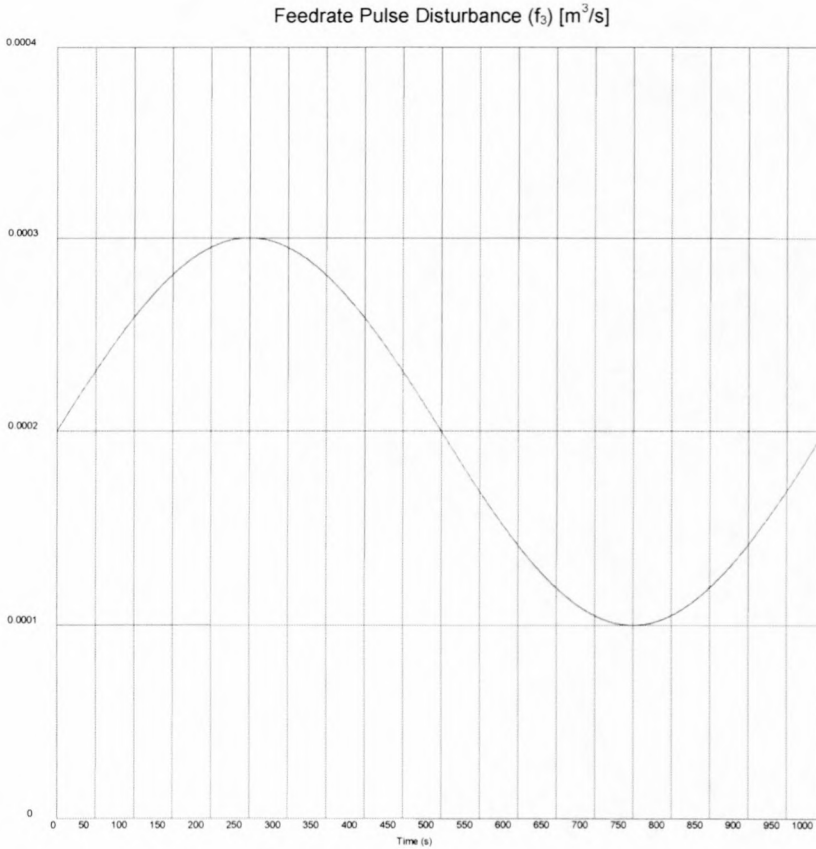

Figure 64: Scenario 6 – valve command signals (dotted line is independent loop response)

Figure 65: Scenario 6 – Feed-rate flow disturbance

Any lower bandwidth feed flow rate (f_3) disturbance as shown in Figure 65 is rejected by the upper tank level control loop and has only a small disturbance effect on the upper tank level (l_2) as illustrated in section 6.5.6. Feed-forward de-coupling cancels this small disturbance effect so that the lower level (l_1) is not affected by the flow rate disturbance as shown in Figure 60.

7.5.7 Scenario 7: Level responses to set-point changes at different steady state feed flow rates.

Scenario 7 as described in section 6.5.7 was repeated here for the SIMuWIN schematic shown in Figure 51. The results are discussed below and shown in Figure 66 and Figure 67.

Upper Tank Level Response (l_2)

Lower Tank Level Response (l_1)
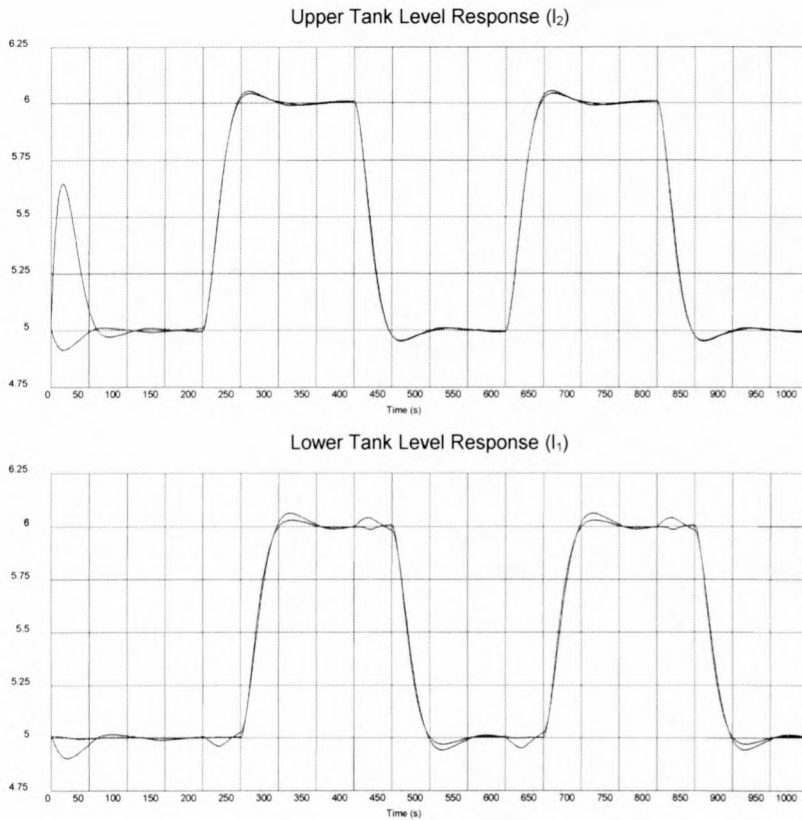
Figure 66: Scenario 7 – levels (de-coupled response compared with independent loop response – de-coupled is the less disturbed response of the lower tank level)

Upper Tank Valve Command (u_2)

Lower Tank Valve Command (u_1)
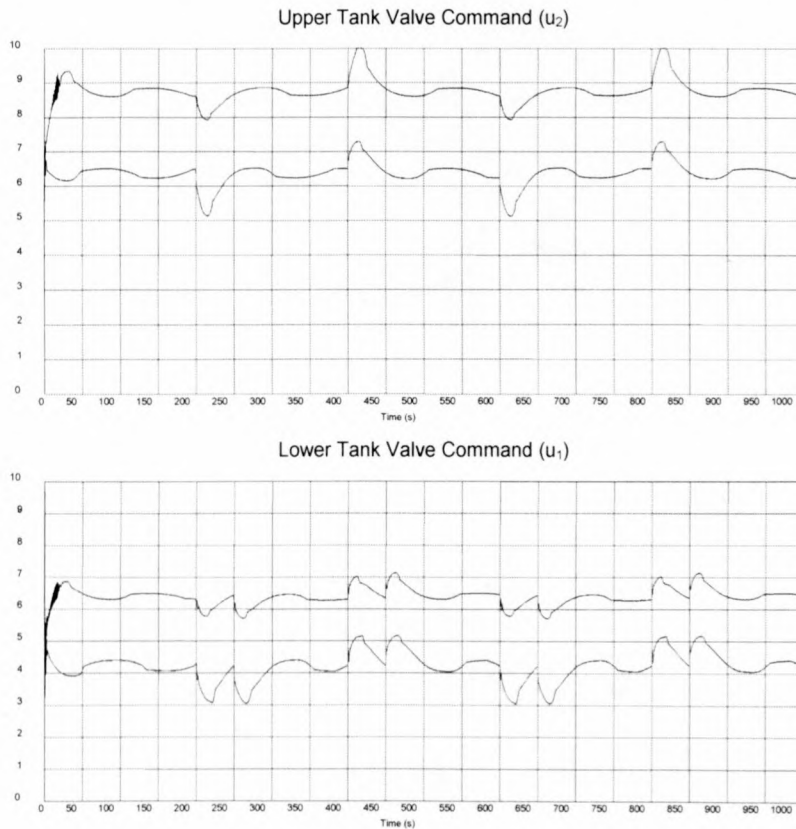
Figure 67: Scenario 7 – valve command signals (de-coupled response compared with independent loop response)

In the absence of feed-forward de-coupling step changes in the upper tank level set-point disturb the closed loop set-point tracking performance of the lower tank level (l_1), as shown in section 6.5.7. With feed-forward de-coupling these disturbance effects are cancelled resulting in upper level set-point changes having no effect on the set-point tracking performance of the lower tank level as specified in section 7.3.

7.5.8 Summary of de-coupled control simulation

Feed-forward de-coupling of consecutive level control loops was illustrated in this chapter. It was shown how feed-forward de-coupling cancels the disturbance effects that upstream control actions have on downstream tank levels. By doing this consecutive control loops are effectively isolated from each other so that each tank level is independently controllable resulting in more consistent closed loop performance. It was also illustrated that accurate feed-forward decoupling is only possible if accurate linear models are available and can only be implemented safely for appropriate model structures which will ensure all time stability as discussed in section 7.4.

Having presented and compared the level control strategies of independent control loops in Chapter 6 vs. feed-forward de-coupling in Chapter 7, Chapter 8 will now conclude on the level control research done for thesis and discuss possibilities for future research.

Chapter 8

Conclusions

In this thesis two control strategies that can be applied to level control in cascaded flotation processes were investigated and compared namely independent PID control loops vs. PID control loops with feed-forward de-coupling. This was done using a two tank cascaded pilot plant with identical tank units and control valves.

8.1 A review of the chapters

Chapter 1 gave an overview of the history and current status of level control in flotation processes and also pointed to the importance of weighing up performance against cost in choosing a control system. Chapter 2 described the pilot plant and experimental set-up used for the level control research done for this thesis also stating control objectives for the pilot plant. In Chapter 3 a comprehensive simulation model of the pilot plant was developed that could be used to design, test and compare different control strategies in a simulation environment which is low cost, risk free and not subject to the time constants of normal plant operations. Chapter 4 considered the range of available control technologies and selected a specific form of PID control as a suitable technique for level control in cascaded flow processes. Chapter 5 showed how linear models could be deduced for the purpose of controller design using data driven system identification and more fundamental techniques and considerations. In Chapter 6 and Chapter 7 the two different control strategies were evaluated and described. The last chapter, Chapter 8, is a summary of the findings of this study, some conclusions and ideas for future research.

8.2 A summary of the results

In giving a summary of the findings of the study as presented throughout this thesis, the following can be said:

It has been illustrated by other studies [19] and was re-confirmed by this study that de-coupled level control outperforms independent control loops in a level control system for cascaded flow processes like froth flotation. Independent control loops propagate level disturbances to downstream tank units because each control valve is unaware of the control actions of upstream control valves. An integrated PID control strategy with feed-forward de-coupling as presented in this thesis compensates for the control actions of upstream valves so that a flow disturbance affects only the first tank level in a cascaded arrangement of tank units. This makes the level of each tank unit independently controllable. The use of the selected PID control law together with the direct pole placement design technique makes it possible for the control engineer to specify explicit closed loop performance in terms of the desired rise time and maximum overshoot, giving the control engineer full control over the behaviour and aggressiveness of the controller. The selected combination of techniques can also easily be extended to a self-tuning strategy by adding an on-line model parameter estimator to the control system. PID control makes the solution simple, cost effective and easy to maintain relative to other more complex control techniques.

The study also pointed out that non-linearities in cascaded flow processes affects the plant models deduced and used for controller design and therefore directly affects control system performance. These non-linearities can not always effectively be compensated for by the control system and should be addressed in the design phases of the process by choosing control valves, instruments, tank units and a process configuration, which ensures linearity and controllability. It is important to realise that the hardware design and configuration of the process determines the controllability of the levels within a cascaded tank system. Crucial hardware design issues in level control include valve sizing, tank shape, sizing and difference in altitude relative to adjacent tanks in the cascaded system. Controllers cannot compensate for issues like incorrect sizing of control valves, lack of gravity pressure head due to shallow levels and incorrect placement of adjacent tanks.

It has also been shown how valuable data driven batch system identification techniques can be in selecting model structures and calculating model parameters, but that it can never be divorced from a thorough fundamental analysis of the process.

8.3 Possibilities for future research

This thesis assumed a time invariant process and proposed a set of controllers based on fixed plant models for a pilot plant using water as a flow medium. In practice these plant model might change over time due to changes in pulp density and composition, which will result in a degrading of closed loop control performance and ask for controller adjustment, a high amount of robustness again model variation or a self-tuning strategy which poses possibilities for further research.

A subject that might deserve more attention is the effect of measurement noise on the proposed control strategy. This thesis focused on meeting certain time domain closed loop specification without placing much emphasis on robustness in the midst of specifically high noise levels. An investigation of the noise properties of the proposed PID control strategy with feed-forward decoupling might be a subject for further research.

As this thesis focused on the use of PID control in cascade flow processes the question remains of how much can be gained in performance and robustness by looking at more complex and advanced control and system identification techniques.

In general the field of cascaded level control and specifically flotation level control is very important, as level control systems are crucial for stability and optimum performance in these processes.

Bibliography

[1] A.F. Taggart, *Handbook of Mineral Dressing*, Wiley (1945).

[2] K. L. Sutherland and I.W. Wark, *Principles of Flotation*, Australasian IMM (1955).

[3] M. Gaudian, *Flotation*, McGraw-Hill (1957).

[4] D.W. Fuerstenau (Ed.), *Froth Flotation - 50th Anniversary Volume*, AIME/SME (1962).

[5] M. Gaudin, *1900 - Flotation*, McGraw-Hill, (1957).

[6] N. Arbiter and C.C. Harris, "Flotation Machines", Ch. 14 in *Froth Flotation - 50th Anniversary Volume*, D. W. Fuerstenau (Ed.), AIME/SME (1962).

[7] C. C. Harris, "Flotation Machines", Ch. 27 in *Flotation - A. M. Gaudin Memorial Volume*, M. C. Fuerstenau (Ed.), AIME/SME (1976).

[8] C. Dorenfeld, "Flotation Circuit Design", Ch. 15 in *Froth Flotation - 50th Anniversary Volume*, D. W. Fuerstenau (Ed.), AIME/SME (1962).

[9] K. Fallenius, "Outokumpu Flotation Machines", Ch. 29 in *Flotation - A. M. Gaudin Memorial Volume*, M. C. Fuerstenau (Ed.), AIME/SME (1976).

[10] V. R. Degner and H.B. Treweek, "Large Flotation Cell Design and Development", Ch. 28 in Flotation - A. M Gaudin Memorial Volume, M. C. Fuerstenau (Ed.), AIME/SME (1976).

[11] T. M. Plouf, "Large Volume Flotation Machine Development Criteria and Plant Testing: Denver Equipment Division's Single Mechanism 1275 ft^3 (36 m^3) DR Flotation Machine", *Proc. 13th Int. Miner. Process. Congr. Warsaw. 1979*, Elsevier (1981).

[12] J.A Finch and G.S. Dobby, *Column Flotation*, Pergamon Press (1990).

[13] D.G. Hulbert and R.G.D. Henning, *Flotation Plant Control*, SAIMM School: Process Simulation, Control and Optimisation, (18-20 August 1993).

[14] D.J. Mckee, *Automatic Flotation Control - A Review of 20 Years of Effort*, Minerals Engineering, Vol. 4, Nos 7-11, pp. 653-666, (1991).

[15] H. W. Smith, *Computer Control in Flotation Plants*, Flotation, M.C. Fuerstenau (Ed.), AIME, New York, N.Y., (1976), pp. 963-993.

[16] J.A. Herbst and O.A. Bascur, *Conductivity Interface Detector for Pulp Level and Froth Level Control*, Patent disclosure, University of Utah, Salt Lake City, (January 15, 1981).

[17] O.A. Bascur, M. Steven and J.A. Herbst, *Sonic Interface Detector for Flotation level and Froth Depth Control*, Patent disclosure, University of Utah, Salt Lake City, (January 20, 1981).

[18] O.A. Bascur and J.A. Herbst, *Light Attenuation Sensor for Flotation Pulp Level and Froth Depth Control*, Patent disclosure, University of Utah, Salt Lake City, (February 15, 1981).

[19] J.H. Schubert, R.G.D. Henning, D.G. Hulbert, and I.K. Craig, *Flotation Control – A Multivariable Stabilizer*, Proceedings of the 19th International Minerals Processing Conference, Vol. 3, (1995), pp 237-241.

[20] R.A. Serway, *Physics for Scientists & Engineers with Modern Physics*, Third edition, Updated version, International edition, Saunders College Publishing, (1992), pp 407.

[21] G. F. Franklin, J. D. Powell, and M. L. Workman, *Digital Control of Dynamic Systems*, 2nd ed. Reading, MA: Addison-Wesely, (1990).

[22] P.E. Wellstead and M.B. Zarrop, *Self-Tuning Systems* Control and Signal Processing, John Wiley & Sons Ltd. (1991)

Appendix A

Level Sensors

Differential pressure transducers were used to measure the water level in each tank. This appendix explains the dynamic behaviour and calibration of the level sensors.

The differential voltage obtained from the differential pressure to voltage transducers used as level sensors were amplified with a simple two-stage operational amplifier circuit with anti-aliasing filtering as shown in Figure 68. Anti-aliasing filtering was necessary to get rid of high frequency energy in a signal that will corrupt the signal when sampled at a specific sample rate.
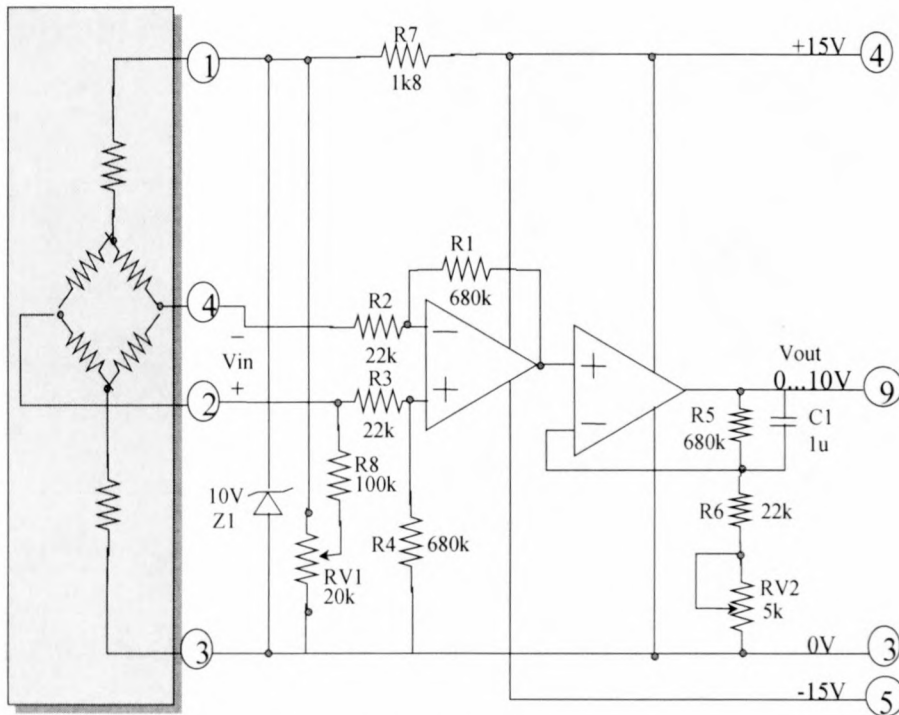
Figure 68: Level sensor circuitry

In the circuit of Figure 68 the variable resistors RV1 and RV2 were used to calibrate the circuit; RV1 to zero the output signal when the tank is empty and RV2 to adjust the amplifier gain to give an output voltage of 10V when the tank is full. Capacitor C1

111

served as the anti-aliasing filter resulting in an amplifier circuit -3dB bandwidth of 0.24Hz as shown in Figure 69.
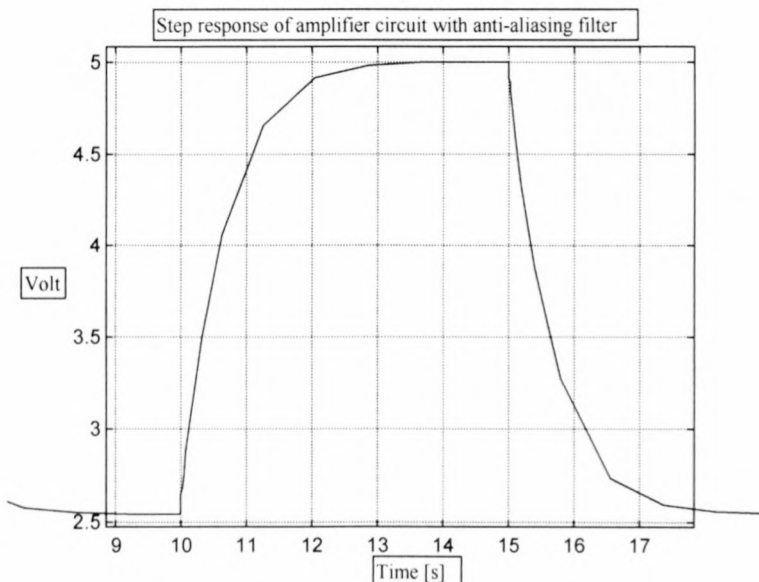
A.1 The Dynamic behaviour of the level sensor circuitry:

The -3dB cut-off frequency of the anti-aliasing filters was 0.24Hz as shown in Figure 69.
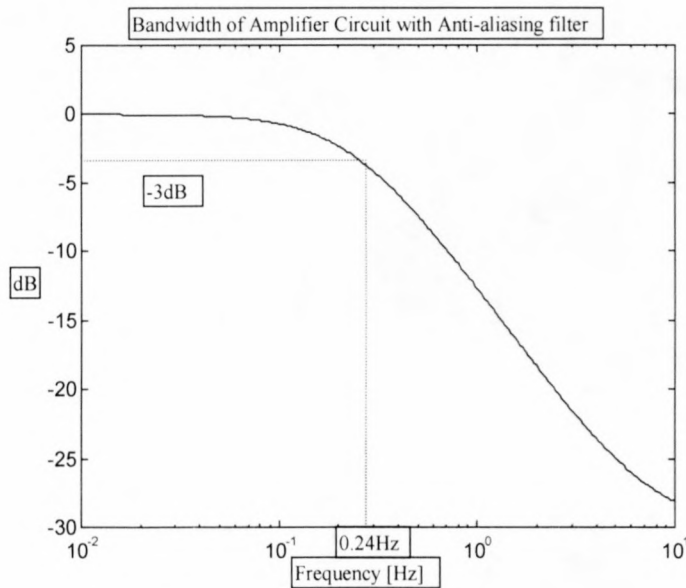
Figure 69: Bandwidth of level sensor circuitry

The step response simulated for the amplifier circuit with anti-aliasing filter is shown in Figure 70. The rise time was approximately 3s with a 66% time constant of 0.6s.

Figure 70: Step response of level sensor circuitry

A.2 Sample rate selection

The Nyquist sampling criterion states that to prevent aliasing, the sample rate should be at least two times higher than the highest frequency component of the signal being sampled. For smooth control however sample rates should not be lower than about 6 times the highest frequency component. From the literature a good sample rate prove to be 20 times the highest frequency component of the signal being sampled. The sample rate was therefore chosen as 4Hz, which is about 20 times the bandwidth 0.24Hz of the anti-aliasing filter.

A.3 Determining the Static Gains of the Level sensors

The sensors gains were determined by taking three voltage and level readings over the range of possible levels and then fitting a first order polynomial to obtain the sensors gains and offsets.
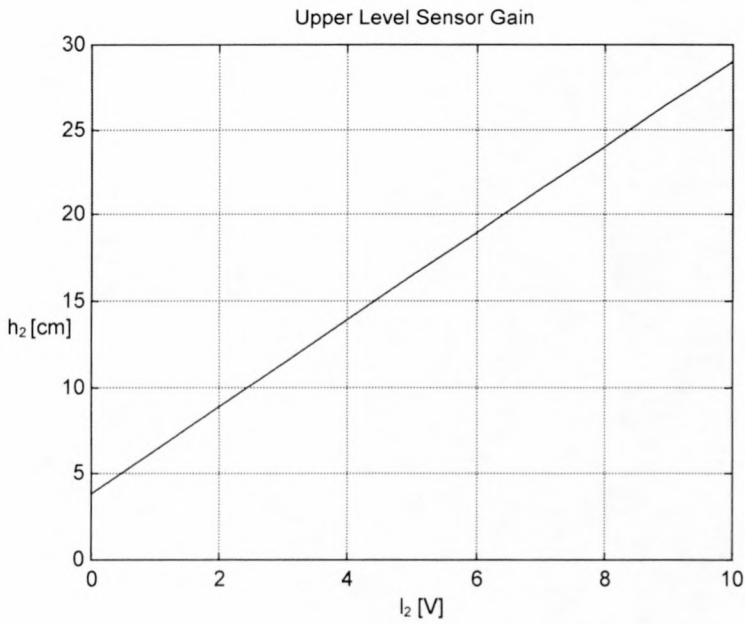
Upper Tank

Tank level – h_2 [cm]	Transducer reading – l_2 [V]
10	2.44
22	7.17
27	9.2

Table 13: Upper Tank – level sensor static gain

A first order polynomial, shown in Figure 71, was fitted through the data points in Table 13.

Figure 71: Upper Tank – level sensor static gain

The level height (h_2) was related to the level sensor reading (l_2) through Equation 56.

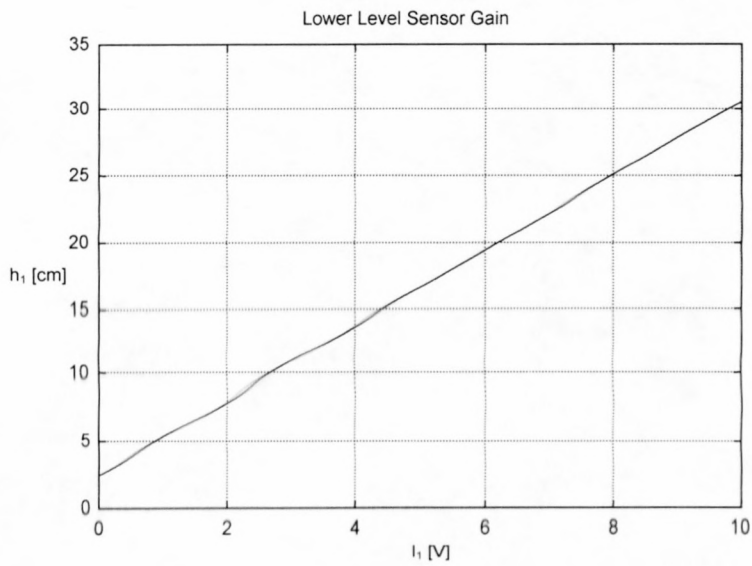**Equation 56**

$$h_2 = 2.52l_2 + 3.87$$

h_2 is the upper tank level [cm] and l_2 is the upper tank transducer reading [V] as shown in Figure 2. The sensor gain was therefore 2.52 and the sensor offset was 3.87.

Lower Tank

Tank level – h_1 [cm]	Transducer reading – l_1 [V]
5	0.87
15	4.46
25	7.97

Table 14: Lower Tank – level sensor static gain

A first order polynomial, shown in Figure 72, was fitted through the data points in Table 14.

Figure 72: Lower Tank – level sensor static gain

The level height (h_1) was related to the level sensor reading (l_1) through Equation 57.

Equation 57

$$h_1 = 2.81 l_1 + 2.54$$

h_1 is the lower tank level [cm] and l_1 is the lower tank transducer reading [V] as shown in Figure 2. The sensor gain was therefore 2.81 and the sensor offset was 2.54.

# Appendix B

Effect of Toricelli's law on Feed Flow Rate

The simulation model developed in Chapter 3 assumes that the feed flow rate f_3 to the upper tank as shown below in Figure 73 is an independent disturbance input variable to the simulation model that can be set to an constant value of choice within its available operating range. This appendix presents the test that was done to determine to what extent that assumption holds true.
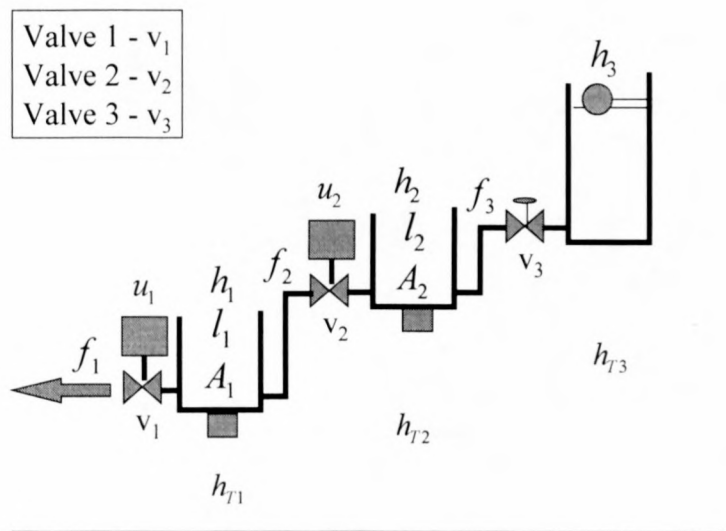
Figure 73: Valves, variables and dimensions

The reservoir feeding the flow system is kept approximately full by means of a floating ball valve. This is to keep a constant pressure at the outlet to the lower tanks. The constant reservoir water level h_3 is about 30 cm, approximately the same as $h_{2\,max}$. The elevation of the reservoir above the upper tank is 57cm. When

opening valve v_3 fully the level of the reservoir tank drops to a lowest point of 25cm before the ball valve opens up enough to keep it constant. To check the effect of Toricelli's law[2] on flow rate f_3 over the full range of l_2, valve v_3 was opened fully with valve v_2 shut, filling the upper tank while recording level l_2 at a sample rate of 4Hz. From this data flow rate f_3 was computed to see how it was affected by changes in the levels of the upper tank and reservoir. In the computations it was assumed that the reservoir level remains constant at 27cm.
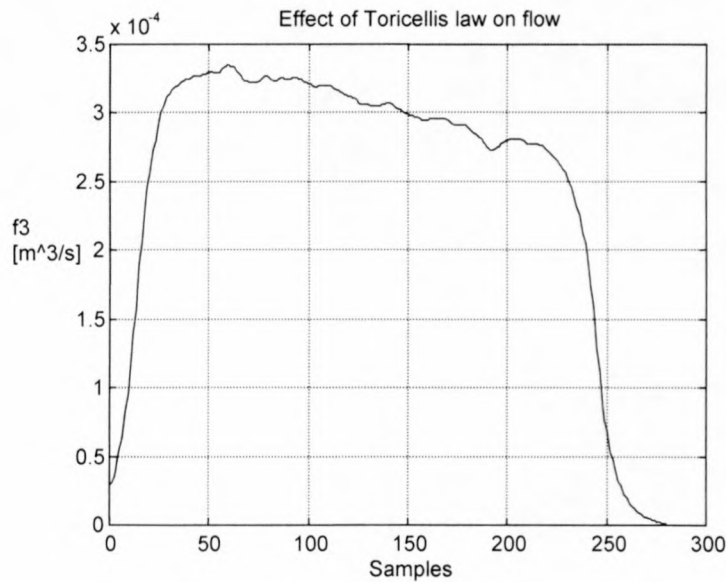
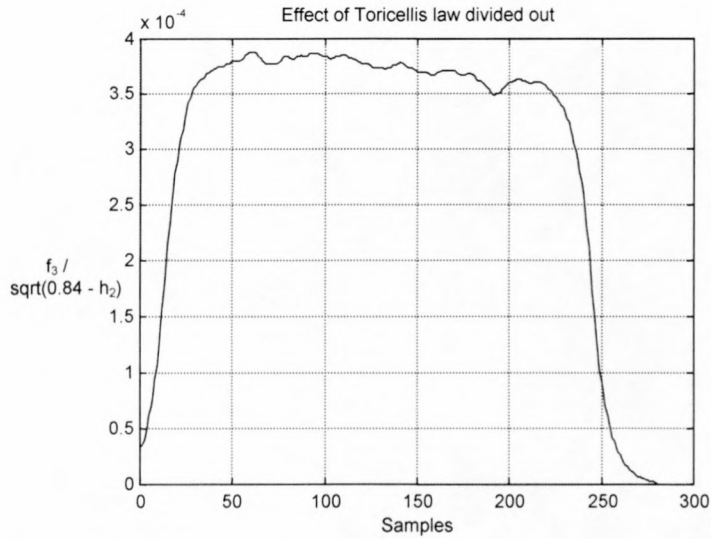**Figure 74:** Effect of Toricelli's law on feed flow rate

It is clear from Figure 74 that the flow was not constant over the recorded period. This was due to changes in level. To confirm the effect of Toricelli's law the flow was divided by a square root factor as shown in Equation 58 and the result plotted against level as shown in Figure 75.

Equation 58

$$\frac{f_3(t)}{\sqrt{(0.57+0.27)-h_2(t)}} = const$$

---

[2] Toricelli's law: The speed of efflux of a liquid from a small hole at the bottom of an open tank is equal to that acquired by a body falling freely through a vertical distance equal to the height of the liquid level above the point of efflux.

Figure 75: Effect of Toricelli's law on feed flow rate divided out

Figure 75 shows that the flow divided by the square root of the level as stated in Equation 58 is nearly constant over time. This confirms the effect of Toricelli's law on flow f_3.

In the simulation model only flows f_1 and f_2 and levels l_1 and l_2 were modelled. f_3 was viewed as a disturbance. It was used as an independent input variable to the model than can be set to any desired value within its maximum and minimum limits and it was assumed to be unaffected by level l_2.

Appendix C

Hysteresis

This appendix describes how hysteresis can be identified and measured in dynamic systems.

Hysteresis or otherwise known as backlash, is a non-linearity commonly found in dynamic systems, especially mechanical systems and other systems with memory or play. To identify and characterize hysteresis in a system it is necessary to consider its affect on system dynamics and control as well as how it differs from other linear system dynamic elements like transportation delays and first order time constants.

The characteristic difference between hysteresis and other system dynamics is that the system response as a result of hysteresis alone remains unchanged regardless of the frequency of the input signal.

C.1 Defining hysteresis

Hysteresis can be mathematically described in the following way with u being the input and y the output variable:

With u increasing and u_0 the value of u when it starts to increase:

$$y = f(u_0) \text{ for } u_0 < u < u_0 + \Delta u,$$
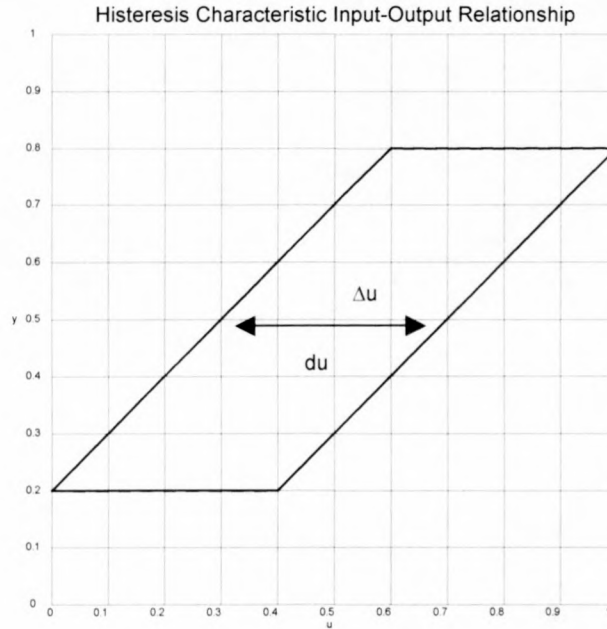
$$y = f(u) \text{ for } u \geq u_0 + \Delta u,$$

With u decreasing and u_1 the value of u when it starts to decrease:

$$y = f(u_1) \text{ for } u_1 - \Delta u < u < u_1,$$

$$y = f(u) \text{ for } u \leq u_1 - \Delta u,$$

with Δu describing the amount of hysteresis present and characterising the non-linearity.

Hysteresis can be graphically represented as shown in Figure 76 below.

Figure 76: Hysteresis characteristic input/output relationship

In Figure 76 the gap (du) is entirely due to and therefore represents the amount of histeresis in the system. As stated before, the amount of histeresis (Δu) in a system is independent of input signal frequency.

C.2 Identifying hysteresis

It is the frequency independent characteristic of hysteresis that is used to distinguish it from other system dynamics. To identify hysteresis or any type of system dynamics, it is necessary to make sure that the input signal stimulates the dynamics or trigger the non-linearity, otherwise it will not be visible in the input/output signal relationship.

The aim is therefore to single out or identify a selected component of the dynamics or a specific non-linearity. It is ideal if only that selected dynamic component or non-linearity is stimulated by the input signal. This is not always possible, but can always be strived towards by choosing the input signal to be as selective as possible.

One method of identifying hysteresis is to stimulate the system with an appropriate input signal and plot the input/output signal relationship (X-Y plot). If the X-Y plot has the form of Figure 76, the gap might be entirely or partially due to either histeresis (Δu) or other system dynamic effects. If the gap (du) is entirely due to histeresis (Δu), du = Δu, as in Figure 76. It can also be that the gap (du) is not due to histeresis, but due to other system dynamic effects as explained in the sections below.

C.2.1 Hysteresis vs. Time constant:

The input/output relationship of system dynamics can look very similar to hysteresis and can easily be mistaken for it. If the input signal is not totally selective the input/output plot can also reflect the combined effect of stimulated system dynamics and hysteresis. There is however ways to quantify the effect of dynamics as oppose to hysteresis contributing to the X-Y plot.
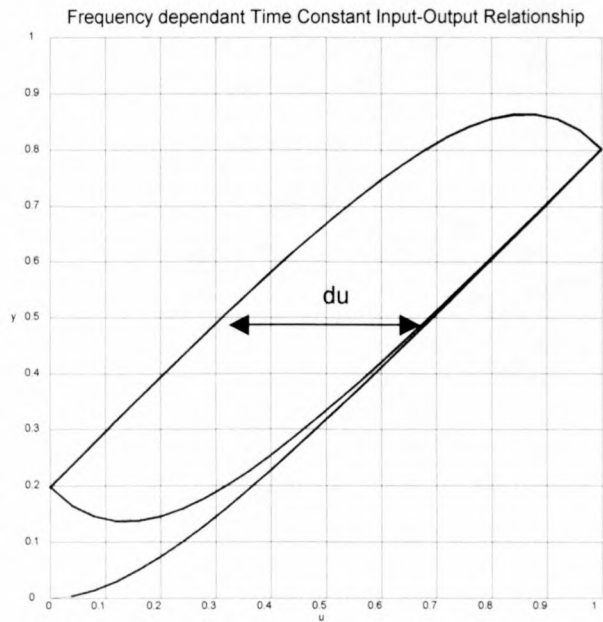
Figure 77: Time constant X-Y plot

Figure 77 shows the X-Y plot of a first order time constant of 0.1s when stimulated with an input signal of frequency 1Hz. Notice that when the input signal changes direction the output still increases for a while (depending on the value of the time constant) before it flattens and starts to decrease, following the input. The gap (du) in the case of a first order time constant can be computed from the relationship:
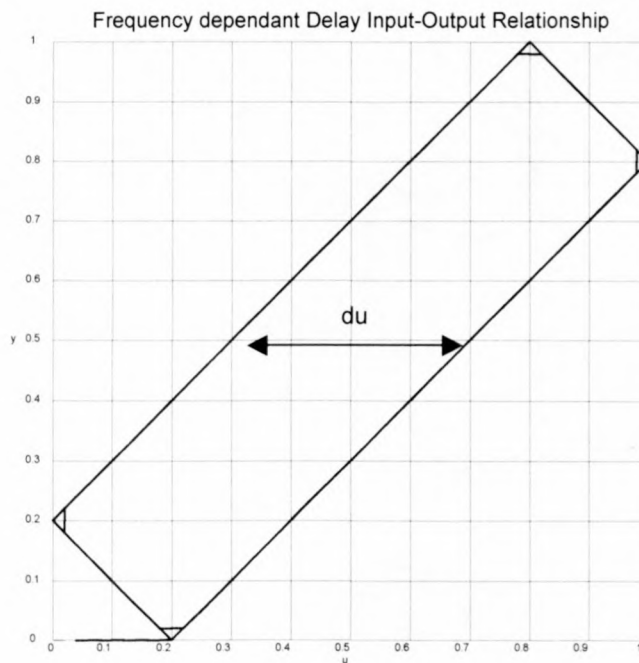
Equation 59

$$du = 4f\tau$$

where f is the frequency of the input signal and τ the time constant. When it is not possible to distinguish from the form of the input/output plot whether it is hysteresis or a time constant revealing itself, Equation 59 states the way to make sure. From Equation 59 it is evident that the gap (du) resulting from a time constant is directly proportional to the frequency of the input signal whereas the gap resulting from hysteresis is fixed regardless of frequency. If the input signal frequency is doubled, du should also double if the gap is entirely due to a time constant. If du remains the same it is entirely due to histeresis (Δu).

C.2.2   Hysteresis vs. Transportation delay:

Figure 78: Transportation delay X-Y plot

Figure 78 shows the X-Y plot of transportation delay of 0.1s when stimulated by an input signal of frequency 1Hz. Notice that when the input signal changes direction in the case of time delay, the output still keeps on increasing for the duration of the delay before it starts to decrease, following the input.

The gap (du) in the case of pure transportation delay can be computed from Equation 60.

Equation 60

$$du = 4f\delta$$

where f is the frequency of the input signal and δ the delay time. When it is not possible to distinguish from the form of the X-Y plot between hysteresis and pure transportation delay, Equation 60 suggests how to make sure. From Equation 60 it is evident that the gap (du) resulting from transportation delay is directly proportional to the frequency of the input signal, just as in the case of a time constant, whereas the gap resulting from hysteresis is fixed regardless of frequency. If the input signal frequency is doubled, du should also double if the gap is purely due to transportation delay. If the gap (du) is due to histeresis (Δu), it should remain constant.

Many times a combination of Transportation Delay, Time Constant and Hysteresis is present in a dynamic system, in which case the choice of an input signal becomes very important to selectively distinguish amongst these elements.

Because it is not always possible to stimulate only one at a time by the correct choice of input signal, it often happens that the input/output plot is the combined result of two or more of the elements in action as shown in Figure 79, which is the result of the system in Figure 80.

Histeresis, Time Constant and Delay combined Input-Output Relationship
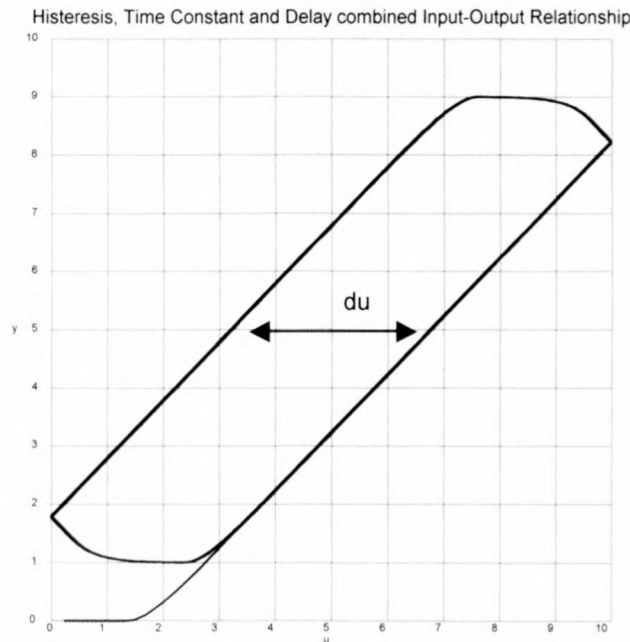
Figure 79: Hysteresis, Time Constant and Transport Delay combined X-Y plot
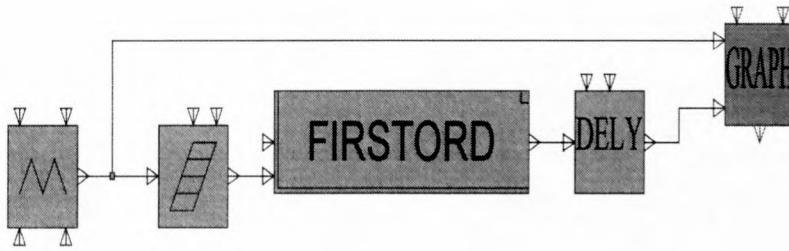
Figure 80: Hysteresis, time constant and transport delay system

In this case the amount of hysteresis can be found in the following way. First plot the input/output relationship for the system with input signal of frequency f_1 and measure the gap du_1. Then plot the input/output relationship for system again, but for input signal of frequency f_2 and measure the gap du_2. The amount of hysteresis can then be found by solving for it from Equation 61 and Equation 62

Equation 61

$$du_1 = \Delta u + y$$

Equation 62

$$du_2 = \Delta u + \frac{f_2}{f_1} y$$

where Δu is the portion of the gap due to histeresis. y is the portion of the gap due to the combination of other frequency dependant system dynamic effects in the X-Y plot for a input signal with frequency f_1.

## C.2.3 Choosing input signals to identify hysteresis:

From Equation 59 and Equation 60 it is evident that when the frequency of the input signal approaches zero, so also does the gap contribution in the X-Y plot due to time delay and time constant dynamics, while the gap due to hysteresis remains fixed. Therefore to measure hysteresis in a system, choose the input signal frequency as low as possible to minimize the effects of system transient dynamics on the X-Y plot.

Shown below is input/output plots for the system if Figure 80 with hysteresis 0.1, time delay 0.1s and time constant 0.1s. Figure 81 is the result of an input signal of

frequency 0.5Hz. The plot is dominated by the effects of the time delay and time constant, with the effect of the hysteresis not even visible. In Figure 82 where the input signal frequency was 0.01Hz, the effects of the delay and time constant on the plot is negligible and the gap is practically only due to the effect of hysteresis.

Time Constant, Time Delay and Histeresis Input/Output Plot
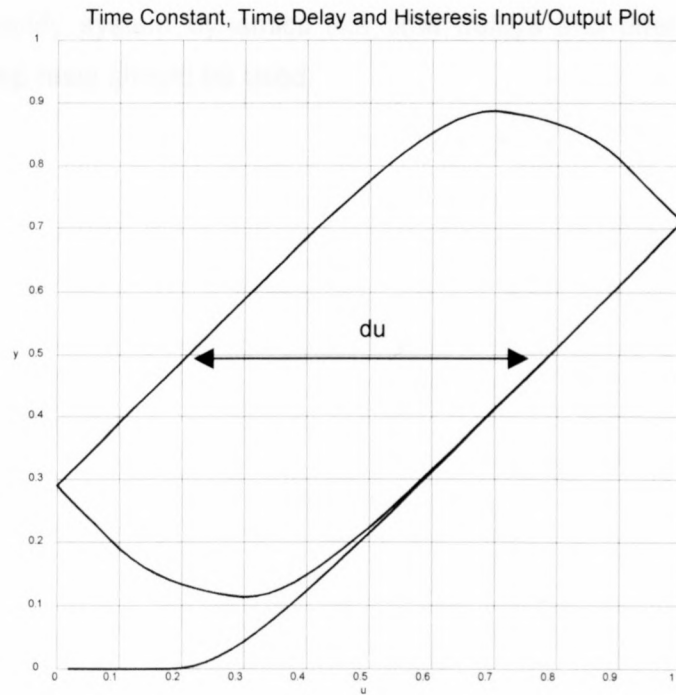
Figure 81: Time constant and time delay dominated X-Y plot

Time Constant, Time Delay and Histeresis Input/Output Plot
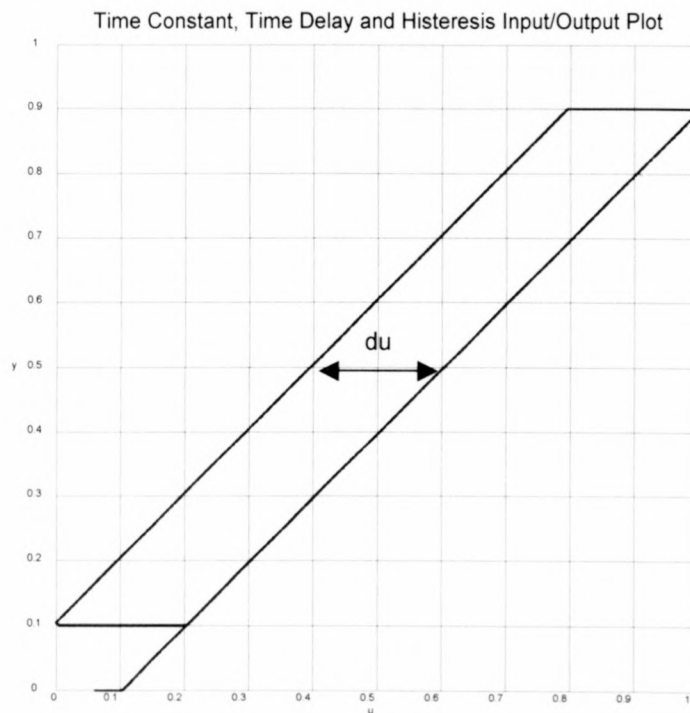
Figure 82: Hysteresis dominated X-Y plot

C.3 Measurement and Identification of system dynamics:
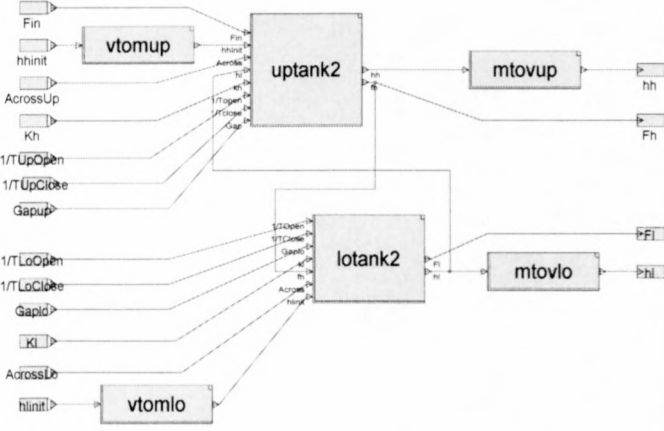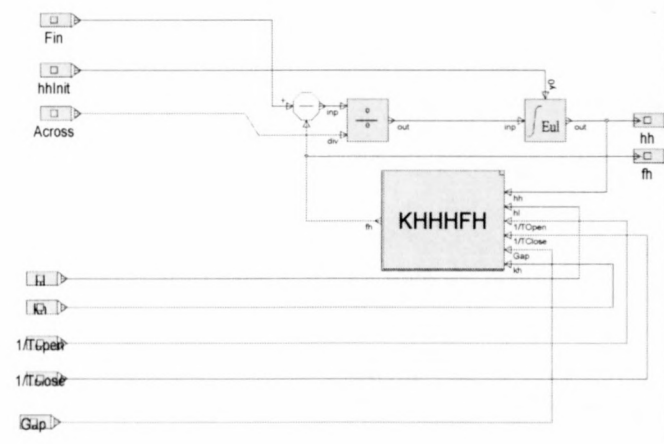
It is not possible to distinguish between and accurately measure time delays and time constants from X-Y plots due to their similar frequency dependence. If the aim is to measure or identify system dynamics like time delays and time constants, other methods like step tests should be used.
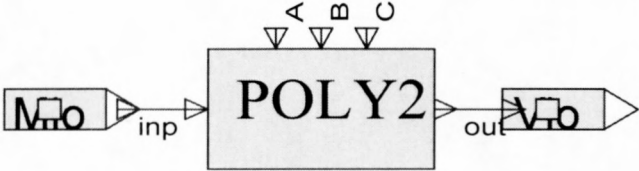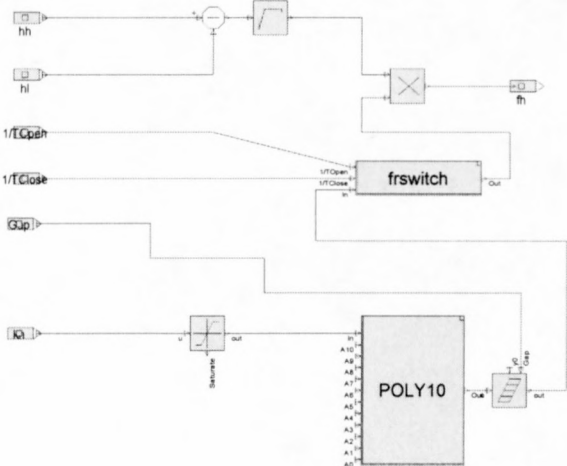
Appendix D

SIMuWIN Implementation

This appendix shows the implementation of the simulation model in SIMuWIN by presenting the contents and parameters of all blocks and superblocks of the complete simulation model in a hierarchical order in Table 15 below.
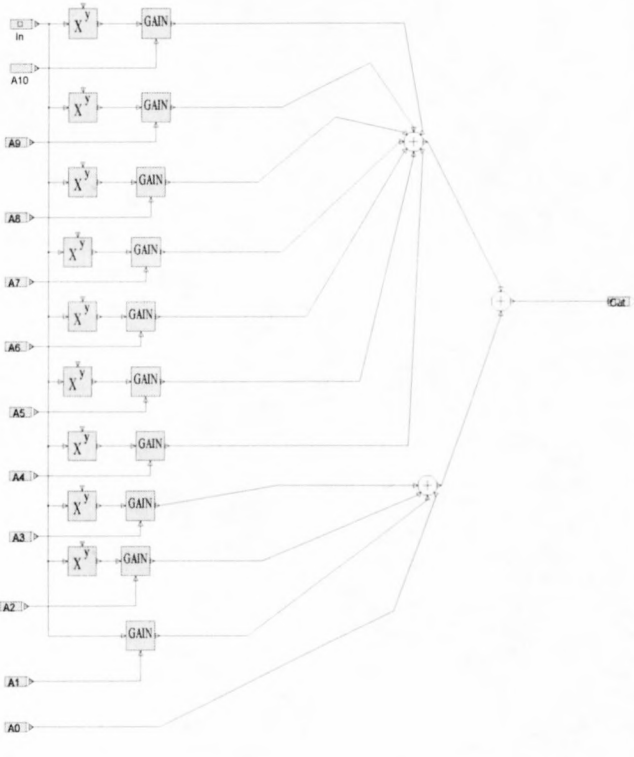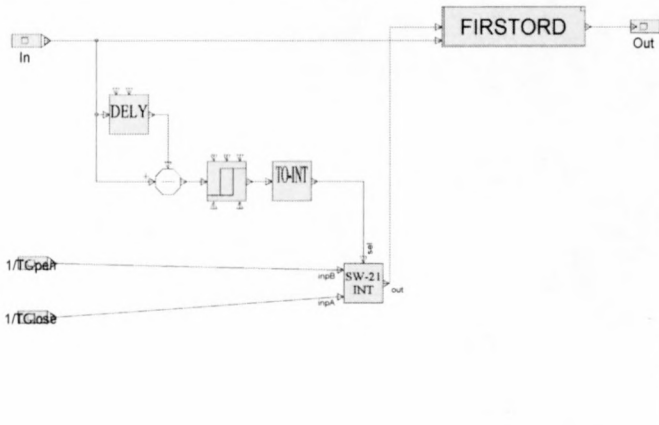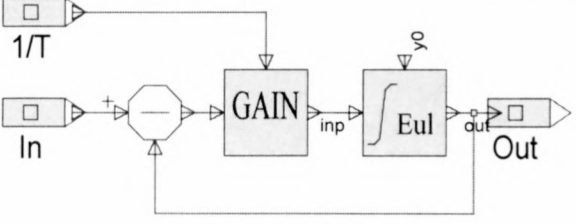
Model SuperBlock	Block Contents	Block Parameters
Simulation Model Superblock	Fin, hhinit, AcrossUp, Kh, 1/TUpOpen, 1/TUpClose, Gapup, Gain, 1/TLoOpen, 1/TLoClose, Kl, AcrossLo, hlinit, Gaplo → **sysmodne** → hh, Fh, Fl, hl	System Parameters: 1/tupopen = 1.5 (1/ valve v_2 open time constant) 1/tupclose = 0.8 (1/ valve v_2 close time constant) 1/tloopen = 0.65 (1/ valve v_1 open time constant) 1/tloclose = 0.9 (1/ valve v_1 close time constant) acrossup = 0.08 (upper tank cross sectional area [m^2]) acrosslo = 0.08 (lower tank cross sectional area [m^2]) gapup = 1.2e-5 (valve v_2 hysteresis $[\frac{1}{2}\Delta u]$) gaplo = 1.1e-5 (valve v_1 hysteresis $[\frac{1}{2}\Delta u]$) Model Initialization: Hhinit (upper tank level h_2

Model SuperBlock	Block Contents	Block Parameters
		initial value) Hlinit (lower tank level h_1 initial value) Feed flow rate input: Fin (f_3) Control inputs: Kl (valve v_1 control signal u_1) Kh (valve v_2 control signal u_2)
Sysmodne		
Uptank2		Euler integrator time step = 0.01

Model SuperBlock	Block Contents	Block Parameters
Lotank2		Euler integrator time step = 0.01
Vtomup		Poly2: $out = A \times in^2 + B \times in + C$ A = 0 B = 0.0246 C = 0.038743
Mtovup		Poly2: $out = A \times in^2 + B \times in + C$ A = 0 B = 40.6504 C = -1.5749
Vtomlo		Poly2: $out = A \times in^2 + B \times in + C$ A = 0 B = 0.028128 C = 0.03

Model SuperBlock	Block Contents	Block Parameters
Mtovlo		Poly2: $out = A \times in^2 + B \times in + C$ A = 0 B = 35.5517 C = -1.0665
KHHHFH		Limiter: Min = 5 Max = 10 Gain = 1 Backlash: $Y_0 = 0$ Subtract: Sub = -0.57 Poly10: A10 = 0 A9 = 0 A8 = 0 A7 = 0 A6 = 0 A5 = 0 A4 = -9.1209e-7 A3 = 2.2697e-7 A2 = -1.9564e-4 A1 = 7.6884e-4 A0 = -1.204e-3

Model SuperBlock	Block Contents	Block Parameters
Poly10		$out = A_{10}in^{10} + A_9in^9 + A_8in^8 + \ldots + A_1in + A_0$
Frswitch		Delay: Dt =0.01 Delay = 0.1 Max Delay = 0.1 $Y_0 = 0$ Switch: Umin = -1e-4 Umax = 1e-4 Ymin = 0; Ymax = 1 $Y_0 = 0$
Firstord		Euler integrator time step = 0.01

Model SuperBlock	Block Contents	Block Parameters
Kloflo		Limit: Min = 3 Max = 10 Gain = 1 Backlash: $Y_0 = 0$; Sum: Sum = 0.57 Poly10: A10 = 0 A9 = 0 A8 = 0 A7 = -5.2168e-8 A6 = 2.3404e-6 A5 = -4.3534e-5 A4 = 4.3418e-4 A3 = -2.5061e-3 A2 = 8.3877e-3 A1 = -1.5042e-2 A0 = 1.1139e-2

Table 15: Simulation model – SIMuWIN Implementation

Appendix E

Simulation Model Evaluation

The appendix presents the results of tests that were done to verify the validity of the simulation model. In a typical test a command signal was applied to the real plant (one or both of the valves) given certain initial tank levels. Then tank level changes were recorded over time and compared with those resulting from a simulation of the plant model where the same command signals were given to the simulation model with the same initial tank levels. The results the tests are shown below.

E.1 Step-test

Upper tank:

With the lower tank empty and the upper tank filled, the upper tank valve command signal u_2 was stepped over a period of 60 seconds as shown in Figure 83 with the resulting simulated and measured level responses l_2 also presented in Figure 83.
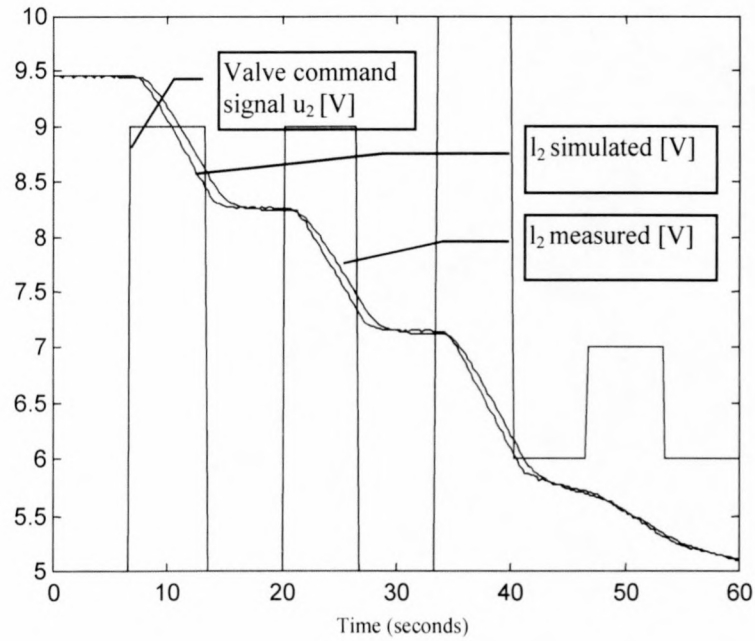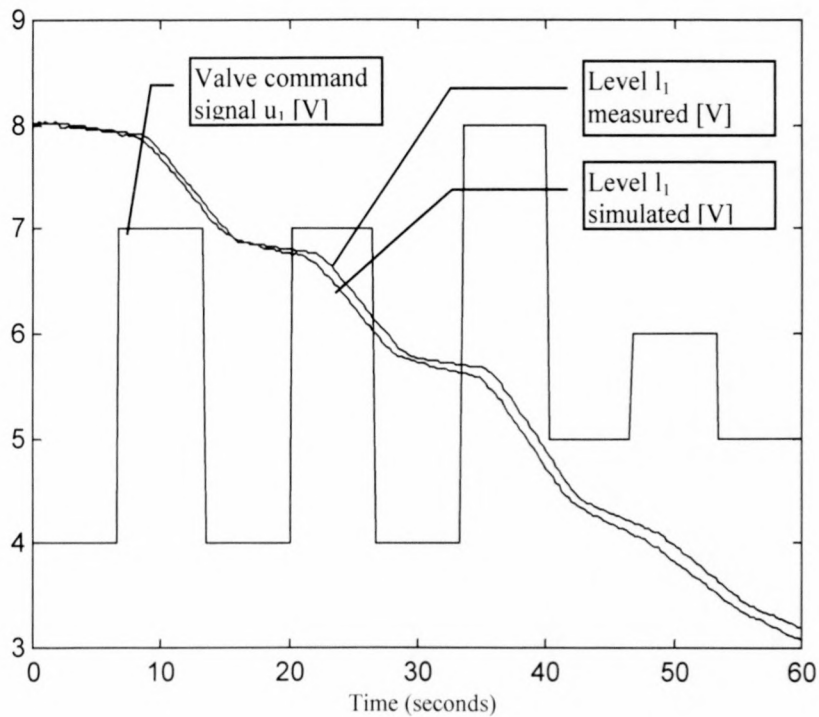
Figure 83: Upper tank – step test

Lower tank:

With the upper tank empty and the lower tank filled, the lower tank valve command signal u_1 was stepped over a period of 60 seconds as shown in Figure 84 with the resulting simulated and measured level responses l_1 also presented in Figure 84.
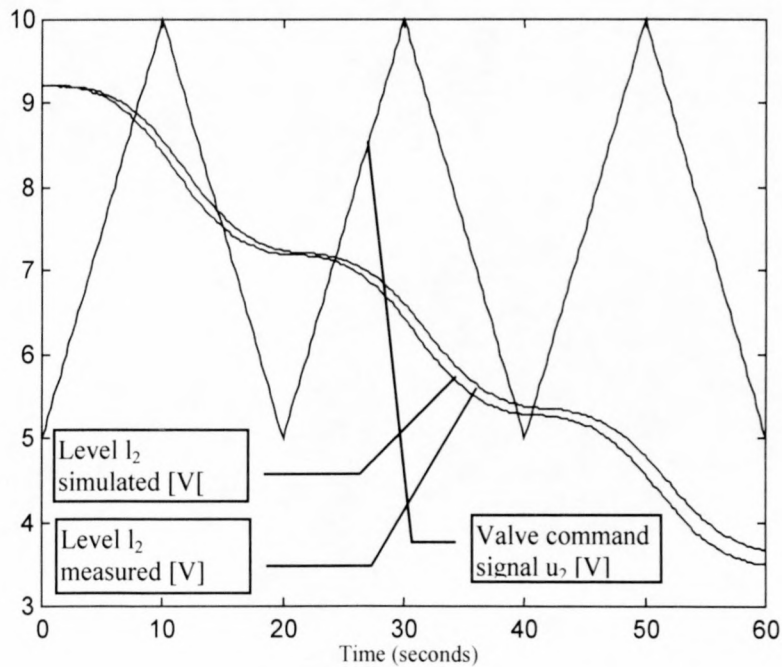

Figure 84: Lower tank – step test

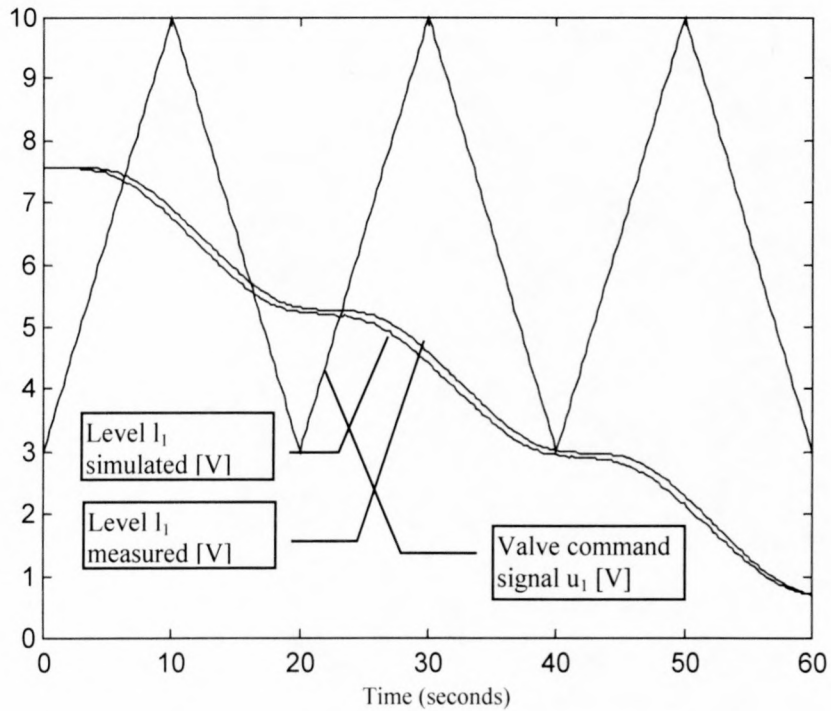## E.2 Triangular test

Upper tank:

With the lower tank empty and the upper tank filled, the upper tank valve command signal u_2 was adjusted in a triangular way over a period of 60 seconds as shown in Figure 85 with the resulting simulated and measured level responses l_2 also presented in Figure 85.

**Figure 85:** Upper tank – triangular test

Lower tank:

With upper tank empty and the lower tank filled, the lower tank valve command signal u_1 was adjusted in a triangular way over a period of 60 seconds as shown in Figure 86 with the resulting simulated and measured level responses l_1 also presented in Figure 86.

Figure 86: Lower tank – triangular test

E.3 Final test – tanks in cascade

In the final test the complete simulation model were tested as a unit with the upper and lower tank modules in cascade. Both the upper and lower tanks were filled. Valve command signals were applied to the simulation model as well as the pilot plant upper valve v2 and lower valve v1 as shown in Figure 87. Resulting level responses from both the simulation model as well as the pilot plant is shown in Figure 88.
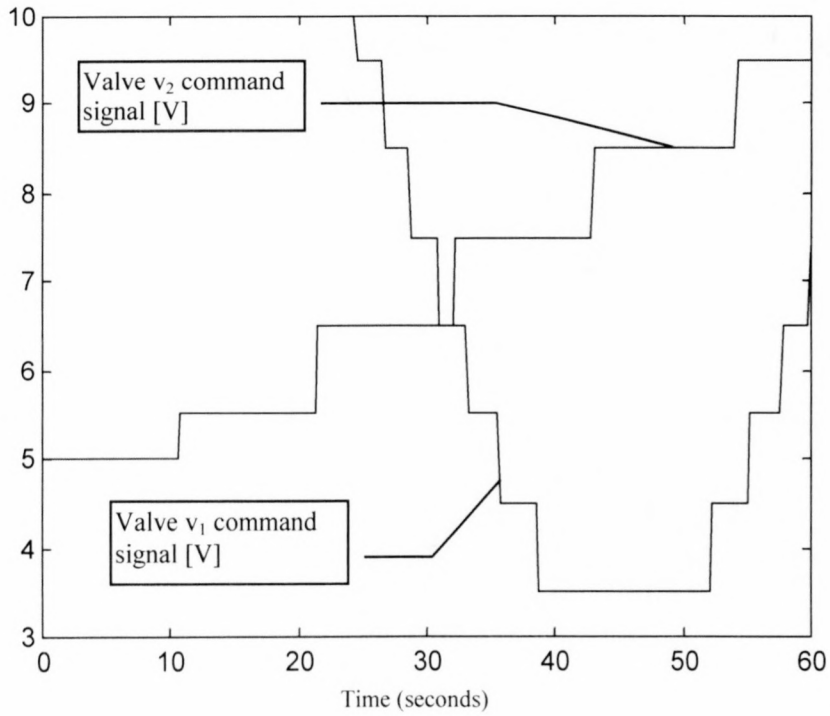
Figure 87: General test – valve commands
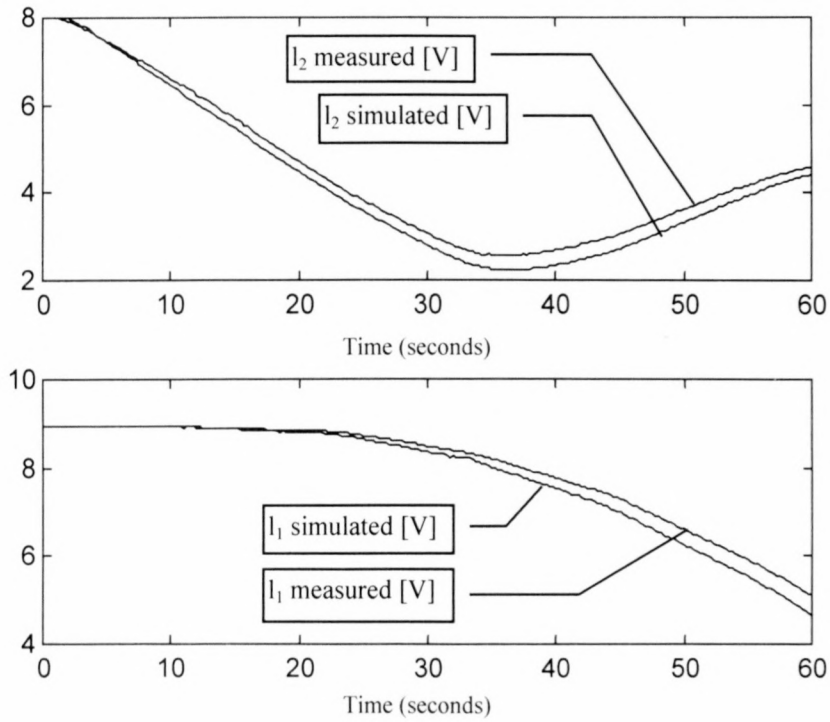
Figure 88: General test – level responses